Thirty Fourth Edition

Photovoltaics International

THE TECHNOLOGY RESOURCE FOR PV PROFESSIONALS

Solar Intelligence The Silicon Module Super League in 2017 and 2018: a data-driven, bottom-up analysis of technology and capacity forecasts

Motech Cu-plated electrodes with laser contact opening on n-type crystalline silicon solar cells

Fraunhofer IKTS High-performance screen-printable pastes for HJT cells

ISFH Ultrafast lifetime regeneration of boron-doped Czochralski-silicon in an industrial belt-line furnace

Imec Use of a perovskite layer to boost the efficiency of CIGS modules

Valencia Nanophotonics Technology Center Improving the efficiency of PV modules using glass with reflective strips

Fourth Quarter, December 2016

www.pv-tech.org

JA SOLAR

www.jasolar.com

Harvest the Sunshine

Premium Cells, Premium Modules

JA Solar Holdings Co., Ltd.

Building No.8, Nuode Center, Automobile Museum East Road, Fengtai District, Beijing

Tel: +86 (10) 63611888 Fax: +86 (10) 63611999 Email: sales@jasolar.com; market@jasolar.com

Photovoltaics International

Published by:
Solar Media Ltd.,
3rd Floor, America House, 2 America Square
London EC3N 2LU, UK
Tel: +44 (0) 207 871 0122
Fax: +44 (0) 207 871 0101
E-mail: info@pv-tech.org
Web: www.pv-tech.org

Publisher: Chris Riley

Head of Content: John Parnell
Managing Editor: Ben Willis
Commissioning Editor: Adam Morrison
Sub-Editor: Steve D. Brierley
Senior News Editor: Mark Osborne
Reporters: Andy Colthorpe, Tom Kenning, Danielle Ola

Design: Tina Davidian
Production: Daniel H Brown, Sarah-Jane Lee

Sales Director: David Evans
Account Managers: Adam Morrison, Graham Davie, Lili Zhu, Matthew Bosnjak, James Linin

Cover image: Unloading of solar cells from a furnace

Image courtesy of Hanwha Q CELLS

Printed by Buxton Press

Photovoltaics International
Thirty Fourth Edition
Fourth Quarter, December 2016
Photovoltaics International is a quarterly journal published in February, May, August and December.

Distributed in the USA by Mail Right International, 1637 Stelton Road B4, Piscataway, NJ 08854.

ISSN: 1757-1197

USPS Information
USPS Periodical Code: 025 313

Periodicals Postage Paid at
New Brunswick, NJ
Postmaster: Send changes to:
Photovoltaics International,
Solar Media Ltd., C/o 1637 Stelton Road, B-4, Piscataway, NJ 08854, USA

Foreword

Welcome to the thirty-fourth issue of *Photovoltaics International*. As always, we bring you insights into the latest in-depth research from the world of solar R&D. A great deal of credit for the headline-grabbing cost reductions since we first published *PVI* can be attributed to innovations we have detailed on these pages.

The breeding ground for these innovations has a similar look. The first edition of *PVI* featured imec, Spire, PI Berlin, Q CELLS and a few other familiar names. But the industry that these breakthroughs have fed into has changed dramatically. A bevy of billion-plus dollar companies now work to bring these developments from lab to fab and with an ever increasing share of the market, the very biggest solar manufacturers are picking technology winners and laying down the path all the others will follow.

In March we will once again assemble a 'who's who' of the PV manufacturing world for our PV CellTech conference in Malaysia. The CTOs and R&D heads of the Silicon Module Super League players, who so dominated the PV industry in 2016 and look set to again in 2017, will discuss their plans at the conference on the 14-15 March in Penang. Finlay Colville, Head of Market Research at our publisher Solar Media, examines the extent of their influence and the benchmarks they will set for wafer quality, cell efficiency and module power ratings (p.16).

With this in mind, our Senior News Editor Mark Osborne's quarterly analysis of manufacturing capacity expansions (p.28) holds additional weight. Cancellations and closures replaced the wave of new additions and upgrades seen earlier in the year. This is clearly bad news in the short term, especially for those impacted directly by job losses. The change could also be seen as a correction, a responsive shift from an agile industry. Overcapacity concerns could well prove to be short lived and the impacts could fail to cut as deeply as we have seen in previous, full-blown cycles of overcapacity.

Elsewhere in this issue, the afore-mentioned imec investigates the benefits of adding a perovskite layer to CIGS cells (p.70). Challenges clearly remain, including improving stability of the material at higher temperatures, but the benefits of pairing perovskite with existing cell technologies are crystal clear. As imec shows, the efficiencies achieved in the lab hold great promise.

Motech reveals how n-type cells with copper-plated electrodes and laser contact opening have enabled efficiency levels of up to 21.3% (p.45). And Fraunhofer IKTS examines a number of new metalization pastes for heterojunction cells (p.60). It set out to match the performance of today's pastes while reducing associated production costs and simplifying the processing and handling requirements and reports for us on its results.

We hope that these papers continue to add value to your work and we hope you can join DuPont, Indeotec, SCHMID, Meyer Burger and a host of other influential PV firms in Penang for PV CellTech 2017.

John Parnell
Head of Content
Solar Media Ltd

Photovoltaics International

Photovoltaics International's primary focus is on assessing existing and new technologies for "real-world" supply chain solutions. The aim is to help engineers, managers and investors to understand the potential of equipment, materials, processes and services that can help the PV industry achieve grid parity. The Photovoltaics International advisory board has been selected to help guide the editorial direction of the technical journal so that it remains relevant to manufacturers and utility-grade installers of photovoltaic technology. The advisory board is made up of leading personnel currently working first-hand in the PV industry.

Editorial Advisory Board

Our editorial advisory board is made up of senior engineers from PV manufacturers worldwide. Meet some of our board members below:

Prof Armin Aberle, CEO, Solar Energy Research Institute of Singapore (SERIS), National University of Singapore (NUS)

Prof Aberle's research focus is on photovoltaic materials, devices and modules. In the 1990s he established the Silicon Photovoltaics Department at the Institute for Solar Energy Research (ISFH) in Hamelin, Germany. He then worked for 10 years in Sydney, Australia as a professor of photovoltaics at the University of New South Wales (UNSW). In 2008 he joined NUS to establish SERIS (as Deputy CEO), with particular responsibility for the creation of a Silicon PV Department.

Dr. Markus Fischer, Director R&D Processes, Hanwha Q Cells

Dr. Fischer has more than 15 years' experience in the semiconductor and crystalline silicon photovoltaic industry. He joined Q Cells in 2007 after working in different engineering and management positions with Siemens, Infineon, Philips, and NXP. As Director R&D Processes he is responsible for the process and production equipment development of current and future c-Si solar cell concepts. Dr. Fischer received his Ph.D. in Electrical Engineering in 1997 from the University of Stuttgart. Since 2010 he has been a co-chairman of the SEMI International Technology Roadmap for Photovoltaic.

Dr. Thorsten Dullweber, R&D Group Leader at the Institute for Solar Energy Research Hamelin (ISFH)

Dr. Dullweber's research focuses on high efficiency industrial-type PERC silicon solar cells and ultra-fineline screen-printed Ag front contacts. His group has contributed many journal and conference publications as well as industry-wide recognized research results. Before joining ISFH in 2009, Dr. Dullweber worked for nine years in the microelectronics industry at Siemens AG and later Infineon Technologies AG. He received his Ph. D. in 2002 for research on Cu(In,Ga)Se2 thin-film solar cells.

Dr. Wei Shan, Chief Scientist, JA Solar

Dr. Wei Shan has been with JA Solar since 2008 and is currently the Chief Scientist and head of R&D. With more than 30 years' experience in R&D in a wider variety of semiconductor material systems and devices, he has published over 150 peer-reviewed journal articles and prestigious conference papers, as well as six book chapters.

Chen Rulong, Chief Technology Officer, Solar Cell R&D Department, Wuxi Suntech

Chen Rulong graduated from Changchun Institute of Optics and Fine Mechanics, majoring in applied optics. He began working in the field of R&D on solar cells from 2001. He is a visiting fellow at the University of New South Wales in Australia and an expert on the IEC Technical Committee 82, which prepares international standards on PV energy systems.

Florian Clement, Head of Group, MWT solar cells/printing technology, Fraunhofer ISE

Dr. Clement received his Ph.D in 2009 from the University of Freiburg. He studied physics at the Ludwigs-Maximilian-University of Munich and the University of Freiburg and obtained his diploma degree in 2005. His research is focused on the development, analysis and characterization of highly efficient, industrially feasible MWT solar cells with rear side passivation, so called HIP-MWT devices, and on new printing technologies for silicon solar cell processing.

Sam Hong, Chief Executive, Neo Solar Power

Dr. Hong has more than 30 years' experience in solar photovoltaic energy. He has served as the Research Division Director of Photovoltaic Solar Energy Division at the Industry Technology Research Institute (ITRI), and Vice President and Plant Director of Sinonar Amorphous Silicon Solar Cell Co., the first amorphous silicon manufacturer in Taiwan. Dr. Hong has published three books and 38 journal and international conference papers, and is a holder of seven patents. In 2011 he took office as Chairman of Taiwan Photovoltaic Industry Association.

Matt Campbell, Senior Director, Power Plant Products, SunPower

Matt Campbell has held a variety of business development and product management roles since joining the SunPower, including the development of the 1.5MW AC Oasis power plant platform, organized SunPower's power plant LCOE reduction programmes, and the acquisition of three power plant technology companies. Campbell helped form a joint venture in Inner Mongolia, China for power plant project development and manufacturing. He holds an MBA from the University of California at Berkeley and a BBA in Marketing, Finance, and Real Estate from the University of Wisconsin at Madison.

Ru Zhong Hou, Director of Product Center, ReneSola

Ru Zhong Hou joined ReneSola as R&D Senior Manager in 2010 before being appointed Director of R&D in 2012. Before joining ReneSola he was a researcher for Microvast Power Systems, a battery manufacturer. His work has been published in numerous scientific journals. He has a Ph.D. from the Institute of Materials Physics & Microstructures, Zhejiang University, China.

About LERRI Solar

A world leading mono-crystalline solar module manufacturer for achieving best LCOE (levelized cost of electricity) solutions.

LERRI Solar is a world leading manufacturer of high-efficiency mono-crystalline solar cells and modules. The company was founded in 2007 and later on acquired by Longi Group in 2014. Longi Group (SH601012) is the largest supplier of mono-crystalline silicon wafers in the world, with total assets above $1.7 billion. (2016)

Armed and powered by the advanced technology and long standing experience of Longi Group in the field of mono-crystalline silicon, LERRI Solar has shipped over 1GW products in 2015 and is estimated to double the revenue by the end of 2016.

With strong focus on R&D, production and sales & marketing of mono-crystalline silicon products, LERRI Solar is committed to providing the best LCOE solutions as well as promoting the worldwide adoption of mono-crystalline technology.

www.lerri.com

LERRI Solar

Visit us at WFES & Solar Expo 2017

Date : Jan 16 – Jan 19
Booth : NO.8120
Venue: Abu Dhabi National Exhibition Centre, Abu Dhabi, UAE

Contents

TALESUN

FEATHER

- “Lighter”、“Higher”、“intelligent”.
- 2 mm thin front glass and 30 mm thin frame.
- Robust design:Certified to 2400 Pa wind load and up to 5400 Pa snow load.
- Fully automated production line:Better consistent product quality.

SMART MODULE

- Integrated with module optimizer from Tigo Energy.
- Eliminate the module’s Current mismatch.
- Increase the number of modules per string of solar array by up to 30%.
- Robust design:Certified to 2400 Pa wind load and up to 5400 Pa snow load.
- More flexible system design:Work with various inverters.

ZHONGLI TALESUN SOLAR CO.,LTD.

E-mail: sales@talesun.com **Web:** www.talesun.com **Tel:** +86 512 8235 5888

Contents

inter solar
connecting solar business

25
1991–2016
YEARS OF INTERSOLAR

INTERSOLAR – POWERFUL PIONEERS FOR 25 YEARS!

Intersolar Europe | Munich | May 31–June 2, 2017
Intersolar North America | San Francisco | July 11–13, 2017
Intersolar South America | São Paulo | August 22–24, 2017
Intersolar Middle East | Dubai | September 25–27, 2017
Intersolar India | Mumbai | December 5–7, 2017
Intersolar Summit Iran | Tehran | November 15, 2016
Intersolar Summit USA East | New York | Spring 2017

Discover the World's Leading
Exhibition Series for the Solar Industry
www.intersolarglobal.com

Product Reviews

EMS

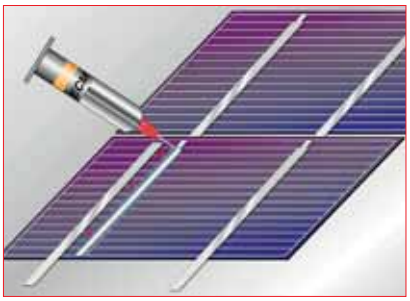

Engineered Material Systems providing low-cost 'snap cure' conductive adhesive for volume stringing

Product Outline: Engineered Material Systems (EMS) has launched a new 561-400 series low-cost 'snap cure' conductive adhesive, which is designed for stringing and shingling crystalline silicon and heterojunction solar modules.

Problem: Snap cure conductive adhesives are mostly employed in high volume production processes, due to dispensing ease and rapid adhesion at relatively low temperatures and high strength on a variety of substrates. They also need to provide low shrinkage after curing and low stress characteristics.

Solution: The EMS 561-400 series is used in modified ribbon stringers as the adhesive is more stress absorbing than solder to withstand the rigors of thermal cycling and processes at lower temperatures than solder. EMS 561-400 series conductive adhesives are claimed to be 60% cheaper than pure silver-filled conductive adhesives.

Applications: Snap curing conductive adhesive for crystalline silicon and heterojunction solar modules.

Platform: The EMS 561-400 series is designed to be used in modified ribbon stringers. The material will snap cure and fix ribbons in seconds at 150°C with enough strength to withstand module manufacturing processes until the adhesive cure is completed during the encapsulant lamination process. EMS 561-400 series conductive adhesives can be dispensed by time-pressure, auger or jetting.

Availability: Currently available.

Maxim Integrated Products

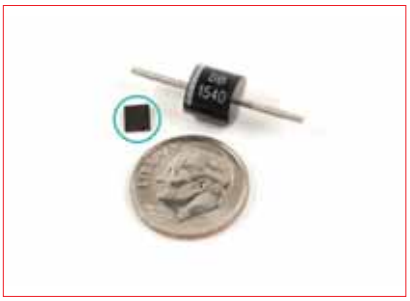

Maxim's analog IC integrated cell-string optimizer replaces bypass diode limitations

Product Outline: Maxim Integrated Products has introduced a new cell-string optimizer technology that is claimed to allow PV panels to harvest more energy.

Problem: Unlike conventional bypass diodes, solar cell optimizers do not bypass weak cell strings. Using bypass diodes in solar panel that experiences shading/soiling at any point within a string limits the maximum current rating to the lowest performing cell in the string.

Solution: Maxim's cell-string optimizers are integrated DC-DC converters that replace the bypass diode and perform maximum power point tracking (MPPT) of the PV panel. By replacing each diode with an MPPT device, the on-off response to performance mismatch is eliminated; every cell-string contributes maximum power without interfering with the power production capability of others. This enhanced degree of flexibility leads to increased energy production, eliminating collateral performance loss. A PV system designer can reconfigure a system design to allow for more inter-row shading that is claimed to deliver 10 to 20% more energy density than a conventional system.

Applications: PV module-integrated replacement for bypass diodes.

Platform: Maxim's solar cell optimizer works by boosting the current of the weak cells to match those of the stronger, eliminating the corresponding performance penalty of the conventional system. The module includes three Maxim solar cell optimizers, which replace the three diodes found in a conventional module junction box.

Availability: Currently available.

Ultrasonic Systems

Ultrasonic Systems offers fast anti-reflective coating with MAX-1200 system

Product Outline: Ultrasonic Systems has introduced the MAX-1200 coating system, enabling uniform high-speed glass substrate module coatings.

Problem: Anti-reflective coatings on glass substrates for PV modules are required to perform for the expected module lifespan. However, studies from NREL and others have highlighted that poor coating can lead to the top layer developing porosity due to variable pore size, in turn leading to defects and reduced performance.

Solution: The MAX-1200 leverages USI's proprietary, nozzle-less ultrasonic spray head technology that features a programmable high-speed X-Y-Z gantry to process glass plates or other substrates up to 1.2 meters wide at a process speed of up to 3.3 meters per minute. The system employs a bi-directional coating application sequence that provides an ultra-uniform coating layer onto the substrate. The company claims an excellent coating transfer efficiency of up to 99% with the finished film thicknesses down to the sub-micron level.

Applications: High-speed glass substrate anti-reflective coatings.

Platform: The MAX-1200 uses the PMP-200 precision metering pump liquid delivery system with a dual pump design for uninterrupted operation and an automatic pump refill system from the coating reservoir. The system is constructed with materials compatible with acidic and caustic coating liquids and has an automated spray head wash down facility with a clean and dry station. The system is also PAC controlled with touch panel HMI and the system can be configured as an in-line system or stand-alone.

Availability: Currently available.

Market Watch

News

Mercom forecasts 76GW in global PV installations in 2016

Global clean energy communications and consulting firm Mercom expects global solar installations to reach 76GW in 2016.

Despite an expected slowdown, global solar demand outlook has improved for 2017, as drops in costly module prices have led to a rebound in China in anticipation of the next round of tariff cuts. Mercom noted in its report that solar installations are expected to hit 70GW.

Raj Prabhu, CEO and co-founder of Mercom Capital Group, said: "Global solar demand will overshoot most forecasts made earlier this year due to an unprecedented level of activity in China. Record installations in China followed by a slowdown resulted in an oversupply situation, which led to a module price crash. Low module prices are helping demand recovery going into 2017."

Credit Sungrow

A surge in deployment in China has helped propel global installations this year towards 76GW.

After installing 15.1GW in 2015, China surpassed its 2016 installation goal of 18.1GW in the first half of 2016 with approximately 22GW installed as developers rushed to complete projects before the country's tariff deadline on June 30.

Mercom's expectation approximately 13GW for the US solar market in 2016. In total, the US market is projected to grow about 78% year-over-year in 2016.

Global

Sonnedix founder launches US$100 million solar and storage fund for emerging markets

An open fund for solar energy and energy storage in various emerging markets has been launched by Franck Constant, the co-founder of Sonnedix Group and director of Sithe Pacific.

The new fund named 'Constant Energy' aims to reach US$100 million by the end of 2017 and, while predominantly aimed at solar, it will have 20% focused on energy storage.

Target nations in Asia include Thailand, Malaysia, Indonesia, Laos, Cambodia, Myanmar, Korea, Taiwan, as well as selected African markets such as South Africa and possibly Kenya.

Constant said: "A lot of these countries already have a tradition of private power generation in the conventional space. It's only a matter of time before they are moving to private power generation in the solar space."

To date, only a few funds have specifically focused on both solar and energy storage.

Constant added: "Storage is today where solar was nine years ago when we started Sonnedix. Probably as a first step, I expect it will be a combined solution, where we get land, we have a solar plant and we add storage to improve the dispatch of the solar plant or to support the grid."

GCL chairman to be next head of Global Solar Council

GCL Holding chairman Zhu Gongshan will head up the second committee of the Global Solar Council (GSC).

Zhu will take over for a two-year term from December 2017. He has targeted a three-pronged approach for the group tackling technology, policy and investment at the same time.

"It's my greatest honour to be the president of GSC's second committee. I promise to leave no stone unturned to promote the global development of the PV industry," Zhu said.

Zhu currently holds positions with the Asian Photovoltaic Industry Association and the China PV Industry Alliance.

He also hinted that he could seek to establish a solar development fund under the auspices of the GSC with the goal of encouraging greater financial innovation in the sector.

Boost for solar as European Commission reveals energy reforms

The European Commission has unveiled a package of policy proposals that would transform the continent's energy market.

While concerns remain that renewables will lose their right of priority dispatch, the new package would enshrine the right of solar owners to sell excess electricity and establish a level playing field for investment via a shared rulebook.

Additional encouragement for cross-border tenders and an emissions limit on technologies participating in capacity mechanisms have also been welcomed.

"We need strong action to ensure that priority dispatch is maintained for renewables, especially if capacity mechanisms are to be allowed – even as a last resort," said Alexandre Roesch, policy director at trade group SolarPower Europe (SPE). "Such mechanisms have a massive negative effect on the electricity price and thus distort investments away from clean technologies to old polluting ones. Renewables and flexibility providers need to be rewarded in the new market."

Despite these concerns, proposals to protect self-consumption drew praise from SPE.

"Solar is a means to democratise energy and we are delighted that for the first time renewable self-consumers will now be recognised at EU level and have a legally binding framework giving them the right to generate, consume, store and sell their own power," added Roesch.

GCL-SI to build 1GW solar plant in Chernobyl

GCL-SI, a subsidiary of China's GCL, is to develop a 1GW solar PV plant at the former contaminated nuclear site in Chernobyl, Ukraine. Construction is expected to start in 2017.

It will be located in what is known as the 'exclusion zone' – the 30km² guarded areas around the original nuclear reactor hall that exploded in 1986 resulting in a historic tragedy.

The plant, which will be developed by GCL-SI in collaboration with the China National Complete Engineering

European Commission

New EU energy market proposals could help solar despite concerns over the loss of priority dispatch.

Corporation (CCEC), is part of the Ukrainian government's plans to revive the exclusion zone with renewable and safer energy sources.

The plan for the plant was announced in October by Ostap Semerak, the country's minister of environment and natural resources: "Its cheap land and abundant sunlight constitute a solid foundation for the project. In addition, the remaining electric transmission facilities are ready for reuse," he said.

Americas

Chile announces plans for 1GW solar park at COP22

Chile plans to develop a solar park of between 750MW to 1GW capacity to power the mining industry in the Atacama region, according to a release from Chilean development agency Corfo.

This would almost double Chile's current solar capacity, having become the first Latin American country to surpass 1GW in January this year.

The new solar park, to be known as the 'Solar District', will require investment of US$4 billion and will generate around 3,000 jobs during construction.

Chile will focus on reducing PV costs by 25% using the extremely favourable conditions of the Atacama Desert, aiming to reach prices of US$0.02/kWh by 2025.

In August, renewables firm SolarPack was awarded a project in Chile to produce 280GWh per annum at what was then a record low tariff US$0.0291/kWh.

Chile will also utilize the availability of lithium salt resources to improve energy storage technology and will invest in the major interconnection between the central and northern grids SIC and SING. A Solar Technology Center in Antofagasta will also be created.

Tesla/SolarCity merger gets go ahead

The US$2.6 billion merger between Tesla and SolarCity has been approved by shareholders.

The combined Tesla and SolarCity will deliver Elon Musk's vision for a world-first opportunity to "generate, store and consume energy sustainably, through a suite of integrated products that add aesthetics and function while reducing cost", according to a company blog.

"By leveraging SolarCity's installation network and Tesla's global retail footprint, we can do this in a way that is seamless for our customers and that we expect will create significant value for our shareholders," it continued.

The deal could "substantially" increase SolarCity's sales, reckons industry veteran Jigar Shah, clean energy entrepreneur and the founder of SunEdison.

"Tesla is sitting on around 300,000 pre-orders for the Model 3 [EV]. So there is a real opportunity for SolarCity to substantially increase sales by selling into the Tesla base. It works the other way too – a lot of people buying SolarCity systems could go out and buy Tesla cars," said Shah.

Asia and Oceania

Thai solar slated to rejuvenate from mid-2017 but long dry spells expected

Political changes over the last four years and the recent death of King Bhumibol have brought some inertia to the Thailand solar market, but industry members expect it will return to strong growth in the second half of 2017.

Speaking at Solar & Off-Grid Renewables Southeast Asia in Bangkok, Franck Constant, co-founder Sonnedix Group, said it has not been easy to develop policy in the current climate following a constitutional referendum in August, which has made foreign

investors hesitate. Far less capacity has come online compared to the 2010/11 period.

Despite a level of "inertia", Constant noted that Thailand is still leading the pack in Southeast Asia with more than 3GW of operating solar PV installations; far more than Malaysia, Indonesia, Laos and Myanmar, although the Philippines is catching up quickly.

Referring to Thailand, Constant added: "I believe the new ministry of finance, the new leadership in the government, is going to very aggressively push for infrastructure implementation from the second half of next year. They want to do green bonds and other interesting things so watch this space on Thailand."

Solar takes its share of Indian electricity to 1%

Solar power produced 1% of India's electricity in 1H 2016/2017, according to data from Mercom Capital.

Between April and September 2016, the country produced 5.79 billion units of electricity from solar, tracking 2.6 billion units ahead of the 2015 figures.

The country has installed more than 10GW of solar with long-term ambitions to increase that level by an order of magnitude.

The rate of commissioning of plants has also gathered pace. According to Mercom's "India Solar Project Tracker", the country has put 3.6GW of solar online in the 2016 calendar year compared to 2.1GW in all of 2015. Mercom expects the 2017 figure to approach 8GW.

Africa and Middle East

PPA under three cents per kWh signed for 800MW Dubai project

What is thought to be the world's lowest priced solar PPA has been signed for an 800MW project in Dubai.

The emirate's utility DEWA signed the contract with Abu Dhabi-based renewable energy company Masdar.

The price appears higher on paper than the winning bid in Abu Dhabi's own 350MW tender. A consortium including JinkoSolar was revealed to have won with an offer of US$0.0242/kWh. That offer includes an increased payment during the summer months.

"The 2.42 cents that has been reported as a record bid is, in fact, not an LCOE for the project. ADWEA, aiming to maximise the plant's use to generate electricity for a summer peak electricity demand, adds a 60% bonus to tariff payments during summer months," said James Kurz, senior consultant at Apricum – The Cleantech Advisory. "The reported tariff of 2.42 cents is a base tariff that is paid from October through May while 3.87 cents is paid from June through September. The bid on a levelised cost of energy basis was 2.94 cents, which is comparable to the DEWA results."

The Dubai PPA is for the third phase Mohammed bin Rashid Al Maktoum Solar Park. The 200MW second phase was awarded a PPA at just under six cents.

Scatec Solar signs PPA for Mozambique's first large-scale solar plant

Scatec Solar and Norwegian private equity firm KLP Norfund Investments have signed a 25-year PPA for a 40MW solar PV plant in Mozambique – the country's first large-scale solar plant.

The US$80 million plant is located in the Zambézia Province and is expected to deliver 77,000MWh per year to the northern regions of Mozambique.

Equity for the project was supplied by Scatec Solar (52.5%), Norfund (22.5%) and EDM (25%). The International Finance Corporation (IFC) and the Emerging Africa Infrastructure Fund intend to provide project finance debt. The parties are expecting financial close and solar plant construction to start in the first quarter of 2017.

"This is an excellent example of how private public partnerships can deliver renewable energy and support further economic growth in Mozambique. EDM and the government of Mozambique have demonstrated strong leadership in taking this project forward and it paves the way for further investments in renewable energy in the country," said Scatec Solar CEO Raymond Carlsen, in a statement.

"Access to reliable energy is a prerequisite for development. Only 3% of the world's electricity is generated in Africa, although 15% of the world's population lives here. Clean energy is a focus investment area for Norfund, and we appreciate being a partner in this first independent solar power producer project in Mozambique together with EDM and Scatec Solar," added Norfund CEO Kjell Roland.

Tata Power Solar

The power from India's growing PV base now accounts for 1% of the country's generation.

Under the Patronage of **H.H. General Sheikh Mohammed bin Zayed Al Nahyan,** Crown Prince of Abu Dhabi and Deputy Supreme Commander of the U.A.E. Armed Forces

SOLAR EXPO

A WORLD FUTURE ENERGY SUMMIT EVENT

16-19 JANUARY 2017

ABU DHABI NATIONAL EXHIBITION CENTRE

Hosted by

Masdar
A MUBADALA COMPANY

Strategic Partner

هيئة مياه وكهرباء أبوظبي
Abu Dhabi Water & Electricity Authority

Strategic Sponsor

غرفة أبوظبي
ABU DHABI CHAMBER

Visit the region's largest exhibition dedicated to SOLAR PV & CSP

REGISTER FOR FREE

solarexpo.ae

EXHIBITION

200+ Exhibiting Companies

20+ Free-to-attend Workshop Sessions

400+ Innovative Products & Services

PRODUCT SECTORS

- Photovoltaic Applications
- Photovoltaic Cells and Modules
- Photovoltaic Components
- Solar Thermal Technologies/Applications
- Smart Grids
- Energy Storage

ABU DHABI NATIONAL EXHIBITION CENTRE | **10 AM – 5 PM**

STAY IN THE LOOP

Download the ADSW Mobile App
Optimise your experience at Abu Dhabi Sustainability Week

Available on the App Store | Google play

Part of ABU DHABI SUSTAINABILITY WEEK BUSINESS

Official Event Partner: MESIA

Chinese TV Partner: CATV

Official Radio Station: dubai eye 103.8

Part of 10th EDITION WORLD FUTURE ENERGY SUMMIT

Co-located with: ENERGY EFFICIENCY EXPO | SUSTAINABLE TRANSPORT

Organised by: Reed Exhibitions

The Silicon Module Super League in 2017 and 2018: a data-driven, bottom-up analysis of technology and capacity forecasts

Finlay Colville, Head of Market Research, Solar Media

ABSTRACT
After several years of increased capital equipment spending and technology upgrades, solar photovoltaic manufacturers are adjusting to rapid pricing declines during the second half of 2016. This is having a direct impact on factory productivity and utilization rates, and has left many unanswered questions when forecasting company plans for 2017. While there are several hundred companies engaged in PV manufacturing today, the decisions on technology and product shipment of the major module suppliers, the Silicon Module Super League, will be critical in setting the benchmarks for wafer quality, cell efficiency and module power ratings during 2017 and 2018.

The solar photovoltaic (PV) industry can generally still be viewed as a growth industry in terms of end-market module shipments, where annual growth rates of 10-20% remain typical. While the factors driving global demand often manifest themselves through changing policies and trade-related duties at the country-specific level, the industry is still at an early adoption phase, and will remain like this for the next few years.

Consistent annual growth generally allows the scope for multiple PV module suppliers to grow market share through increased shipment levels, accompanied by capacity increases and production line upgrades. As a result, the industry follows typical cyclic trends related to overcapacity, oversupply and capital equipment budgets.

In recent years, a select group of seven solar PV module suppliers has emerged, labelled the 'Silicon Module Super League' (SMSL). The SMSL consists of Canadian Solar, GCL (including both GCL Poly and GCL Systems Integration), Hanwha Q CELLS, JA Solar, JinkoSolar, LONGi Silicon Materials (including its cell and module subsidiary operations under LERRI Solar) and Trina Solar. Collectively the SMSL has moved from having a market share of module supply at approximately 30-40% a few years ago to nearly 50% currently, and will likely approach 60% of end-market supply during the next couple of years.

With module shipment levels at the multi-gigawatt (GW) level today, and in some cases well above 6GW, the SMSL is the most important group of companies in the PV industry, broadly setting the benchmark for all other producers of components and suppliers of modules to the end market. Furthermore, the SMSL includes the two most important upstream (ingot/wafer) suppliers in the industry today: GCL Poly and LONGi Silicon Materials. These two companies are poised to play a leading role in p-type crystalline silicon (c-Si) technology and cell efficiencies over the next two years, with LONGi dictating p-type mono market-share gains against p-type multi, and GCL Poly being critical to the adoption of diamond wire saws for slicing p-type multi wafers and black silicon texturization of p-multi cell lines.

This article presents the current forecasting from the PV Tech market research team relating to the SMSL when considered as a single entity. The data and analysis is collected in-house, with the graphics coming directly from our manufacturing model created for each of the SMSL companies. The data and graphics form a subset of the full industry analysis presented in the January 2017 release of the "PV Manufacturing & Technology Quarterly report" [1]. The discussion provided within this article also considers the impact of the forecasting, with respect to the PV Tech conference, PV CellTech, in Penang, Malaysia on 14-15 March 2017.

"With module shipment levels at the multi-gigawatt level today, and in some cases well above 6GW, the SMSL is the most important group of companies in the PV industry, broadly setting the benchmark for all other producers of components and suppliers of modules to the end market."

Hanwha Q CELLS

A small group of module suppliers has pulled away from the rest of the market in recent years and looks set to continue their dominance.

Automatic $POCl_3$ / BBr3 / TMA Chemical Distribution System

HORIBA's fully automated bulk chemical distribution systems safely deliver chemical to the point of use. No exchanging fragile quartz bubblers at height, reduced labor cost, risk and chemical waste with the benefits of improved process, safety and higher uptime.

SYSTEM BENEFITS

- Reduced risk
- Lower labor cost
- Reduce scrap
- Reduce chemical handling
- Improved process stability
- Higher uptime
- Enhanced operator safety

Solar Power award winner

SCAN ME

HORIBA UK Ltd
Moulton Park
Northampton
NN3 6FL
United Kingdom

+44 1604 542 600
+44 1604 542 696
enquiries.hil@horiba.com

www.horiba.com

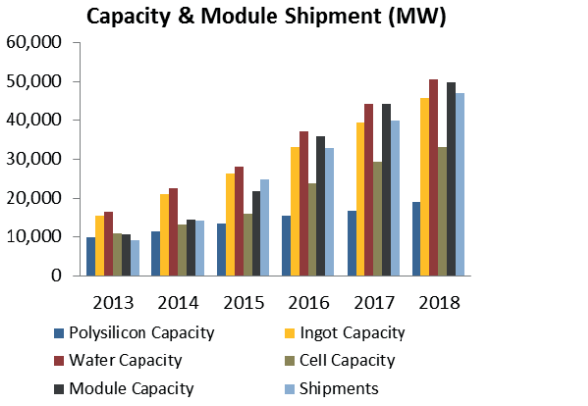

Figure 1. Effective annualized capacities from the SMSL companies will see further growth during 2017 and 2018, with branded module shipments exceeding 40GW in 2018.

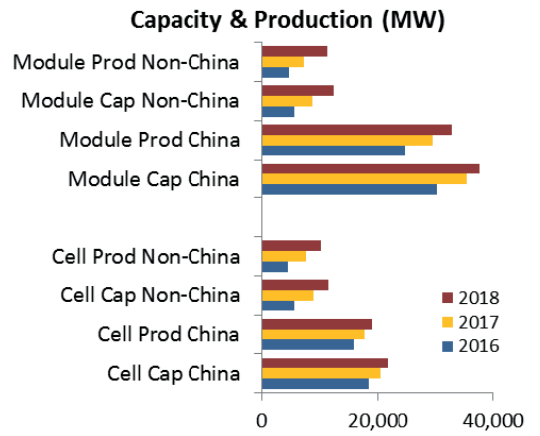

Figure 2. Capacity and production from cell and module lines operated by the SMSL, outside China, are expected to more than double between 2016 and 2018.

In-house capacity and module shipments keep on growing

When one looks across the entire PV manufacturing universe (encompassing several hundred companies engaged in various stages from polysilicon to module production, thin-film manufacturing and end-market module shipments), there is a wide range of strategies being employed. One of the most important leading indicators of each company's market strength and durability relates to effective capacity, expansions and utilization rates. Note that we refer only to annualized effective capacity rates in the graphics that follow, reflecting capacity taken offline, mothballed, or added across any specific calendar year: this differs from the often-cited year-end nameplate capacity figures that have little significance in assessing actual productivity rates.

While many companies have been forced to take capacity offline in the past 12 months, or scale back expansion and capital expenditure (capex) plans for 2017, the SMSL continues to bring capacity online, often by creating new production facilities across Southeast Asia (and shortly India). This is shown clearly in Figure 1, alongside the cumulative end-market module shipment levels, for the SMSL grouping.

A very simple comparison of the SMSL shipment growth rates with those coming from end-market demand (as it relates specifically to module shipments, as opposed to government-cited connections/accreditation) reveals the true intentions of the SMSL to increase market-share levels further. This supports the basic premise discussed above, namely a group of just seven module suppliers moving quickly from 30% to 60% market-share.

Aside from polysilicon metrics shown in Figure 1 (arising purely from only one company active in polysilicon supply, GCL Poly), the other key takeaway relates to the imbalance from in-house cell manufacturing. This is mainly due to the legacy role (and continued relevance) of pure-play Taiwan-based cell makers that dates back to 2006. Indeed, most Taiwan cell companies still tend to be heavily biased towards cell production, and continue to be key cell suppliers to the SMSL today, also from cell lines that have been relocated from Taiwan to Southeast Asia in recent years.

While the SMSL draws heavily on Taiwan-managed Southeast Asia operations for trade-free module shipments to Europe and the US, the SMSL can also call upon pure-play (or nominally contract manufacturing) cell producers located in mainland China, in order to fulfil module supply demand for downstream project activity in China or India.

Southeast Asia expansions risk overcapacity outside China

The emergence of Southeast Asia as potentially the most important region for solar cell manufacturing has been driven by two key factors: the preference among US/Europe/Japan-headquartered companies to prioritise the region for low-cost mass production activities (such as the original moves from SunPower, Q-CELLS, the REC Group, and Panasonic/Sanyo); and the choice of the region by Chinese and Taiwanese cell and module producers to negate the cell/module made-in-China/Taiwan duties for shipments to Europe and the US.

Collectively, these two factors have seen the emergence of Malaysia, Singapore and the Philippines, followed by Thailand, Indonesia and Vietnam. For geographic purposes, we include South Korea within our Southeast Asia grouping, but we keep India as a unique manufacturing/end-market location.

Figure 2 shows the effective annualized cell and module capacity (and production) for the SMSL grouping, broken down into China and non-China regions. The non-China segment is dominated by Southeast Asian countries, notwithstanding the use of third-party OEM cell and module companies in the region that act as a buffer for short-term cell and module supply needed by the SMSL for (mostly) US-bound modules.

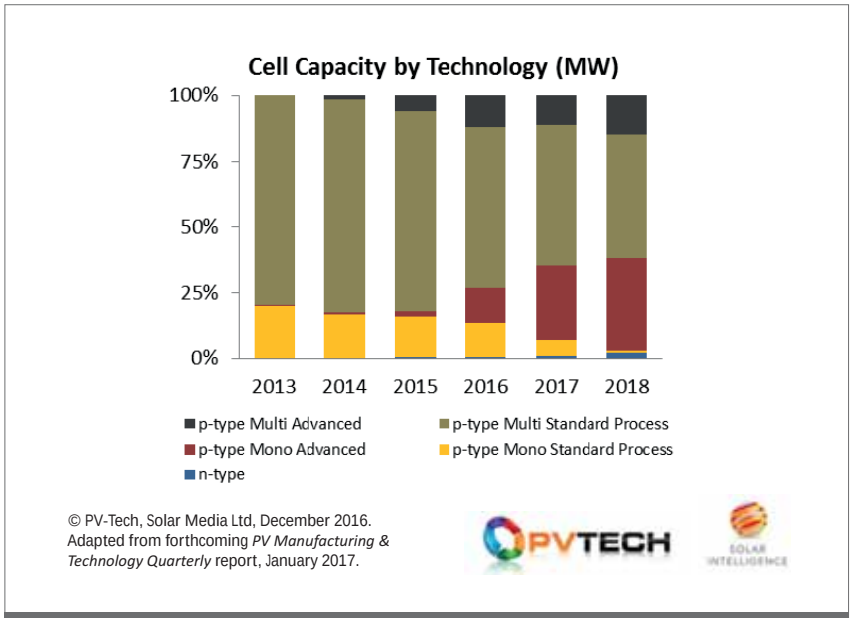

Figure 3. Cell capacities from the SMSL are forecast to remain almost exclusive to p-type c-Si substrates, with advanced process flow types increasing to 2018 mainly for PERC (p-mono) and black-silicon (p-multi).

During 2018 for example, the fraction of cell production from the SMSL coming from company-owned operations outside China will approach 50%. The number of cells actually used by the SMSL made outside China will be higher, due to the large portion of cells that are required to be outsourced.

With the SMSL far from alone in choosing Southeast Asia for increased cell and module capacity, it is inevitable that the region will move into a localized overcapacity, in particular when the typical production levels are sufficient to supply a significant portion of European and US module demand. Changes also to existing wording related to the US- and Europe-based trade duty restrictions would also impact on Southeast Asia. While this is unlikely to become a threat during 2017, it is something that could start to have an impact during the back half of 2018.

Technology roadmap of the SMSL sets benchmark for competition

During the four-year period from 2013 to 2016, the solar industry has seen some of the most significant advances in cell manufacturing, with previously cited high-efficiency concepts finally becoming commonplace. This time period has also seen module power, reliability and quality increased. Module suppliers not offering the higher performance panels have been left with restricted supply channels and very low average selling prices (ASPs).

While most of the gigawatt-based cell producers have largely kept to known technology types (choosing to perform process flow upgrades), many others have spoken in public about gigawatt-scale market entrance using bespoke customized technologies and equipment.

With the exception of GCL Systems Integration within the SMSL, the other cell and module suppliers have followed a broadly similar technology enhancement strategy. This makes the collective analysis

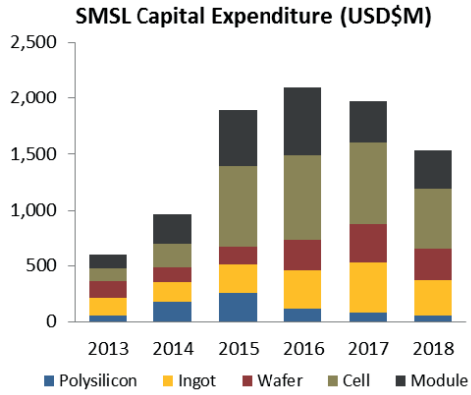

Figure 4. Capex from the SMSL is forecast to decline in 2017 and again in 2018, compared to the peak seen in 2016. Scope for upside at the wafer stage may come from a greater adoption of diamond wire sawing for the SMSL companies currently operating p-multi ingot/wafer capacity.

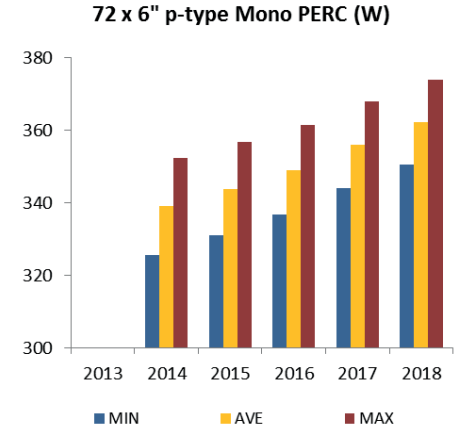

Figure 5. Average module power ratings (at STC) using 72-cell p-mono PERC cells are setting the benchmark for many competing companies and PV technologies, with this panel type expected to form a large portion of utility scale shipments during 2018.

of the SMSL, as shown in Figure 3, highly significant, and allows us to talk generally about what has been happening (and is forecast) for each of p-type mono and multi variants.

Indeed, the fact that the SMSL contains the leading suppliers to the industry of c-Si multi (GCL Poly) and mono (LONGi Silicon Materials) wafer makes the collective analysis all the more pertinent.

The change in technologies adopted across the cell lines of the SMSL between 2013 and 2018 is seen clearly within Figure 3. Back in 2013 and 2014, the SMSL cell capacity was largely confined to the standard p-mono and p-multi cell technologies of the time. Increases in module power levels were typically provided by moving from two- to four-busbar operation, improvements in silver paste and increased wafer quality.

However, from 2015, there has been a clear shift to high-efficiency cell operation (assigned as advanced cell types), both on p-multi and p-mono. Furthermore, the ratio of capacity (and corresponding production) from p-mono has grown, at the expense of p-multi.

In fact, while many industry observers still cling to a technology roadmap entrenched in n-type variants, the output from Figure 3 for the SMSL is the most valuable indicator for technology roadmap evolution in the industry, with the SMSL expected to remain focused on p-type options.

The move to advanced cell types has seen strong adoption. For p-mono, this is mostly coming from passivated emitter rear contact (PERC) additions. For p-multi, it is a combination of p-multi PERC (initially) and 'black-silicon' texturization upgrades. The shift to black silicon for p-multi is directly connected with the rate of adoption of diamond wire saws being implemented for p-multi wafer slicing. Diamond wire saws would see an increase in productivity of about 10-15% per multi block being sliced, in turn shaving around 1-2c/W off final wafer costs.

Capex to decline after peak of 2016

Capex remains one of the key inputs to any factor analysis that is applied to rank companies by strength, or as an indicator of sustained profitability.

Capex from the SMSL saw strong growth during 2013 to 2016, mainly at the cell and module stages, with contributions from capex due to Southeast Asia expansions playing a key part. As shown in Figure 4, we are forecasting consecutive year-on-year declines in capex from the SMSL during 2017 and 2018, with upgrades (across ingot-to-cell stages) having increased significance for PV equipment suppliers.

Indeed, when looking at the contributions to the overall SMSL capex, GCL and LONGi/LERRI are the major spenders, and any pull-back on their long term growth plans during 2017 and 2018 could have a profound effect on the forward-looking part of Figure 4.

Currently, few if any of the other SMSL players are guiding capex for 2017. This is mainly due to the year-end uncertainties ahead of 2017 shipment forecasts, and related operating profits stemming from a low-ASP module environment.

Benchmarking against 72-cell p-mono module powers in 2018

Just a couple of years back, the main threat to competitors both within and outside the SMSL was expected to come from 60-cell p-type multi panels, then being widely used for large-scale utility solar installations. However, the availability of low-cost, high-quality mono wafers (driven by LONGi), the move to add PERC tooling to p-mono cell lines and the shift to increased production of 72-cell module designs have led to the 72-cell p-mono PERC module becoming the benchmark for both power (at elevated temperatures) and costs (cost of goods sold).

Figure 5 shows a blended analysis of modules being supplied today consisting of 72-cell p-mono PERC cells. We show here typical min/max power levels, all at standard test conditions (STC), noting that

Enhance your PERC Technology

Rear side polishing and selective emitter for more efficiency

more energy yield!

Expect Solutions.

SCHMID's Inline System for alkaline polishing improves your cell efficency by 0.1 %. It produces no nitrogen oxide and hence reaches a perfect back side at low cost. **Gain another 0.3 – 0.4 % cell efficiency** by using a selective emitter on the front side! The upgrade is done by simply integrating two machines: The SCHMID SE Jet that prints etch masks with high precision using inkjet technology and the SCHMID wet process machine for etching back the emitter and for stripping the wax. Contact us under pv@schmid-group.com and discover the difference!

www.schmid-group.com

SCHMID
Expect Solutions

power related temperature coefficients are largely aligned to historic c-Si variants (at approximately -0.4%/oC).

We have then forecasted the average power ratings from our control set of p-mono PERC module suppliers, by factoring in expected cell efficiency improvements out to the end of 2018. This provides the output down in Figure 5, with the average of 360W during 2018.

Upside to this exists from a stronger industry adoption of 156.75mm wafers, the full shift to five-busbar designs, and any other incremental improvements such as half-cut or singulated assembly designs. Collectively, these could see the average power levels move closer to 400W going into 2019.

Other factors to consider, aside from the SMSL grouping

While this article has focused specifically on the SMSL grouping of seven manufacturers (and module suppliers), the rest of the PV manufacturing community will play a key role in overall technology trends during 2017 and 2018. In this respect, however, we need to segment out these 200-300 manufacturers into various categories.

Importantly, many of the other c-Si companies outside the SMSL are operating today with very low capex, minimal research and development activity, and at best break-even company operations. Their scope to drive any change is almost negligible, and these companies typically follow the minimum requirements in order to stay competitive. Many of these company types are located in China or Taiwan. Much of the India-based manufacturing can be treated similarly to this, not to mention new capacity now located within Vietnam.

SunPower and REC Solar then form the main threat for alternate technology adoption benchmarking, although the cell capacity levels from these companies are well below those of the multiple gigawatts from most of the SMSL players.

The only other company supplying PV modules to the market that retains the scope to set a benchmark for c-Si companies is First Solar. This company has only recently announced one of the most aggressive technology roadmaps seen in the PV industry, moving from its Series 4 module CdTe technology ('2x4' size) to Series 6 sizes ('4x6'), at the same time as introducing further process flow enhancements. While the final module size from First Solar's Series 6 panels is marginally bigger than the 72-cell six-inch c-Si cell 'equivalent,' it is interesting to note that First Solar is targeting module powers (at STC) by the end of 2018 at (or above) the 400W level.

As we move into 2017, the companies making up the SMSL will start to announce capacity and technology plans for 2017, and this timing will overlap well with the PV CellTech meeting in Penang in March. All the topics discussed above will be reviewed and examined in further detail, with the chief technology officers (CTOs) and heads of R&D from the SMSL companies presenting on stage. Their thoughts will ultimately provide a reference point as to the accuracy of the two-year forecasting analysis outlined within this article.

Further information on PV CellTech 2017 is available at celltech.solarenergyevents.com

References

[1] Colville, F. 2016, "PV Manufacturing & Technology Quarterly", Solar Media Ltd.

About the Author

Finlay Colville is Head of Market Research at Solar Media Ltd, also the publisher of *PV Tech* and *Photovoltaics International.* Prior to this, Dr. Colville was Head of Solar at NPD Solarbuzz between 2010 and 2014. As the leading market analyst tracking PV manufacturing, technology and equipment spending trends, Dr. Colville has been active in the solar industry for more than a decade. Prior to NPD Solarbuzz, he held various senior sales and marketing positions at leading capital equipment supplier, Coherent Inc.

Fab & Facilities

News

Tesla picks Panasonic to operate SolarCity's 1GW Buffalo fab in major strategy shift

As part of the merger between Tesla and SolarCity, the electric car manufacturer has tentatively agreed with Japanese electronics firm Panasonic to begin solar cell and module production at SolarCity's Riverbend production plant in Buffalo, New York state, in 2017.

Panasonic is the main partner of Tesla in relation to its battery technology and production at its Gigafactory in Nevada.

Tesla intends to provide a long-term purchase commitment for solar cells from Panasonic. It also expects to use the cells and modules in a complete solar energy system that would be deployed with Tesla's Powerwall and Powerpack energy storage products.

The move by Tesla to team with Panasonic for PV modules raises significant doubts over SolarCity and its subsidiary Silevo's ability to execute on ramping the 1GW Riverbend facility in 2017.

Credit: SolarCity

The Tesla/SolarCity merger will see Panasonic produce solar cells and modules at SolarCity's Riverbend plant in New York State.

Silevo was acquired by SolarCity for its low-cost, high-efficiency cell technology and was expected to be driving the eventual ramp at the Riverbend facility. The move was designed to facilitate the aim of producing a significant percentage of its PV module needs internally in the US.

However, it remains unclear if Panasonic would produce its HIT cells or takeover production of Silevo's cell technology. Either way, delays in ramping the facility could be expected.

Job losses

SolarWorld to lay off 500 temporary manufacturing workers

Integrated PV manufacturer SolarWorld will lay off around 500 temporary manufacturing workers in the fourth quarter of this year due to significant PV module price declines on the world market.

The lay-offs, which started on 1 October, include 300 temporary workers at its facility in Freiburg and 200 in Arnstadt, but permanent staff will not be affected.

Milan Nitzschke, vice president at SolarWorld, said that the "elasticity" of demand is low in the solar market, which results in offers for prices below the cost of production. As a result, every manufacturer in the industry has to take action to adjust production.

SolarWorld, which had continued to hire more staff until a few weeks prior to the lay-offs, has to reduce manufacturing production in Q4 with "modest adjustments". In line with this, the firm will also have to reduce its workforce and lay off some temporary workers.

REC trims workforce by 3% but upgrades at Singapore production plant continue

Integrated PV module manufacturer REC Group has trimmed its global workforce by 3%, roughly 65 jobs out of approximately 2,200 employees.

Due to global solar market conditions, including significant price pressure on PV modules, REC, like several other leading manufacturers in the solar industry, has had to implement some organizational restructuring.

The company will continue the US$48 million in capital expenditure plans to upgrade all production at its manufacturing facility in Tuas, Singapore, to its half-cut PERC cell technology. This technology is used in its 'TwinPeak' series modules.

REC Silicon cuts more jobs and polysilicon production in second half of 2016

Polysilicon producer REC Silicon ASA has responded to weak demand seen in the third quarter of 2016 with 70 job cuts and a further curtailment of polysilicon production through the second half of the year.

Tore Torvund, CEO of REC Silicon said: "In order to maintain liquidity and manage inventory, the company is announcing additional cost cutting initiatives and has reduced production capacity utilization to approximately 50% at the Moses Lake facility. As part of the cost-cutting initiatives, the company is announcing a reduction in headcount of approximately 70 employees."

The polysilicon production cuts relate to third quarter 2016 revenue falling to US$50.9 million, compared to US$71.1 million in the previous quarter, which led to inventory build by 2,132MT.

Mission Solar closing n-type mono cell line with 87 job losses

US-based integrated PV manufacturer Mission Solar Energy will close its n-type mono solar cell line with the loss of 87 jobs and will focus on module assembly to remain competitive.

The San Antonio, Texas-based manufacturer recently launched four new PV modules, although two of the products were based on passive emitter rear contact (PERC) solar cells rather than n-type mono cells. Mission Solar's spokesperson confirmed the solar cell line closure, while the company would purchase cells from Asia to remain competitive.

Mission Solar Energy, formerly known as Nexolon America, a joint venture with Korean-owned OCI Solar Power and partner of Texas-based CPS Energy started n-type monocrystalline solar cell production in June 2014.

Canadian Solar cutting jobs at Ontario module assembly plant - reports

'Silicon Module Super League' (SMSL) member Canadian Solar has cut 130 manufacturing jobs at its PV module assembly plant in Guelph, Ontario.

The headcount reduction at the plant was due to a decline in demand for modules and increased competition as module prices have fallen.

The company recently revised its capacity expansion plans and failed

Credit: Meyer Burger

Meyer burger is streamlining its operations, resulting in around 250 job losses.

to highlight whether the previously announced plans to double (500MW) module assembly production at the Ontario plant, would proceed.

Canadian Solar, in reporting second quarter financial results, said that it expected global in-house module capacity to reach 5.8GW by the end of year, instead of previous guidance of 6.43GW.

Meyer Burger streamlining business with 16% workforce reduction

Leading PV manufacturing equipment supplier Meyer Burger Technology has announced a major restructuring plan to become more flexible to market dynamics by lowering its operating cost base by CHF50 million (US$40.5 million) per annum and reducing its workforce by around 16% by the end of 2016.

As a result of the streamlining, around 250 jobs would be lost with around 33% of the job losses at facilities in Thun, Switzerland, the company said.

Some of the job losses are expected to be made through early retirement schemes. The latest restructuring includes a focus on strengthening its strategic technology units with a focus on high-end solar user markets.

The company also plans to boost its global service business with a focus on key customers and applications. Meyer Burger's 'Technology and Production Centers' will also be further optimised via capacity adjustments in Asia.

Production

SunPower reducing IBC solar cell production capacity on competitive issues

High-efficiency PV module producer and project developer SunPower is to reduce the manufacturing capacity of its IBC solar cells that have the industry leading conversion efficiencies above 24%.

Restructuring strategies have already seen the company close its PV module assembly operations in the Philippines

and takeover its joint venture solar cell manufacturing operations in Malaysia from Taiwan-based former partner AUO.

The company cited PV module ASP declines of 25% in recent months, due to industry overcapacity and PV power plant PPA pricing pressure. As a result, its strategy includes mothballing an unspecified number of both solar cell and module manufacturing lines to match expected weaker demand in 2017.

Management inferred that its latest X-Series IBC cell capacity, produced at its 350MW Fab 4 in the Philippines, was not affected by the reduction in capacity; instead this would primarily relate to its second highest efficiency E-Series cell and module production.

Aleo Sunrise starts PERC solar cell production in Prenzlau, Germany

PV module manufacturer aleo Sunrise has started production of its 'CELCO' high-efficiency PERC solar cells at its production plant in Prenzlau, Germany.

Aleo Sunrise announced in September 2015 that it would add solar cell production at its module assembly plant. After nine months of construction and 'renovation' phases, its annual production capacity of the two production lines was 100MW.

The facility is capable of accommodating four production lines and 200MW of nameplate capacity. "We can produce three, four and five-busbar cells and thanks to the group's proven CELCO technology achieve average efficiencies above 21% in mass production," noted Alexander Kasic, head of cell production at aleo.

RenewSys opens 100MW cell line at Hyderabad production plant

India-based PV module and EVA encapsulant manufacturer RenewSys India Pvt Ltd has started ramping its 100MW highly automated multicrystalline solar cell line at its Hyderabad facility.

Deploying primarily European production equipment, German consultancy firm Solsol GmbH has helped in the commissioning of the line, which was first announced back in January 2016.

The decision to invest in solar cell production was based on the Indian Government policies that supported domestic manufacturing. RenewSys expects to increase both cell and module production further in 2017.

With the confidence that this support will be on-going, RenewSys intends to enhance its EVA/POE encapsulant and backsheet material capacity.

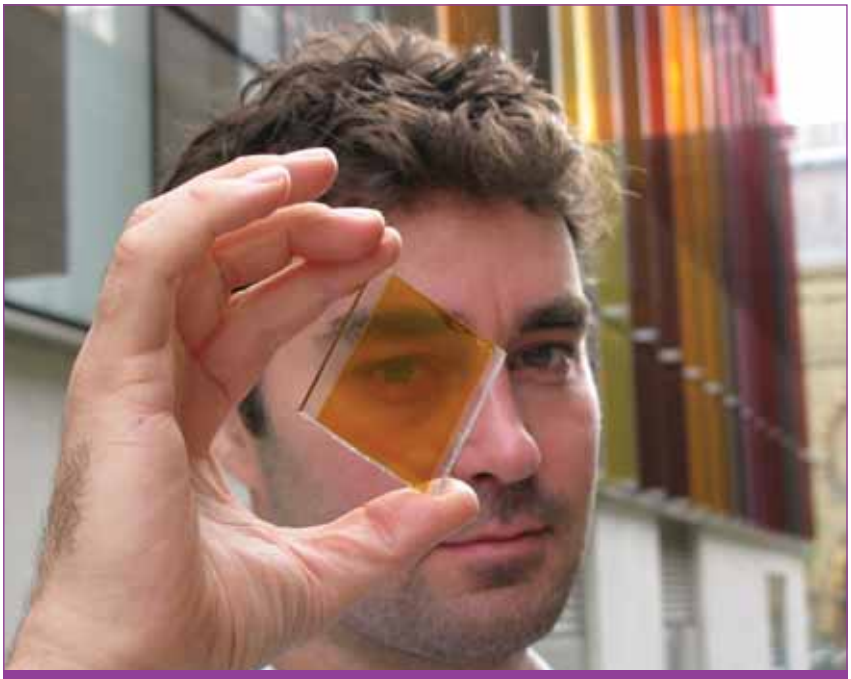

Credit Oxford PV

Perovskite producer Oxford PV has secured fresh investment for its IP licensing.

Company news

Bankruptcy court approves GCL-Poly's US$150 million bid for SunEdison's FBR polysilicon assets

Polysilicon and wafer producer GCL-Poly Energy Holding says the US bankruptcy court dealing with renewable energy firm SunEdison's Chapter 11 bankruptcy has approved the sale of its electronics-grade granular polysilicon produced with fluidized bed reactor (FBR) technology assets, primarily held by Korean-based production plant SMP.

GCL-Poly had previously placed a US$150 million bid for the FBR technology with a US$50 million deposit.

FBR technology potentially offers the lowest-cost polysilicon while achieving high purity levels close to those achieved with the dominant Siemens process used by the likes of GCL-Poly.

The Korean plant was initially built with a 10,00MT nameplate capacity but technical issues prevented the plant from entering volume production. GCL-Poly had previously attempted FBR production, but was believed to have also suffered technical issues. Only REC Silicon has a history of successful FBR volume production.

LDK Solar liquidation approved and buyer selected

Liquidation proceedings in the Cayman Islands and bankruptcy in mainland China for former integrated PV manufacturer LDK Solar have resulted in major creditor losses and its wafer and cell production operations being acquired.

Creditors were said to expect to lose around 80% of their investments in the company. However, instead of the expected acquisition of LDK Solar's assets, which included two idled polysilicon plants, wafer (4GW) and module assembly (1.5GW) capacity by SFCE, its wafer and module assets have been acquired by Henan Yicheng New Energy Co, which is a major supplier of wafer cutting materials.

It is not clear what the plans are for LDK Solar's manufacturing operations under publicly listed Yicheng New Energy and it remains unclear whether LDK Solar's idled polysilicon plants will secure a buyer.

Oxford PV garners more funding to avoid 'valley of death' commercialisation

Perovskite solar cell developer Oxford Photovoltaics has secured another round of funding to support its IP licensing business model.

This comes off the back of plans to produce working solar cells for customer evaluations after purchasing the former Bosch Solar CIS thin-film site in Brandenburg an der Havel, Germany.

It expects the facility to be operational within months. Staff recruitment has already begun, with the region's solar expertise a major attraction to the British start-up.

The latest funding amounts to £8.1 million (US$10.3 million) and follows a series C funding of £8.7 million. This funding was led by Statoil ASA, Legal & General Capital and an unidentified technology-focused, family fund investor.

MENA'S LEADING SOLAR TRADE EVENT

Providing international suppliers with direct access to thousands of the regional market's top project decision makers, influencers, utilities and government policy makers. Grow or introduce your business to the region, strengthen relationships with existing clients and make essential new connections.

For booking and more information
info@solarmiddleeast.ae
www.solarmiddleeast.ae

Discover more
www.energisingtheindustry.com

Brought to you by

MIDDLE EAST ELECTRICITY

SOLAR MIDDLE EAST

ENERGISING THE INDUSTRY

14 – 16 FEBRUARY 2017
DUBAI WORLD TRADE CENTRE, UAE

PV manufacturing capacity expansion announcement plans and analysis for Q3 2016

Mark Osborne, Senior News Editor, Photovoltaics International

ABSTRACT
In this quarterly report on global PV manufacturing capacity expansion announcements we cover the third quarter of 2016 and the month of October. The period under review is in stark contrast to the high level of activity seen in the first half of the year, marking a major slowdown in new announcements and fears of a new wave of overcapacity across the supply chain. This has already led to manufacturing underutilization, and line and plant closures with significant job losses.

July 2016

New capacity expansion plans in July amounted to only 20MW and were an update to plans already announced in 2016, by Malaysia-based solar cell producer, Tek Seng.

However, local news reports appeared in July indicating JA Solar planned to build a manufacturing plant in Vietnam in the same industrial park as OEM module producer, Boviet Solar. JA Solar deferred providing further information, while the local reports did not cite any nameplate capacity figures.

In the same month, TBEA SunOasis was reported to have signed agreements with the Egyptian government to build a 1GW PV power plant in the country that also included an unspecified integrated PV manufacturing plant. TBEA has not directly released any information on these plans.

Therefore, preliminary July expansion plans amount to only 20MW, the lowest monthly levels by a huge margin, since 2013.

August 2016

August fared little better than July. Announcements included 'tentative' plans (subject to government policy) by Taiwan-based solar cell producer, Inventec Solar Energy, to expand capacity from around 950MW to 1,600MW. However, tentative plans already existed to boost production to 1,450MW in 2016. Local news reports cited a number of countries outside Taiwan where the expansions may take place.

Local reports also appeared in Oman, regarding a PV project developer, Nafath Renewable Energy, considering establishing a PV module assembly plant in the country, although no further information was provided.

The significant decline in new capacity expansion plans in the last two months follows a downward trend that started in May 2016. That month marks a key point in time for global PV manufacturing capacity expansion announcements as they revealed only 4.04GW of total new plans and a significant slowdown of over 58%, compared to the previous month.

The month of June confirmed a second consecutive month of announcement declines, with a total of 3.52GW of planned expansions unveiled, around a 12% decline from the previous month.

Canadian Solar revises capacity expansion plans

August was also noteworthy as 'Silicon Module Super League' (SMSL) member Canadian Solar made a third major revision to its planned manufacturing capacity expansion plans for 2016, while reiterating previously guided PV module shipments and revenue for the year.

Canadian Solar said it was revising its cell manufacturing nameplate capacity expectations for the end of the year, primarily due to the impact of tornado damage at its JV solar cell factory in Funing County, Jiangsu Province, on 23 June 2016.

The Funing facility will be out of action until the first quarter of 2017, with volume production back online in the second quarter. The Funing plant would have added a further 500MW of capacity by July 2016 to reach a nameplate capacity of 1GW.

As a result, Canadian Solar expects in-house cell capacity to reach around 3.05GW by the end of 2016, compared to the last revision expectation of 3.9GW.

Cell expansions of 850MW are going ahead via a new cell manufacturing plant located in an unspecified location in Southeast Asia, which the company said at the time was due to be commissioned in September of 2016. Interestingly, the

Credit JA Solar

JA Solar was one of the few leading module suppliers to announce any significant capacity expansions in the third quarter of 2016.

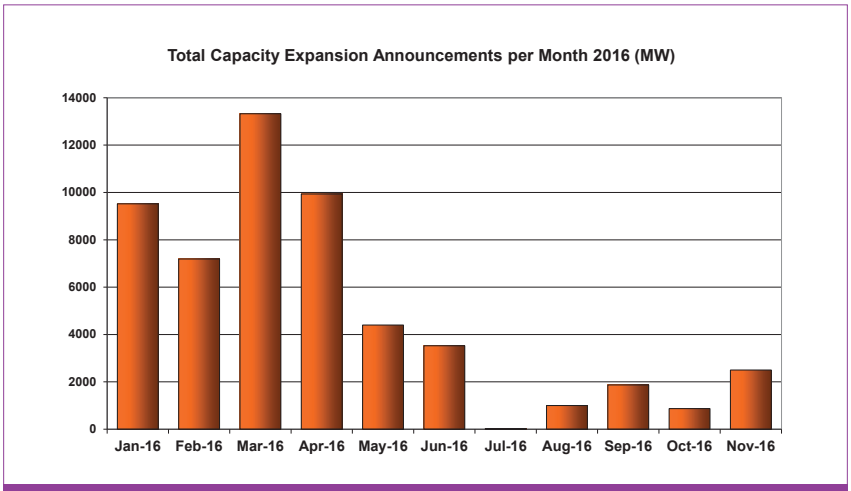

Total monthly capacity announcements, July to October 2016.

nameplate capacity at the Southeast Asia cell plant has been increased twice. Initially, Canadian Solar said that plant would have a nameplate capacity of 500MW, yet that was later raised to 700MW.

However, Canadian Solar also noted that it would be curtailing PV module capacity expansions due to the threat of overcapacity, increased ASP declines and an overall industry downturn. Management noted that keeping strong control of module inventory would be a key strategy during this period.

Canadian Solar said that it expected in-house module capacity to reach 5.8GW by the end of year, instead of previous guidance of 6.43GW. Our analysis puts the company's module assembly capacity at 6.4-6.6GW at year-end.

Capacity expansions that have continued include its new 650MW module assembly plant at an unspecified location in in Southeast Asia, which Canadian Solar said been commissioned in early August 2016. Again, this would seem to be a capacity increase of around 50MW from the previously stated 600MW, based on previous management commentary and PV Tech's analysis.

A new JV assembly plant on Brazil with an initial 360MW of nameplate capacity was also expected to be commissioned in September of 2016, providing the remaining majority of expansions. Again, this would seem to be a capacity increase of around 60MW more than previously guided.

Based on Canadian Solar's expected module capacity by the end of 2016, only around 460MW of module assembly capacity would seem to have been added at its facilities in Suzhou, Jiangsu Province, and Luoyang, Henan Province. Various module assembly expansion plans previously announced, such as in Vietnam (300MW) and Indonesia (30MW), were not updated.

September recovery of sorts

September's analysis indicates a small recovery from the July and August lows, yet the key module assembly expansion plans (1.5GW) announced by India-based Vikram Solar are spread out through to 2019, indicating a cautious approach characteristic of the company, with previous expansion announcements (250MW) made in May 2015 and completed in 2016.

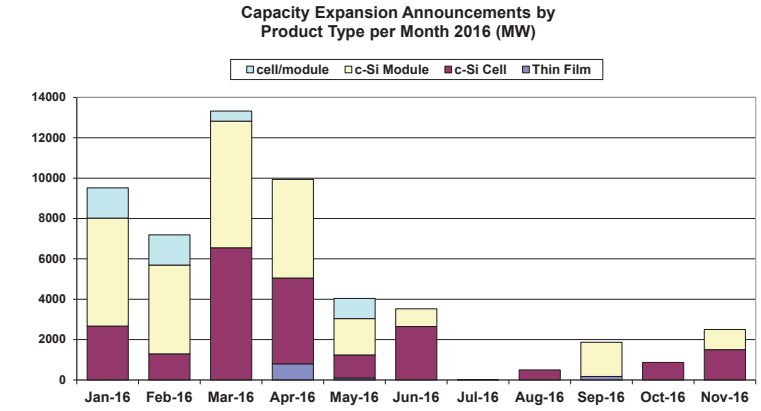

Capacity expansion announcements by product type monthly, July to October 2016.

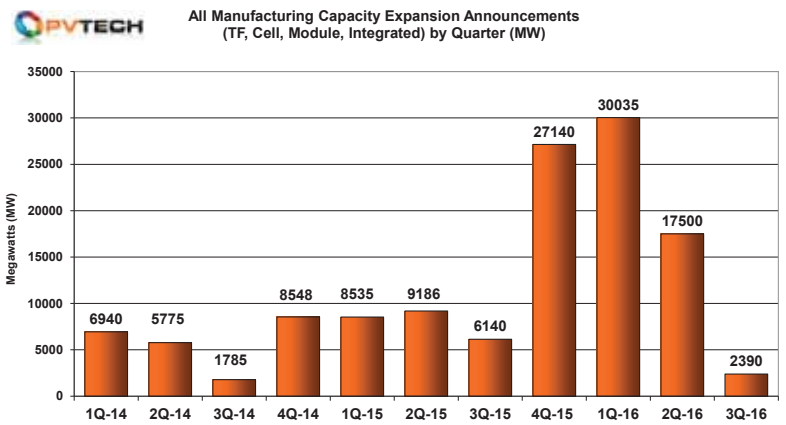

Total manufacturing capacity expansion announcements in Q3 2016

Q3 2016 Analysis

The analysis of global PV manufacturing capacity expansion plans in the third quarter of 2016 highlights an absence of China-based solar cell and module manufacturers making new announcements for either domestic or overseas production.

Considering a total of over 13GW of combined (thin-film, cell, module and integrated) capacity expansions had been announced for China in the first half of 2016, the absence of China-based announcements in the third quarter of the year is noteworthy.

The significant curtailment in expansion plans mirrored the beginning of weak end-market demand in China, overcapacity warnings and plummeting average selling prices (ASPs) across the supply chain.

Curtailment was quickly followed by the start of manufacturing restructuring and consolidation, resulting in job losses that reached over 2,500 at the end of the third quarter of 2016, according to ongoing analysis.

High-efficiency PV module producer and project developer SunPower was the first to react to the changing industry landscape in August with the closure of its module assembly plant in the Philippines and the relocation of production tools to its Mexican facility with the loss of around 1,000 jobs.

This was later followed by the company acquiring AUO's portion of the two companies' joint-venture solar cell facility in Melaka, Malaysia.

Canadian Solar confirmed in second quarter financial results its lower in-house module capacity of 5.8 rather than 6.43GW. This was then followed by confirmed reports of 130 manufacturing job losses at its PV module assembly plant in Guelph, Ontario.

Integrated PV module manufacturer SolarWorld also announced the loss of 500 'temporary' workers at its three manufacturing facilities in Germany, while Taiwan-based solar cell and module manufacturer Motech Industries announced job losses of 200.

Other producers trimming headcount include Malaysia-based solar cell producer TS Solartech, Singapore-based REC Group and US-based Mission Solar, which recently announced with 87 job losses the closure of its 200MW solar cell manufacturing lines.

Combined capacity expansion announcements in the third quarter of 2016 reached only around 2.4GW, driven primarily by 1.7GW of module assembly plans, 520MW of solar cell plans and 170MW of CIGS thin-film plans.

It should also be noted that Vikram Solar accounted for the majority of module assembly expansion plans in September, which only totalled 1.7GW.

Bucking a four-month trend, September also saw the revival of some activity in the thin-film segment. Germany-based OPC flexible thin-film producer Heliatek announced the equivalent of around a 140MW expansion with a major investment round.

However, preliminary analysis indicates that no new solar cell or integrated cell and module manufacturing expansion plans were announced in September.

October

Global PV manufacturing capacity expansion plans in October reflected the continued reaction to the rapid descent into overcapacity at the beginning of the second half of the year. Total new planned capacity expansions in October reached 870MW from only two PV manufacturers, JA Solar and Suniva.

The 870MW plans only relate to solar cell expansions, indicating that no thin-film, dedicated module assembly or integrated cell/module expansions were reported in October.

SMSL member JA Solar said it was expanding capacity at its solar cell plant in Malaysia from 400MW initial nameplate capacity to 1GW. The plant was initiated in the first quarter of 2015 and started ramping in the fourth quarter of 2015.

JA Solar has been one of the fastest growing SMSL members in recent years but lagged behind in having either solar cell or module assembly production outside of China, unlike some of its rivals. The company has also had little penetration of the US market, with the smallest share in the US, by a wide margin compared to its SMSL rivals. The initiation of anti-dumping duties had prevented further market traction.

As its capacity expansions in recent years have matched its overall market share gains, the Malaysian plant is therefore central to its US ambitions as well as circumventing US anti-dumping duties. Recently, JA Solar also left the European Union's minimum import price arrangement imposed under anti-dumping measures, as the Malaysian plant also circumvents these duties.

JA Solar doubled module shipments to the US in the second quarter of

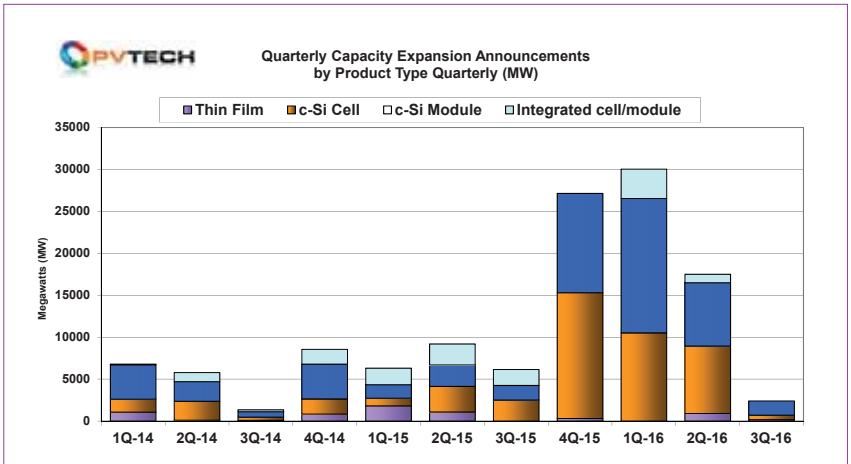

Quarterly capacity expansion announcements by product type in Q3 2016

2016 to 105MW, representing 9% of total shipments in the quarter, while Europe represented 3.7% of shipments. Therefore, the Malaysian cell plant expansion should not come as a surprise, despite the current levels of global overcapacity. However, the Malaysian expansion is using previously upgraded cell lines from China.

Meanwhile, US-based PV manufacturer Suniva, majority owned by China-based Shunfeng International Clean Energy (SFCE), had expanded cell and module capacity from 200MW in 2014 to 430MW in the third quarter of 2016.

In similar circumstances to JA Solar, SFCE had little US market presence, despite its best efforts, and anti-dumping duties were a barrier to market re-entry. As the Suniva expansion came on stream, reports indicated that SFCE was planning a further expansion to 700MW by mid-2017.

On a geographical basis, October expansion plans further highlight the lack of expansion plans in China, last reported back in June 2016, equating to a four-month lapse.

Although Suniva's completed expansion and future plans are good for manufacturing in the US, recent news that Mission Solar was permanently shutting its 200MW in-house solar cell plant in Texas essentially negates the small growth in the PV manufacturing base in the US.

The four months of the second half of 2016 have so far generated only 3,260MW of new capacity expansion announcements, compared to almost 40GW reported for the first four months of the year.

Conclusion

The PV manufacturing landscape has changed considerably in 2016, clearly pointing to a year of contrasting halves. Although a number of companies have reacted quickly to the changing landscape and new capacity expansion announcements have almost stopped, with total global expansion plans in the first half of 2016 having exceeded 47.53GW – almost as much as the total for 2015 – more push-outs and cancellations will clearly be required to bring end-market demand in line with effective capacity.

Penang, Malaysia | 14-15 March 2017 | #PVCELLTECH

SAVE 10% WITH CODE PVI

CONFERENCE PVCELLTECH

Now it's in second year after a sell-out inaugural conference PV Celltech is already established as the leading c-Si cell manufacturing and processing event of the year, don't miss it!

TESTIMONIALS

"The PVCellTech conference was a **fantastic opportunity** to discuss PV manufacturing issues, opportunities and prospects with key players and prepare this industry for the TW level."
Dr. Pierre Verlinden, PhD VP, Chief Scientist and Vice-Chair of State Key Lab (PVST) Technology Dept, **Trina Solar**

"A very well organised event with **impressive selection of speakers** and topics covered."
Stuart Wenham, Centre Director, **UNSW**

"Truly a **phenomenal opportunity** to imbibe the latest cutting edge, real time & in the near future, technical developments at all Global Tier 1 PV Manufacturers." **Paul Gupta,** Managing Director, **Indosolar India**

"It was **absolutely amazing** to me to see such a good conference with outstanding talks along with a networking opportunity with all the most important experts who are driving and dominating the PV industry."
Dr. Christian Buchner, Vice President | Business Unit PV, **SCHMID Group**

"It was truly **one of the best PV conferences** I have participated in."
Homer Antoniadis, CTO, **DuPont Photovoltaic Solutions**

"This was an **outstanding and worthwhile** event." **Peter Cousins,** VP R&D, **SunPower**

"This is **hands down the most valuable conference t**o learn about, and interact with, the photovoltaic industry."
Malcolm Abbott, Director, **PV Lighthouse**

"PVCell tech is really the **grand meeting for technology leaders.**"
Carl Yang, Technical Marketing Manager, **JA solar**

Sponsors:

ASM | ae · Besi · DUPONT · h.a.l.m. · HORIBA · INDEOtec · MacDermid Enthone · MEYER BURGER · MIDA · SCHMID · VITRONIC

celltech.solarenergyevents.com

To get involved either as a speaker, partner or attendee please email: **marketing@solarmedia.co.uk**

PVTECH · Photovoltaics International · SOLAR MEDIA

Materials

34

Dominic C. Walter[1], Thomas Pernau[2] & Jan Schmidt[1,3]

[1]Institute for Solar Energy Research Hamelin (ISFH), Emmerthal; [2]centrotherm photovoltaics, Blaubeuren; [3]Department of Solar Energy, Institute of Solid-State Physics, Leibniz Universität Hannover, Germany

News

Perpetual polysilicon overcapacity to hit producers - Bernreuter Research

Wacker Chemie

Polysilicon producers are facing perpetual overcapacity conditions.

Specialist polysilicon market research firm, Bernreuter Research has warned of continued overcapacity that will force pricing down below many producers' cash cost levels and threatens the existence of high-cost producers in 2018.

"Slowing demand from the photovoltaic industry on the one hand and increasing production capacities on the other will cause turmoil on the polysilicon market," noted Johannes Bernreuter, head of Bernreuter Research.

According to the latest Bernreuter report, 'The Polysilicon Market Outlook 2020', polysilicon spot prices are expected to decline from more than US$14/kg currently to below US$12/kg in 2018, as the supply of polysilicon has increased more rapidly than demand from the PV industry, which consumes approximately 90% of polysilicon produced worldwide.

Bernreuter highlighted that global polysilicon production output went from 313,000MT in 2014 to 363,000MT in 2015, which drove the spot price down to a record low of US$12.93/kg in January 2016.

"Only the massive Chinese PV installation rally in the first half of 2016 saved the polysilicon industry from even more serious oversupply," noted Bernreuter.

Major issues are ahead as new polysilicon capacity of around 141,000MT is expected to come on stream between 2017 and 2019, with around 70% located in China. The disparity between supply and demand is expected to result in strong cut-throat competition that could lead to six or more producers exiting the sector in this timeframe.

Production

HIUV completes PV encapsulant expansion to 10GW

PV module encapsulant producer Shanghai HIUV New Materials Co (HIUV) has completed the expansion of its production capacity to 130 million m² or 10GW.

HIUV said that an extra 12 encapsulant production extrusion lines were installed at the end of August, bringing the number of high-speed lines in production to 24.

The expansions were primarily undertaken in partnership under joint venture agreements with customers. Min Li, HIUV CEO said the company would also pursue international markets and support further production expansions with JV partners in 2017.

The company has also listed in BOM (balance of materials) approved suppliers for a number of downstream PV power project developers such as Sino-Elec Power Group, CECEP Solar and CLP.

GCL-Poly's polysilicon and wafer production down in Q3

Leading polysilicon and wafer producer GCL-Poly reported a 15% cut in production of polysilicon in the third quarter of 2016, compared to the prior-year period, due to weak China end-market demand.

GCL-Poly said in its third-quarter business performance report that it produced 16,160MT of polysilicon, representing a decrease of approximately 15% compared with 19,003MT over the same period of last year and down around 10.6% (18,078MT) from the previous quarter.

External polysilicon sales in the quarter were approximately 1,398MT, representing a 70.0% decrease compared with 4,653MT over the same period of last year. External polysilicon sales fell 54%, quarter-on-quarter.

Polysilicon production volume for the first three quarters of 2016 was approximately 52,488MT, representing a decrease of approximately 5.9% compared with 55,771MT over the same period of last year.

External polysilicon sales were approximately 7,787 MT of polysilicon for the first three quarters of 2016, representing a decrease of approximately 33.2% compared with 11,658 MT over the same period of last year.

Overall polysilicon production capacity remains at 70,000MT on an annual basis.

LONGi Silicon's sales dive 54.8% in Q3

Leading integrated monocrystalline PV manufacturer Xi'an LONGi Silicon Materials has reported a 54.8% decline in third quarter 2016 revenue as the impact of a major demand slump in China after June's feed-in tariff changes seriously curtailed PV power plant construction in China.

LONGi Silicon reported unaudited third quarter 2016 revenue of around US$290 million, compared to around US$642 million in the previous quarter, a 54.8% decline, quarter-on-quarter, the peak in downstream PV demand in China through the first nine months of the year.

The significant decline in LONGi's third quarter revenue could be viewed as a benchmark for China-based PV manufacturers that have a major domestic market position.

LONGi Silicon reported unaudited revenue for the first nine months of 2016 of around US$1.26 billion, up 204% from the prior year period.

Daqo cites strong polysilicon and wafer demand recovery since October

China-based polysilicon and wafer producer Daqo New Energy reported third quarter 2016 financial results

that characterized the abrupt demand slowdown from PV manufacturers at the beginning of the quarter but cited a strong rebound in demand since October.

Daqo New Energy said it suffered a significant slowdown in demand in the third quarter, which resulted in polysilicon ASPs declining to US$15.64/kg from US$17.24/kg in the previous quarter.

Solar wafer sales volume plummeted to 14.4 million pieces, compared to 25.0 million pieces in the second quarter of 2016. As a result, Daqo reported total revenue of US$54.3 million in the quarter, compared to US$71.0 million in the second quarter of 2016.

Revenues from polysilicon sales to external customers were US$44.4 million, compared to US$50.5 million in the second quarter of 2016. External sales volume was 2,838MT in the third quarter of 2016, compared to 2,931MT in the second quarter of 2016.

Daqo had planned to undertake annual maintenance and certain upgrades to facilities in the quarter, which would have partially limited polysilicon output in the quarter. However, the company noted that delayed component deliveries meant the work did not start until late September and did not resume to full capacity until early November,

Revenues from wafer sales in the quarter were US$9.9 million, compared to US$20.5 million in the second quarter of 2016.

The decline in ASPs was said to have resulted in some rival polysilicon producers cutting production.

Solargiga's monocrystalline product sales and shipments sink in Q3

Integrated China-based monocrystalline PV producer, Solargiga Energy Holdings has reported certain unaudited operating figures for the third quarter of 2016, indicating a significant revenue and shipment decline, compared to the previous quarter.

Solargiga reported total preliminary third quarter 2016 revenue of around RMB 687 million (US$102 million), down over 24% (US$134.5) million from the previous quarter.

Revenue for the first nine months of 2016 was RMB2,410 million (US$357.5 million), up 23.5% (US$289.4 million) from the prior-year period.

Total product shipments, which included processing service, sales of silicon solar ingots, wafers, cells and photovoltaic modules and the engineering, procurement and construction of photovoltaic systems service reached 376MW in the third quarter, down around 15% from the previous quarter when shipments reached 442MW.

Shipments in the first nine months of 2016 reached 1,125.5MW, up from 763.9MW in the prior year period, a 47.3% increase from the prior year period.

Company news

JA Solar agrees to accept polysilicon supply contract with Hemlock in lawsuit settlement

Chinese module manufacturer JA Solar has agreed to settle a long-term 'take or pay' contract for the purchase of polysilicon from US-based polysilicon producer Hemlock Semiconductor.

In April Hemlock Semiconductor filed a suit against JA Solar for non-compliance with the supply contract signed in 2011 and sought damages totalling up to US$921.1 million from JA Solar.

Hemlock Semiconductor has previously filed a similar law suit against SolarWorld's former subsidiary, Deutsche Solar for breaching a 'take or pay' contract as well as against Japanese module producer Kyocera.

Under the deal, JA Solar, its holding company, JA Solar (BVI) Limited, and its manufacturing subsidiary, JA Solar Yangzhou, have entered into a new long-term polysilicon supply agreement with Hemlock Operations on a quarterly basis until 31 October 2026. Terms of the deal were not disclosed.

However, due to anti-dumping duties imposed on Hemlock in China, direct supply to JA Solar's manufacturing operations is highly unlikely, impacting production costs and making JA Solar uncompetitive.

Although JA Solar has established solar cell and module manufacturing operations outside China, in-house wafer production remains in China.

GT Advanced Technologies appoints new CEO

Crystal growth equipment supplier GT Advanced Technologies (GTAT) said it had accepted the resignation of CEO, Dave Keck (pictured) and appointed board member and former employee, Greg Knight as its new CEO.

GTAT did not say why Keck had resigned his position within the company.

"The solar industry is at an inflection point, where significant cost-down opportunities have reached their limits and the market needs technologies that deliver ever greater efficiency," said Knight. "GT's unique positioning in photovoltaics presents a number of exciting opportunities to work with our world-class roster of customers and partners to drive the necessary technical innovation in solar and to generate significant growth for the company."

Knight had been the director of process engineering at GT Solar before the company changed its name to GTAT and started his solar industry career at in 2002 at Schott Solar, where he was the manufacturing director for solar cell fabrication and silicon wafer fabrication.

Peter Pauli stepping down as CEO of Meyer Burger as part of major reshuffle

Leading PV manufacturing equipment supplier Meyer Burger Technology has made some major made changes to its senior management and plans for new board directors, led by the stepping down of CEO for 14 years, Peter Pauli.

Pauli stepped down from the board of directors of Meyer Burger on 2 December 2016 but will remain available to the board and the new CEO in a consulting role. The role is expected to be supporting major customer relationships.

Alexander Vogel, designated chairman of the board, said: "Peter Pauli has led the company as CEO for the past 14 years and has made a very significant contribution to building Meyer Burger into a globally recognised market and technology leader in the photovoltaic industry. We sincerely thank him for his deep commitment which was exemplary and very impressive."

The new CEO, effective 1 January 2017 will be Hans Brändle, previously the CEO of Oerlikon Coating, which notably focused on PVD and PECVD technologies that are now being used in the solar industry for PERC and heterojunction cells.

Meyer Burger

Peter Pauli is stepping down as Meyer Burger's CEO after 14 years in the post.

Ultrafast lifetime regeneration of boron-doped Czochralski-silicon in an industrial belt-line furnace

Dominic C. Walter[1], **Thomas Pernau**[2] & **Jan Schmidt**[1,3]

[1]Institute for Solar Energy Research Hamelin (ISFH), Emmerthal; [2]centrotherm photovoltaics, Blaubeuren; [3]Department of Solar Energy, Institute of Solid-State Physics, Leibniz Universität Hannover, Germany

ABSTRACT

Solar cells made of boron-doped, oxygen-rich Czochralski-grown silicon (Cz-Si) wafers suffer degraded efficiency when illuminated, an effect sometimes labelled *light-induced degradation (LID)*. This is caused by a specific defect centre within the silicon bulk, often referred to as a *BO defect*, which activates its recombination properties under illumination, leading to a degradation in carrier lifetime. However, the BO defect centre can be permanently deactivated, and the lifetime permanently recovered, by illumination at an *elevated* temperature. In this paper the focus is on transferring ISFH's lab-type BO deactivation process to an ultrafast high-throughput process, employing an industrial-type belt furnace especially designed by centrotherm photovoltaics AG for this very purpose. By using this industrial furnace, inline regeneration in a solar cell production line becomes feasible. The investigations clearly demonstrate that the industrial belt furnace is well suited to permanently deactivating the BO complex; in addition, excellent stability of the lifetimes after regeneration is demonstrated.

Introduction

In boron-doped oxygen-rich Czochralski-grown silicon (Cz-Si), illumination – or, more generally, the injection of excess carriers – leads to a degradation in the carrier lifetime [1], a phenomenon sometimes labelled *light-induced degradation (LID)*. This lifetime degradation can strongly affect the conversion efficiency of silicon solar cells fabricated on Cz-Si wafers, and may lead to a severe degradation in efficiency of up to 10%$_{rel.}$ [2]. A multiplicity of studies have been carried out to identify the defect responsible for the lifetime degradation [3,4], and it has been concluded that the simultaneous presence of boron (B) and oxygen (O) in the silicon material is directly related to the magnitude of the degradation [5]; hence, the corresponding defect centre is often referred to as a *BO defect*.

> "BO defects can be permanently deactivated under illumination at elevated temperatures."

For a decade it has been known that BO defects can be permanently deactivated under illumination at elevated temperatures [6]. Naturally, this deactivation is accompanied by a permanent recovery in carrier lifetime. After this recovery process, the lifetime shows no (or only very weak) degradation upon illumination at room temperature as well as at typical module operation temperatures [7]. This paper discusses the transfer of ISFH's lab-type deactivation process to an ultrafast high-throughput process, employing an industrial-type belt furnace [8] especially designed for this very purpose by centrotherm photovoltaics AG. ISFH's lab-type deactivation process, using a hotplate and a halogen lamp, is transferred to the belt furnace, which enables inline regeneration to be implemented in solar cell production lines.

Inline regeneration in the C.REG 6.200

For the study reported in this paper, the C.REG 6.200 industrial-type inline regeneration belt furnace [8] from centrotherm photovoltaics, shown in Fig. 1, was used to regenerate the lifetime of Cz-Si samples of various resistivities. Within the C.REG 6.200 tool, the belt speed, temperature and illumination intensity were varied, defining four different processes referred to as P1–P4. A value of 8 or 9m/min was chosen for the belt speed, while the regeneration temperature was varied up to either 237°C or 256°C,

Figure 1. The C.REG 6.200 inline regeneration tool from centrotherm used in this investigation, which is suitable for solar cell production lines.

measured directly on the lifetime samples. The illumination intensity was set at either 100% or 90% of the maximum possible intensity within the regeneration zones. The details of the different processes are summarized in Table 1.

The belt furnace exposes the samples for approximately 32s to the deactivation conditions. The lifetimes are measured on four different materials directly after the regeneration process; the results are shown in Fig. 2. Sample processing included a phosphorus diffusion, subsequent removal of the phosphorus-diffused regions, passivation of both surfaces with Al_2O_3/SiN_x stacks, and a fast-firing step in a centrotherm belt-firing furnace. (More details about the exact sample processing have been reported elsewhere [9].) After the inline regeneration in the C.REG 6.200, the lifetimes measured on the different materials were independent of the applied process and also independent of the doping concentration at a lifetime level of $\tau_{0p} \approx 450\mu s$, measured at a fixed injection level of 1/10. Before the regeneration process was applied, the lifetimes after complete degradation indicate, as expected, a pronounced dependence on the base resistivity of the Cz-Si materials.

For float-zone silicon (FZ-Si) reference wafers, processed in parallel, with a base resistivity of 1.2Ω·cm, a lifetime of τ_{0p} = 920±160µs on average was measured after the belt furnace regeneration process, compared with a value τ = 1,600±180µs measured before the C.REG 6.200 process was applied. The decrease in lifetimes of the FZ-Si samples indicates that the surface passivation quality suffered slightly under the regeneration conditions applied in the belt furnace (i.e. high illumination intensity at increased temperature).

According to Sproul [10], the surface recombination velocity S can be calculated for sufficiently low surface recombination velocities from the equation:

$$S = \frac{W}{2} \times \left(\frac{1}{\tau} - \frac{1}{\tau_{int}} \right) \quad (1)$$

where W = sample thickness, τ = measured effective lifetime and τ_{int} = intrinsic lifetime. Inserting the corresponding values for the FZ-Si reference samples results in an average surface recombination velocity of S = 17.4cm/s after application of the inline regeneration process. When this S value is used, the observed independence of the lifetime of

	Illumination intensity (zones 1–4) [%]	Belt speed [m/min]	Temperature (set) [°C]
P1	100, 100, 100, 100	9	270
P2	90, 90, 90, 90	8	270
P3	100, 100, 100, 30	9	300
P4	90, 90, 90, 30	8	300

Table 1. Details of the regeneration processes P1–P4 investigated in this study.

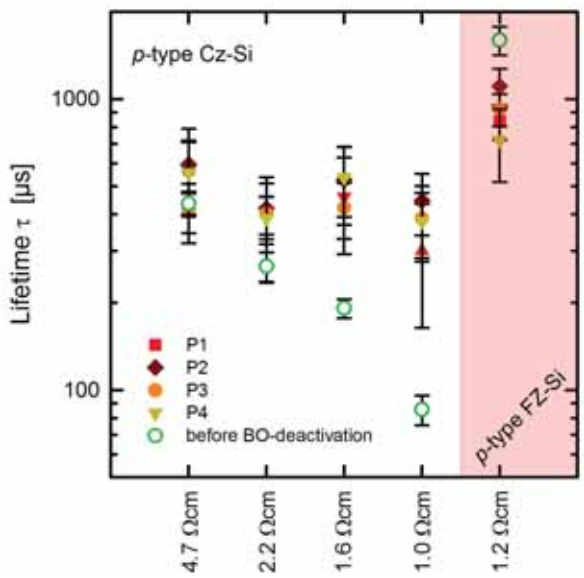

Figure 2. Lifetime τ measured for four different Cz-Si materials in this investigation. Before BO deactivation (open green circles), a clear dependence on the base resistivity can be observed. After BO deactivation (filled coloured symbols) the measured lifetimes are independent of the base material and also independent of the applied process. On the far right, the lifetimes measured for FZ-Si references, processed in parallel, are also shown.

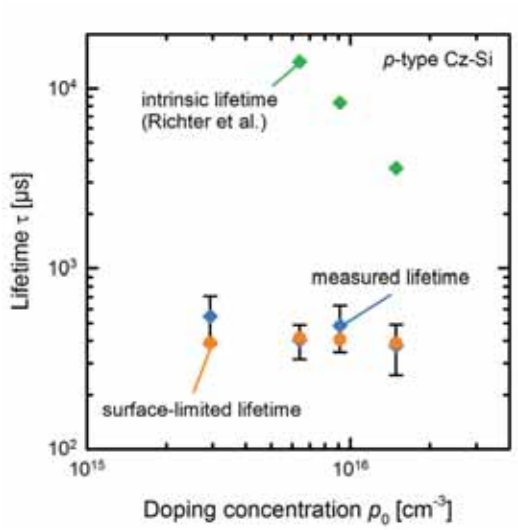

Figure 3. Measured effective lifetime τ of process P2 (blue diamonds) as a function of the doping concentration p_0. The green diamonds represent the intrinsic lifetime limit according to Richter et al. [11], while the orange circles show the calculated surface-limited lifetime using Equation 1, including the intrinsic lifetime limit and the surface recombination velocity of S = 17.4cm/s. The surface-limited lifetime is around the same level as the measured effective lifetime, indicating that the measured lifetimes are entirely limited by surface recombination.

the Cz-Si samples from the doping concentration can be consistently explained.

Fig. 3 shows a plot of the lifetime measured after process P2 versus the doping concentration of the base material; for comparison, the intrinsic lifetime limit according to the most accurate parameterization by Richter et al. [11] is also displayed. Using these values, as well as the measured thicknesses of the Cz-Si samples under investigation and the determined surface recombination velocity, we can calculate an expected effective lifetime, assuming that the measured lifetime is dominated by surface recombination (orange circles in Fig. 3). As can be seen from Fig. 3, the expected lifetime does not depend on the doping concentration p_0. As the actual measured lifetime is around the same level as the expected surface-limited lifetime, it is concluded that the lifetime after the belt furnace regeneration process is mainly limited by the surface recombination. Hence, the lifetime within the Cz-Si bulk is much larger than the measured effective lifetime, proving that the permanent deactivation of the BO defect centre was indeed successful.

Note that photoluminescence (PL) images of the samples under investigation showed features which might originate from scratches introduced to the surface either by sample handling before the regeneration process or by the metal belt within the furnace. This suggests that the reduction in surface passivation quality is not expected to limit the conversion efficiency of solar cells treated in the furnace if the solar cell is fully metallized on the rear side. In fact, the inline regeneration of Cz-Si solar cells using the C.REG 6.200 reduces LID by up to 80%$_{rel.}$ compared with the fully degraded state when no regeneration is employed.

"The inline regeneration of Cz-Si solar cells using the C.REG 6.200 reduces LID by up to 80%$_{rel.}$"

Lifetime stability

Although the surface recombination velocity S seems to be lower after the inline industrial-type regenerator processing, lifetime investigations show that the passivation quality is stable upon further illumination at room temperature.

The stability of the lifetime after the regeneration process was examined by exposing the lifetime samples to a light intensity of 0.1 suns at room temperature. In Fig. 4, the measured lifetime is plotted versus the illumination time after regeneration for four groups of different Cz-Si materials which have been regenerated in the inline furnace using process P2. Only one sample (with the highest measured lifetime) from each group (consisting of five samples) is shown. However, note that all samples from the same material group demonstrate the same trend for the evolution of the lifetime after regeneration.

As can be seen in Fig. 4(a), the

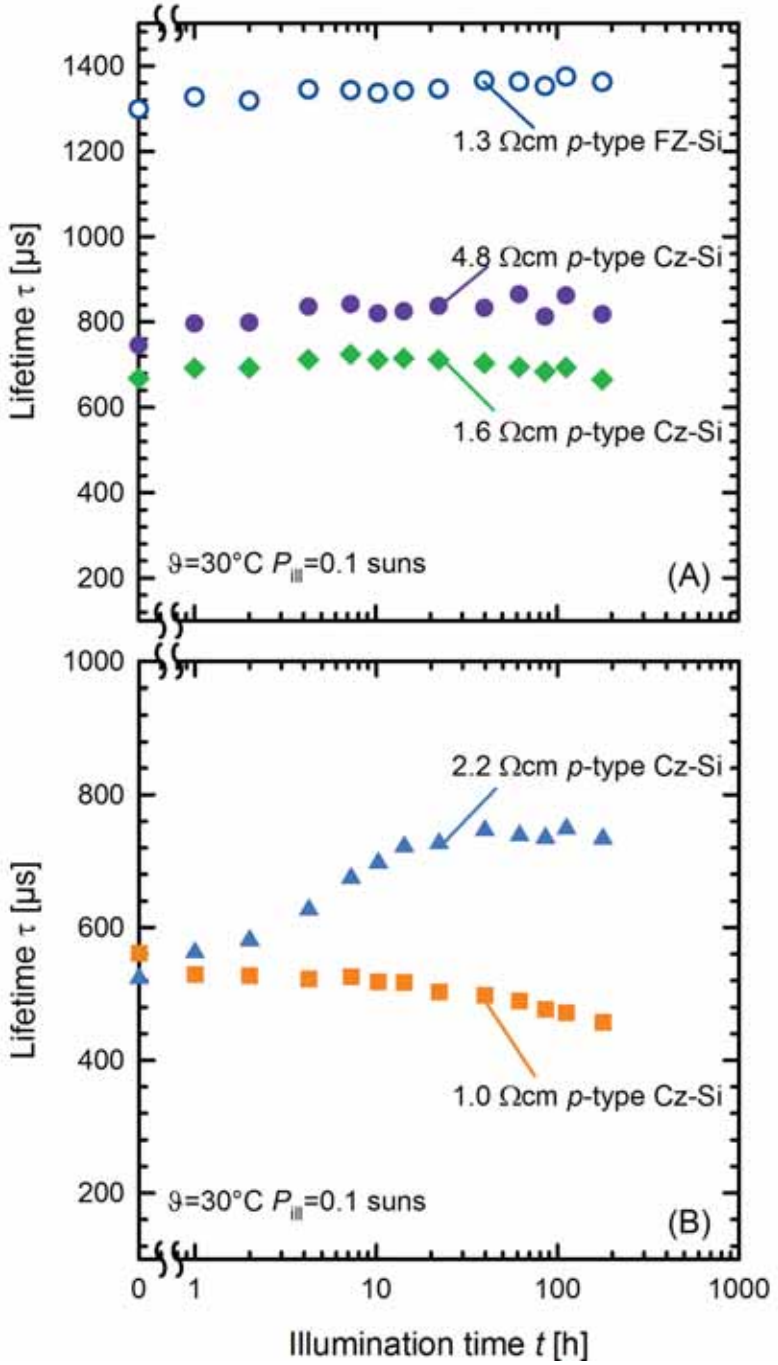

Figure 4. Lifetime τ as a function of illumination time t at room temperature, with exposure to 0.1 suns light intensity, for four Cz-Si materials treated using process P2: (a) two examples of Cz-Si materials featuring a stable lifetime after regeneration; (b) two examples of Cz-Si materials with varying lifetimes. The FZ-Si reference sample in (a) features a stable lifetime.

lifetimes of some Cz-Si materials, in this case with base resistivities of 1.6 and 4.8Ω·cm, are extremely stable upon illumination at room temperature. However, the lifetime of some other materials, specifically the 1.0Ω·cm sample, degrades slightly, while the lifetime of the 2.2Ω·cm material actually increases, as observed in Fig. 4(b).

These essentially different lifetime evolutions can be attributed to different background defects, which are expected to be present within the different Cz-Si materials and which limit the lifetime to a value usually below that for defect-lean FZ-Si. Although the detailed nature of these defects is as yet unknown, it is very likely that they are not related to the BO defect which causes the typical LID in boron-doped Cz-Si, because (for example) no clear trend depending on the boron concentration is observed. Further experiments are therefore necessary with regard to investigating the lifetime-limiting defects once the limitation due to a BO defect has been overcome. However, the recombination activity for these defects is much lower than that for a BO defect, and hence the efficiency potential is greatly enhanced after the inline regeneration process has been performed.

Figure 5. The c.FIRE REG inline integrated fast-firing and regeneration tool from centrotherm photovoltaics used in this investigation, which is suitable for solar cell production lines.

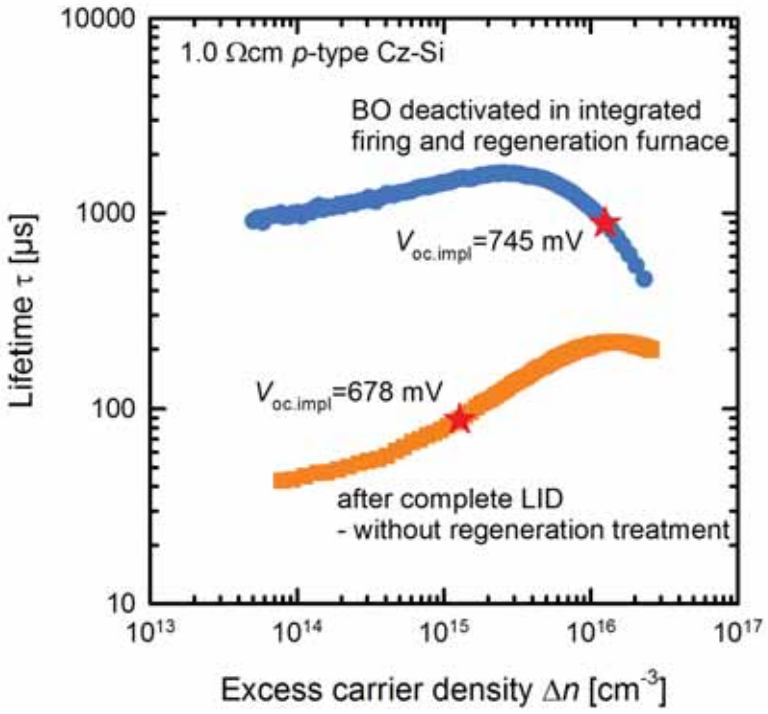

Figure 6. Injection-dependent lifetimes measured after permanent deactivation of the BO defect in the integrated firing and regeneration furnace (blue circles), and after complete LID (orange squares) without deactivation treatment. The red stars indicate the lifetime and excess carrier density at an illumination intensity of 1 sun.

Integrated fast-firing and regeneration

Centrotherm photovoltaics has very recently developed an integrated fast-firing and regeneration furnace, called *c.FIRE REG* (Fig. 5). Apart from the integrated regeneration, this new furnace features the additional benefit of increased cooling rates during the fast-firing step, compared with previous models, which enables a fast regeneration that results in very high lifetimes [12].

In the c.FIRE REG furnace, the wafers are directly transferred to the regeneration unit after firing. For the regeneration conditions, a light intensity of 85% was chosen for all regeneration zones; during the regeneration process the sample temperature reaches a maximum of 234°C. In total, the samples are illuminated for 17s at temperatures above 200°C in the regeneration zone of the furnace.

Lifetime investigations were performed on 1Ω·cm Cz-Si wafers; a dramatic increase in lifetime was observed after applying the integrated process in the c.FIRE REG furnace. Without the regeneration, lifetimes after complete degradation of the order of $\tau_d \approx 100\mu s$ were measured, whereas after the integrated process, an average very high lifetime of $\tau_{0p} = 1{,}460 \pm 80\mu s$ was measured. Fig. 6 shows the injection-dependent lifetimes of two different samples: one sample was treated in the integrated fast-firing furnace (blue circles), while the other sample did not undergo a regeneration process after fast-firing (orange squares). The red stars additionally represent the excess carrier density at 1 sun illumination intensity where

the implied open-circuit voltages $V_{oc.impl}$ of both samples are extracted. A significant increase in the $V_{oc.impl}$ values was observed – from 678mV in the state after complete LID, to 745mV after integrated firing and regeneration. It is therefore concluded that an optimal permanent deactivation of the BO defect occurs under the applied conditions in the combined fast-firing and regeneration furnace.

Summary

ISFH's lab-type deactivation process of the BO-related defect centre has been transferred to industrial belt-line furnaces which use intense illumination at elevated temperatures.

The C.REG 6.200 inline regenerator from centrotherm photovoltaics exposes the samples for approximately 32s to the regeneration conditions. These conditions were varied in four different regeneration processes with regard to the belt speed, the temperature and the illumination intensity. For a large number of Cz-Si materials with different base resistivities between 1 and 5Ω·cm, a constant average lifetime of 450µs, independent of the regeneration process and the base resistivity, was achieved after regeneration. This constant lifetime was limited by surface recombination, which was confirmed by FZ-Si reference samples processed in parallel. The findings indicate that the bulk lifetime for the different Cz materials was significantly higher than the measured effective lifetime of 450µs. It was therefore concluded that the inline regeneration furnace is in fact suitable for effectively suppressing LID in Cz-Si solar cells.

> "The use of a furnace with an integrated regeneration zone is excellently suited to next-generation PERC production lines"

The initial results of lifetime regeneration experiments using a novel inline integrated fast-firing and regeneration tool (centrotherm c.FIRE REG) have also been presented. In this tool the samples are exposed to temperatures between 200 and 234°C for 17s in the regeneration zone. After applying the optimized process, stable lifetimes well above 1ms were obtained for 1Ω·cm Cz-Si material. The very high lifetimes achieved clearly prove that the use of a furnace with an integrated regeneration zone is excellently suited to next-generation PERC production lines.

Acknowledgements

This work was funded by the German State of Lower Saxony and the German Federal Ministry of Economics and Energy (BMWi) within the 'Upgrade Si-PV' research project (Contract No. 0325877B).

References

[1] Fischer, H. & Pschunder, W. 1974, "Investigation of photon and thermal induced changes in silicon solar cells", *Proc. 10th IEEE PVSC*, Palo Alto, California, USA, p. 404.

[2] Knobloch, J. et al. 1996, "Solar cells with efficiencies above 21% processed from Czochralski grown silicon", *Proc. 25th IEEE PVSC*, Washington DC, USA, p. 405.

[3] Schmidt, J., Aberle, A.G. & Hezel, R. 1997, "Investigation of carrier lifetime instabilities in Cz-grown silicon", *Proc. 26th IEEE PVSC*, Anaheim, California, USA, p. 13.

[4] Glunz, S.W. et al. 1998, "On the degradation of Cz-Silicon solar cells", *Proc. 2nd World Conf. PV Solar Energy Conv.*, Vienna, Austria, p. 1343.

[5] Schmidt, J. & Bothe, K. 2004, "Structure and transformation of the metastable boron- and oxygen-related defect center in crystalline silicon", *Phys. Rev. B*, Vol. 69, p. 024107.

[6] Herguth, A. et al. 2006, "A new approach to prevent the negative impact of the metastable defect in boron doped Cz silicon solar cells", *Proc. 21st EU PVSEC*, Dresden, Germany, p. 530.

[7] Walter, D. et al. 2014, "Investigation of the lifetime stability after regeneration in boron-doped CZ silicon", *Proc. 29th EU PVSEC*, Amsterdam, The Netherlands, p. 555.

[8] Pernau, T. et al. 2015, "Rather high speed regeneration of BO-defects: Regeneration experiments with large cell batches", *Proc. 31st EU PVSEC*, Hamburg, Germany, p. 918.

[9] Walter, D.C., Pernau, T. & Schmidt, J. 2016, "Ultrafast lifetime regeneration in an industrial belt-line furnace applying intense illumination at elevated temperature", *Proc. 32nd EU PVSEC*, Munich, Germany, p. 469.

[10] Sproul, A.B. 1994, "Dimensionless solution of the equation describing the effect of surface recombination on carrier decay in semiconductors", *J. Appl. Phys.*, Vol. 76, No. 5, p. 2851.

[11] Richter, A. et al. 2012, "Improved quantitative description of Auger recombination in crystalline silicon", *Phys. Rev. B*, Vol. 86, No. 16, p. 165202.

[12] Walter, D.C. et al. 2014, "Lifetimes exceeding 1 ms in 1-Ω cm boron-doped Cz-silicon", *Sol. Energy Mater. Sol. Cells*, Vol. 31, p. 51.

About the Authors

Dominic Walter studied physics at the Albert Ludwig University of Freiburg, Germany, and received his degree (Dipl.-phys.) in 2011 for his work on lifetime analysis of crystalline silicon thin-film material, conducted at Fraunhofer ISE. He then joined ISFH as a Ph.D. candidate, working on BO-related defect centres in Cz-silicon.

Thomas Pernau studied physics at the University of Konstanz and obtained his diploma in 1999 on spatially resolved minority-carrier lifetime measurements. He continued his work within the PV group, leading to his Ph.D. thesis on CVD processes for industrial solar cells in 2003. Since 2001 he has been working on centrotherm turnkey projects as a process integration specialist, and is currently the R&D project leader and product manager for firing and regeneration furnaces.

Jan Schmidt received his Ph.D. degree in 1998 from the Leibniz University of Hanover. He is head of the PV department at ISFH and also a full professor of PV materials research at the University of Hanover. His research interests include the development of novel solar cell concepts and fabrication processes, with a focus on surface passivation schemes and selective contacts, and the analysis and manipulation of defects in mono- and multicrystalline silicon. He is a scientific committee member for several conferences and workshops in the field of PV, as well as editor of the *IEEE Journal of Photovoltaics.*

Enquiries

Dominic C. Walter
Institute for Solar Energy Research Hamelin (ISFH)
Am Ohrberg 1
D-31860 Emmerthal
Germany

Cell Processing

News

PERC solar cell production to exceed 15GW in 2017

Credit Taitra

PERC was a hot topic of discussion at PV Taiwan this year.

Global passivated emitter rear contact (PERC) cell capacity has the potential to double next year according to Andreas Liebheit, president of metallization paste producer Heraeus Photovoltaics.

Speaking to *Photovoltaics International* sister website, *PV Tech*, at the PV Taiwan exhibition in Taipei, Liebheit said the technology is slowly growing and has been successfully brought in by roughly 10 companies globally to date, and accounts for around 10-15% of the worldwide market.

He added: "Newcomers in PERC still have their initial trouble to get it ramped up, but I think it's more and more feasible now."

Liebheit said the technology is complex and its growth can be limited by the long lead times for equipment as well as the readiness of some companies to invest in it. On the other hand, within this fairly slow market, PERC providers have been selling out, which shows that there is a demand for high-efficiency cells based on PERC.

"Maybe it doesn't sell for the big price premium as some of them expected, but at least it sells, whereas others which have standard efficiency sit on their stocks, so that's a big differentiator." Liebheit said.

He also said his forecasts are in line with the IRTPV roadmap which predicts PERC to have a 70% share by 2018/19.

When asked about whether Taiwan's new feed-in tariff that favours high-efficiency modules will lead to a greater focus on PERC in Tawian, Liebheit said: "I really do hope so. At the moment the Taiwan industry is slightly in defence because they have to justify their advantage towards mainland China. They have to explain that they are better in quality or technology than mainland China and they have higher costs.

"Now in mainland China, you have quite some PERC players so the difference is not that obvious anymore. The issue with the Taiwanese; some of them have been seen as being a bit conservative in investing. So, except one playing in PERC, all others still have limited capacity in PERC. Everyone is doing a little bit about it, but I think [...] the local programme will maybe stimulate them to ramp up faster in PERC."

Tools

RENA wins major alkaline texturing tool order from LERRI Solar

Specialist PV manufacturing equipment supplier RENA Technologies has secured a significant tool order from China-based LERRI Solar said to be in the double-digit million euro range to meet more than 2GW of monocrystalline PERC solar cell production.

RENA noted that the tool order included its 'BatchTex' texturing tools that provide high-throughput IPA-free alkaline texturing and its 'InOxSide+' Inline systems that combine junction isolation and rear side smoothing for high efficiency solar cells.

"Our successful long-term business relationship and the outstanding characteristics of the RENA tools convinced us to place the order with RENA," said Jack Zou, general manager at Xi'An Longi Silicon Materials Corp.

LERRI Solar is a subsidiary of Xi'an LONGi Silicon Materials Corp., the world's largest manufacturer of monocrystalline silicon wafers. LONGi had already announced plans in July, 2015 to build a new large-scale manufacturing complex in Taizhou City, Jiangsu, China as part of its 2GW plans of integrated cell and module production.

Subsequently, LONGi raised around US$290 million via a private placement of new shares to fund the ground-up manufacturing complex through several expansion phases expected to take several years to complete.

"The project award is an important achievement, demonstrating again the leading market position of RENA Technologies' new equipment generation for wet processes in solar cell manufacturing" states Dr. Tobias Luecke, CEO of RENA.

Meyer Burger secures US$74 million 200MW heterojunction order in Turkey

Leading PV manufacturing equipment supplier Meyer Burger Technology has signed an initial order with an unidentified customer that plans a fully-integrated 200MW heterojunction production plant with expectations to reach 1GW of nameplate capacity by 2021.

Meyer Burger said that the initial order was valued at around US$74 million (€67 million) with prepayment expected to be received during the first quarter of 2017.

Based on the prepayment in the first quarter of 2017, Meyer Burger said that the tools would be delivered in the third quarter of 2017, while production ramp would be expected by the first quarter 2018.

The customer prepayment for this contract is expected to be received during the first quarter 2017. The order will be reflected in the incoming orders, once the prepayment has taken place. Delivery of the contract equipment is expected as of the third quarter of 2017. The customer plans to start production by the first quarter 2018.

Meyer Burger also noted that the customer planned to achieve a total production capacity of about 1GW in the next five years, indicating that the 1GW nameplate capacity would be reached in 2021.

The initial order includes Meyer Burger's diamond wire cutting systems for monocrystalline wafering, heterojunction (HJT) solar cell coating technology and its 'SmartWire' connection technology.

The order also includes software

for production control (MES) along the entire PV value chain as well as the on-site training of process operators to ensure the production of high-efficiency solar modules.

Singulus raised funds to focus on CIGS and HJ solar cell development

Specialist PV manufacturing equipment supplier Singulus Technologies has issued new shares valued at around €8 million to provide liquidity for supplying CIGS thin-film production equipment orders and the development of heterojunction (HJ) solar cell processing tools after securing an (MOU) with Golden Concord Holdings, majority shareholder in GCL-Poly and GCL System.

Stefan Rinck, chief executive of Singulas, said: "The capital increase for cash marks the successful conclusion of the company's financial restructuring. We will invest the funds from the capital increase mainly in financing growth in the solar area as well as for research and development work to advance the new business areas. We have achieved an important success in clinching the major contract for CIGS production machinery."

SoLayTec receives follow-on order for three ALD systems

Atomic layer deposition (ALD) equipment specialist SoLayTec, a subsidiary of Amtech Systems has received a follow-on order for three solar cell ALD systems.

Amtech said that it expected to ship the order to a solar cell manufacturer in Asia within the next six months.

Fokko Pentinga, CEO and President of Amtech said: "This latest order is another indication of the growing recognition in the solar industry of the outstanding performance of SoLayTec's spatial ALD system to improve the cost of ownership of our customers' PERC cell processes."

SoLayTec had previously noted a number of new tool orders from a range of customers planning p-type PERC, n-type IBC and bi-facial solar cell production in 2016. Customers are located in China, Japan, Europe and Taiwan.

ALD is typically used to deposit a thin, uniform amorphous aluminium oxide (Al2O3) layer as the rear side passivation for PERC solar cells.

Efficiency records

Trina Solar sets 19.86% aperture efficiency record for p-type multicrystalline cell

Trina Solar has set a new world record of 19.86% aperture efficiency for a p-type multicrystalline solar cell-based module, independently verified by the Fraunhofer ISE CalLab in Germany.

The record was set with half-cut cell interconnection, passivated emitter and rear contact (PERC) technology and highly efficient light trapping on a module area of 1.514m2.

The new record represents an increase of more than 0.7 percentage points, or approximately 3.8% higher than the previously held efficiency record of 19.14% on a 1.515m² module aperture area announced in April 2015. As with previous developments the work was carried out at Trina Solar's State Key Laboratory of PV Science and Technology of China (SKL PVST).

Dr. Pierre Verlinden, Vice-President and Chief Scientist of Trina Solar said: "The efficiency of PV modules is one

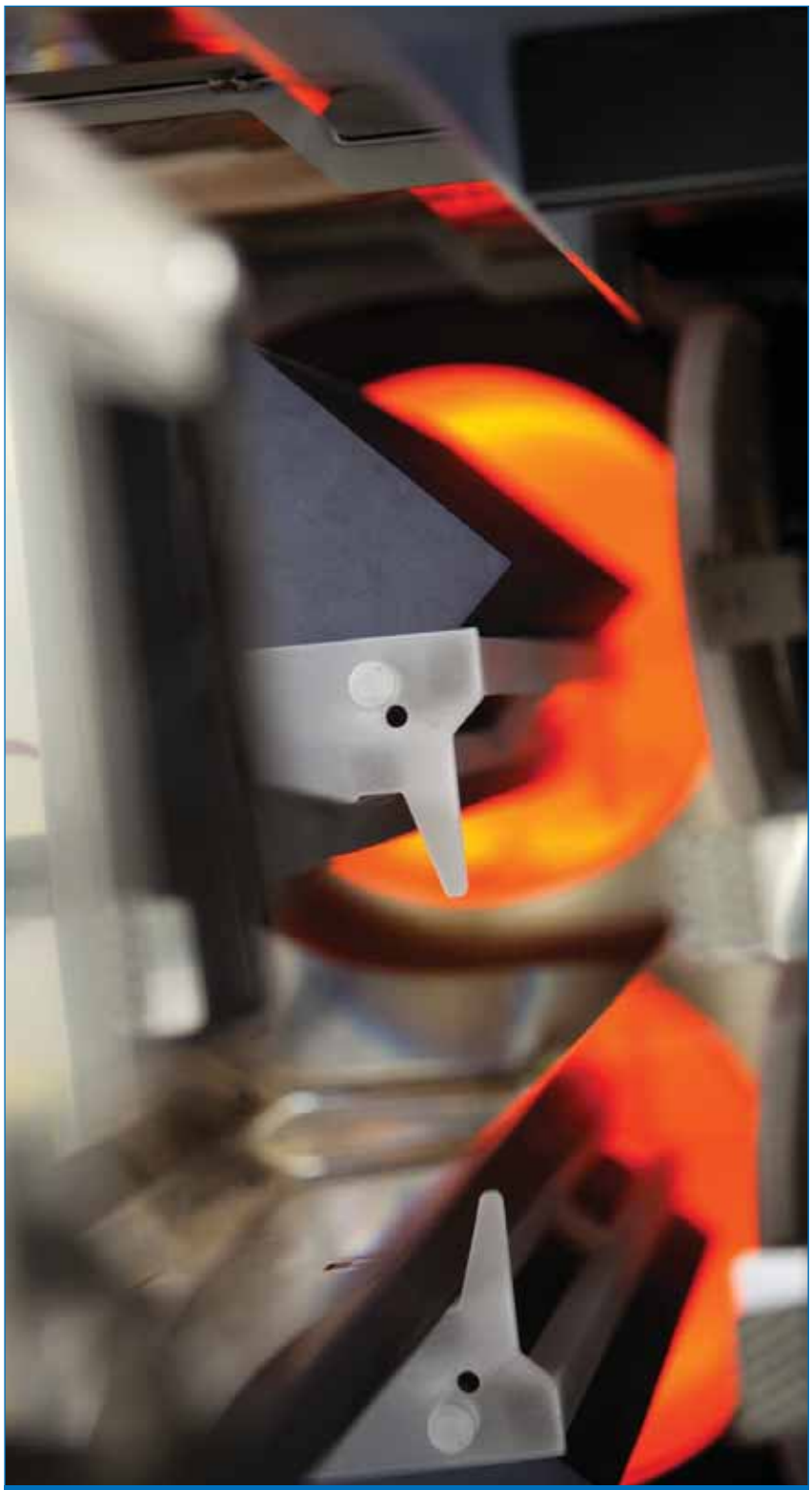

Trina Solar

Trina Solar has achieved a new aperture efficiency record for a p-type multi cell.

of the key parameters to estimate the final Levelised Cost of solar Electricity (LCOE). This 19.86% aperture efficiency result that Trina Solar achieved demonstrates the huge potential for future multicrystalline p-type silicon research. It is also a leap forward in the trend of continuous efficiency improvements of crystalline silicon solar modules."

Trina Solar had recently said it had achieved an average efficiency of 21.1% for its industrially-produced P-type monocrystalline cells (156x156 mm) with PERC technology at its 'golden' pilot production line.

REC touts best production line multicrystalline cell efficiencies of 20.47%

Integrated PV module manufacturer REC Group has claimed that a pre-production batch of multicrystalline solar cells at its manufacturing plant in Singapore achieved a best conversion efficiency of 20.47% measured by an in-house tester with an external calibration cell.

The company noted that upgraded wafer-to-cell processes were responsible for achieving an average cell efficiency of 20.21%, with the best cell at 20.47%. The process developments would be applied to REC's production lines at the beginning of November 2016, according to the company.

"This great achievement is a strong testament to our R&D efforts at each step in the value chain," noted Steve O'Neil, chief executive of REC.

The company had recently confirmed to *PV Tech* that it was trimming its global workforce with 65 jobs losses out of approximately 2,200 employees but was still committed to spending US$48 million to upgrade all production to its half-cut PERC cell technology, used in its 'TwinPeak' series modules.

Results

Neo Solar Power cites deferred orders for slump in November sales

Taiwan-based merchant cell and module producer Neo Solar Power (NSP) reported an unexpected slump in November sales after several months of recovery, which was said to be due to deferred customer orders.

NSP reported November, 2016 sales of NT$ 898 million (US$28.2 million), a 20.03% decline from the previous month.

Sales for 2016 have reached NT$ 15,410 million (US$485.4 million) as of November 2016, a 21.28% decrease from the prior year period.

The company also noted and confirmed that its relocation of production equipment to its new facility in Southeast Asia had been completed with the expectation that the facility would start ramping before year-end.

Rival cell producers had yet to report November results at the time of publication. However, cell maker Gintech Energy reported a slow but meaningful sequential monthly increase in sales in October 2016. It reported revenue of NT$822 million (US$26.1 million), compared to NT$716 million in September 2016, a 14.7% increase. However, revenue remains 41% down, year-on-year.

Meanwhile Solartech Energy Corp reported its first increase in revenue since June, 2016. Its sales in October were NT$461 million (US$14.6 million), up 2.6% from the previous month but still down 56.6%, year-on-year.

Cu-plated electrodes with laser contact opening on n-type crystalline silicon solar cells

Kuang-Chieh Lai, Yueh-Lin Lee, Ming-Shiou Lin, Chia-Chih Chuang, Chi-Chun Li & Chien-Chun Wang,
Motech Industries, Inc., Tainan, Taiwan

ABSTRACT

This paper presents the fabrication of front-junction n-type silicon solar cells with Cu-plated electrodes, using laser contact opening and forward-bias plating. The cells feature a back-surface field formed by a phosphorus implant, and a diffused boron emitter with aluminium oxide passivation. Laser ablation of the front-side dielectric layers is followed by a metallization based on Ni/Cu forward-bias plating, while sintered metal paste is used for the rear electrode. The results show improved line conductivity and contact resistivity for the plated electrode, leading to higher solar cell efficiency than for cells made with conventional Ag/Al paste. On 6" n-type Czochralski wafers, cell efficiencies of up to 21.3% have been demonstrated, with an open-circuit voltage of 654mV, a short-circuit current of 40.8mA/cm^2 and a fill factor of 79.8%.

Introduction

It is well recognized that n-type crystalline silicon solar cells offer higher efficiency potential than p-type cells, as n-type wafers are: 1) more tolerant of common metallic contaminations, such as iron [1]; 2) provide higher minority-carrier lifetime; and 3) do not suffer from light-induced degradation (LID), which significantly impacts the performance of p-type cells created from boron-doped Czochralski (Cz) wafers [2–4].

N-type silicon solar cells are often made with a bifacial structure, which utilizes the light incident on the rear surface to produce even more power. Motech has developed n-type bifacial cells based on a passivated emitter, rear totally diffused (PERT) structure, and has previously reported efficiencies higher than 20.6% for n-PERT cells made with screen-printed electrodes on both sides of the cell [5]. A performance ratio gain of 20% has also been demonstrated for bifacial modules using n-PERT cells in outdoor tests [5].

The conventional metallization approach, however, is relatively expensive for bifacial cells: compared with p-type cells, the usage of Ag pastes on bifacial n-type cells is roughly double. A low-cost alternative to Ag paste metallization, such as the Cu plating method studied in this work, is therefore particularly important for n-type cells. In addition to the material cost savings, the electrical performance of the solar cell also benefits from Cu plating, because the bulk conductivity of plated Cu is higher than that of Ag pastes, and the contact with Si of plated Ni/Cu is superior to that of sintered Ag. The Cu fingers defined by laser contact opening (LCO) can also be made thinner than screen-printed Ag fingers, further reducing the shading losses.

Cu-plating metallization has been used for the front electrodes of p-type cells with an Al back-surface field (BSF) and for passivated emitter and rear cells (PERCs) [6], as well as for the front electrodes of rear emitter n-PERT cells [7]. Those electrodes on the n$^+$ surface of the cells were created by the light-induced plating (LIP) method. However, LIP is not suitable for plating the boron-doped p$^+$ surface; instead, the forward-bias plating (FBP) method [8] is used, whereby the cell is placed under forward bias to enable the plating process. FBP is used to create the Ni seed layer on the p$^+$ surface of the cells, as well as the Cu conductor on top of Ni. The deposition rate is easily controlled by the applied current.

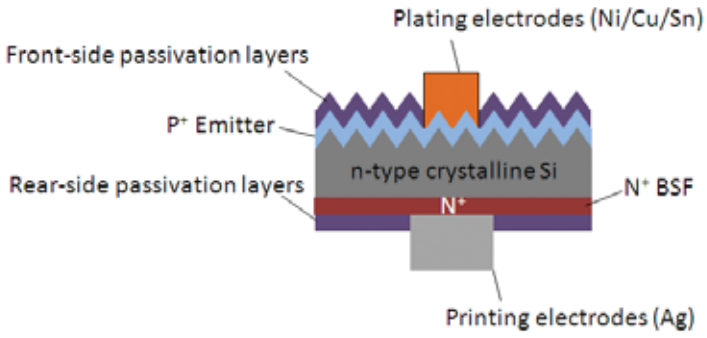

Figure 1. Schematic cross section of an n-type silicon solar cell.

Solar cell structure and process flow

A schematic diagram of the solar cell structure is shown in Fig. 1. As the starting material, 6" n-type Cz wafers were used, with a thickness of ~170µm and a resistivity of 3–5Ω·cm. The front surface was textured with random pyramids to reduce optical reflection. The p$^+$ boron emitter was established near the front surface, and homogeneous phosphorus doping on the rear side formed the BSF. Amorphous SiN_x thin film was deposited on the rear to passivate the n$^+$ doped surface, while a stack of Al_2O_3/SiN_x was deposited on the front

to passivate the boron emitter and to serve as an anti-reflection coating (ARC) at the same time. Conventional screen-printed/sintered Ag paste was used for the rear-side electrode. A Ni/Cu/Sn stack, plated on the Si surface exposed by laser ablation of the ARC, was used for the front-side electrode.

The process flow for the front-junction n-PERT cells is shown in Fig. 2. Standard alkaline etching was used to create the random pyramid texture, followed by BBr_3 diffusion for the emitter, with a sheet resistance of 75±5Ω/sq. After the removal of borosilicate glass, the wafers were subjected to a phosphorus implant and annealing process to form an n^+ BSF on the rear side. An Al_2O_3 layer for the emitter passivation was deposited using atomic layer deposition (ALD) equipment. A SiN_x coating was deposited by plasma-enhanced chemical vapour deposition (PECVD) on the front side as the ARC, and also on the rear side as a capping layer.

Commercially available Ag paste for the n^+ surface was used to create the rear-side electrode by printing and sintering. The thermal budget also helped improve the passivation. The ARC was then ablated using a 532nm green nanosecond laser to define the front-electrode pattern. Ni and Cu were then deposited by FBP, followed by Sn electroplating. Finally, a rapid thermal annealing was performed in a belt furnace to form a nickel silicide layer in order to improve the front-contact resistance.

"Laser ablation of the ARC for front-side contact opening is one of the key processes for Cu-plated n-PERT cells."

Figure 2. Process flow for front-junction n-PERT cells.

Laser ablation process

Laser ablation of the ARC for front-side contact opening is one of the key processes for Cu-plated n-PERT cells. First, it needs to completely remove the ARC in the targeted area, so that Ni can be directly plated onto Si. Second, to reduce the plated finger width and to maintain good finger conductance, the laser opening itself has to be narrow and uniform. Third, the quality of the boron emitter should be maintained after its modification by laser. Because a 532nm nanosecond laser source was used, the thermal effect of the ablation was expected to change both the emitter doping profile and the silicon surface morphology.

Various combinations of laser parameters – including peak power, scan speed, light focus and pulse frequency – were tested in the ablation of the front-side dielectric layers. Fig. 3 shows the scanning electron microscope (SEM) images of the laser contact opening in the experiments.

A good ablation process should lead to a clearly defined removal of the dielectric layer, and minimum laser damage to the Si surface. Fig. 3(a) shows the ablation with too little laser energy: the textured surface was only slightly modified, but the SiN_x film was not fully removed, as indicated by the nitrogen signal in the energy dispersive X-ray spectroscopy (EDS) for the ablated area. In contrast, the high energy case, shown in Fig. 3(c), indicates a seriously damaged surface, with melted Si splashed over the region of the laser opening. Fig. 3(b) shows an example of appropriate laser energy, with a thin line and uniform width: an average width of 15.7µm and uniformity of 1.5% (by measuring widths at different positions across the wafer) were achieved. Complete removal of the dielectric layers was confirmed in this case by the 100% Si signal in the EDS for the ablated area.

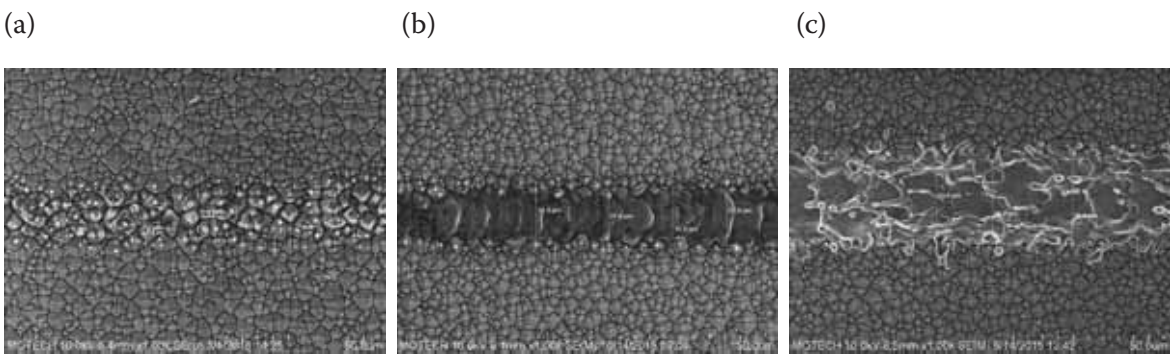

Figure 3. SEM images of front-side contact opening using different laser energies: (a) low; (b) medium; (c) high.

As regards the emitter profile, samples suitable for electrochemical capacitance–voltage (ECV) measurement were created; the results are shown in Fig. 4. The sample before the LCO process indicated a shallow emitter with a peak concentration of ~9E+19cm^{-3}; the sheet resistance was 75Ω/sq. After LCO, the emitter profile was changed in such a way that the surface concentration was reduced to less than 2E+19cm^{-3}, and the junction moved deeper, to ~0.7µm; the sheet resistance became 95Ω/sq. Although such a low surface concentration falls outside the range suitable for contact by sintered Ag paste, it is still practical for a nickel silicide contact. The deeper profile could help reduce carrier recombination in the metal contact region, and prevent a vertical shunting path when nickel silicide is formed during the annealing process.

Front-side metallization

After LCO is completed, the cell is placed in a plating tank with a bias applied via the rear-side Ag electrode in order to start the FBP process; Fig. 5 shows the SEM images of the cell at different stages of the metallization process. The metal deposition of FBP is isotropic, which means that the finger width is roughly the sum of the laser opening width and twice the metal thickness.

Because of Motech's cell design, it was decided not to push the line width to its lower limit, and so a LCO width of 20µm was used instead, as shown in Fig. 5(a). Fig. 5(b) shows the deposition of a 1µm Ni layer by FBP; the finger width was about 22µm. Subsequent Cu FBP processing increased the finger width to 46µm, with a Cu thickness of 12µm, as shown in Fig. 5(c) and (d). Finally a 1µm Sn protection layer was plated; the completed metallization is illustrated in Fig. 5(e).

A GPsolar 4-TEST four-point probe tool was used to perform line resistance R_{line} measurements, yielding the resistance per unit length of the fingers. A comparison of samples created using Ag/Al paste and Cu plating is given in Table 1. The average value of R_{line} readings at five different positions across the wafer was 0.38Ω/cm for Ag/Al paste, and 0.25Ω/cm for Cu plating. By multiplying the respective cross-sectional area of the fingers, the line resistivity of Ag/Al was estimated to be 2.7µΩ·cm, and that of a Cu finger to be 1.9µΩ·cm. This result highlights the advantages of using plated Cu fingers: with a higher finger conductivity, it is possible to implement thinner lines, thus reducing the shading on the front side of the cell.

> "With a higher finger conductivity, it is possible to implement thinner lines, thus reducing the shading on the front side of the cell."

Emitter experiment

In the case of solar cells with screen-printed metallization, the emitter profile is significantly constrained by the contact capability of the sintered Ag or Ag/Al paste. The nickel silicide contact with the Si is expected to be superior, with a contact resistivity below 1mΩ·cm^2 at a doping level of 1E+19cm^{-3} [9]. This provides a lot of room for emitter optimization for higher cell efficiency, even though the emitter is modified in the contact area if a laser is used. In the work reported here, several emitter profiles were tested: a shallow emitter (denoted E1) with a low surface concentration (2E+19cm^{-3}), and several others

(E2–E5) with increasing junction depth and/or concentration. The results of *I–V* measurements are shown in Fig. 6.

The carrier recombination will be enhanced under heavier doping conditions, resulting in a downtrend in short-circuit current (J_{sc}). On the other hand, a heavy doping profile reduces the emitter sheet resistance and hence the series resistance. The dependence of open-circuit voltage (V_{oc}) on doping is generally characterized by an interplay between the recombination in the emitter and the field effect of the emitter. The results show that, except for the heaviest doping condition (E5), the efficiency is consistently higher than 20.6%, with an expected trade-off between fill factor (FF) and J_{sc}. The front-metal patterns were kept the same in all these experiments, and so improved electrode design is certainly a possibility for further increasing cell efficiency.

Contact resistivity was measured by the transfer length method using the GPsolar 4-TEST tool. The resistivity was found to be around 1mΩ.cm^2, even for the lowest doping condition; it should be possible to improve this by further optimizations of the Ni deposition and annealing for silicide formation.

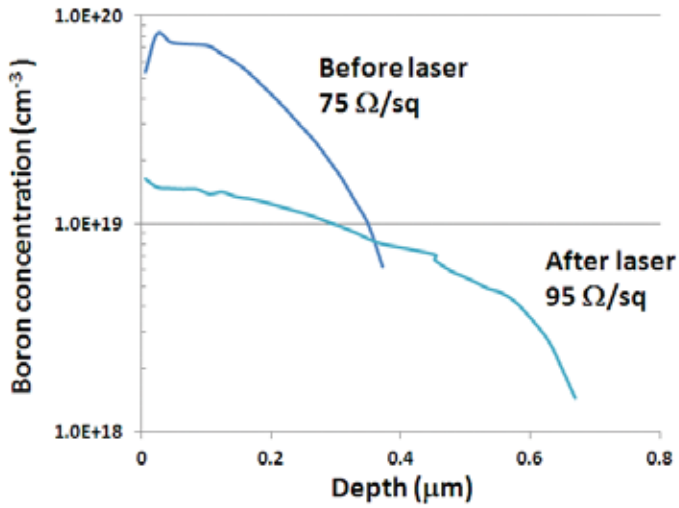

Figure 4. Emitter profile before and after the LCO process.

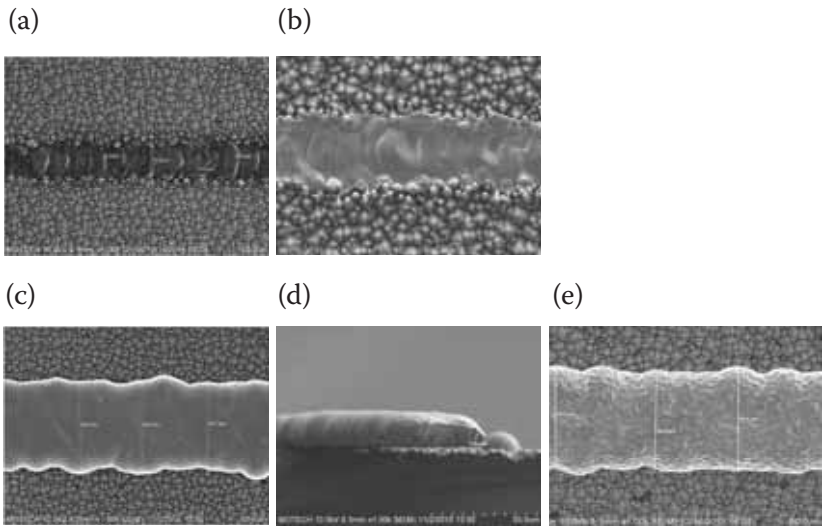

Figure 5. SEM analysis of laser opening and front-side metallization: (a) after green nanosecond LCO; (b) after Ni plating; (c) after Cu plating; (d) after Cu plating, side view; (e) after Sn plating.

Plated vs. printed

One concern about plated electrodes is that the diffusion of Cu into the active area of the solar cell could become a major source of recombination. A Ni layer with proper silicidation can be used as a diffusion barrier to Cu, but the series resistance may increase if the Ni is too thick, because of its lower conductivity. The method in Hernández, J. et al. [10] was followed, and Cu diffusion in the solar cells was checked by *I–V* and Suns-V_{oc} measurements before and after a thermal stress of 500°C for one minute. No change in either V_{oc} or pseudo-fill factor (pFF) was found after the thermal stress, indicating that there was no Cu diffusion into the p-n junction or into the bulk of the wafer.

Compared with a conventional printed Ag/Al finger, the plated Cu finger exhibits a narrow line width, a good aspect ratio, well-defined finger edges, a smooth surface and a solid bulk (Fig. 7). These characteristics indicate that plated Cu is a better conductor for Si solar cells. The fine-line capability enables a more optimal combination of the electrode pattern and the emitter profile. Furthermore, the incident light could be increased as a result of the reflection from the smooth finger edges.

It was possible to improve the efficiency of the plated n-PERT cells to over 21%; the *I–V* curve of one of the best cells is shown in Fig. 8, with a V_{oc} of 654mV, J_{sc} of 40.8mA/cm^2 and FF of 79.8%.

A comparison of the performance of n-PERT solar cells with different metallizations is given in Table 2. The Cu-plated n-PERT cells showed an efficiency improvement of 0.2%$_{abs.}$ over the printed cells. One apparent benefit of Cu fingers was the improved current density J_{sc}, which resulted mainly from the thinner line width. The V_{oc} of n-PERT cells made using the Ag/Al paste firing process usually degrades

	R_{line} [Ω/cm]						Resistivity
	Position 1	Position 2	Position 3	Position 4	Position 5	Average	[µΩ·cm]
Ag/Al paste	0.389	0.409	0.398	0.378	0.331	0.381	~2.7
Cu plating	0.253	0.255	0.259	0.258	0.223	0.250	~1.9

Table 1. Line resistance data and resistivity for sintered Ag/Al fingers and plated Cu fingers.

significantly from the implied V_{oc} value measured before metallization. Even though no Cu diffusion was observed in the plated cells, their average V_{oc} was slightly less than that of the printed cells. It is suspected that the laser used in this study introduced damage to the contact area, and that the silicidation process needs to be improved. With regard to the FF, a further increase is expected when the electrode pattern design is optimized for specific emitter profiles.

> "The Cu-plated n-PERT cells showed an efficiency improvement of 0.2%$_{abs.}$ over the printed cells."

Conclusion

A Ni/Cu/Sn metallization has been developed for the front-side electrode of an n-PERT cell, using forward-bias plating and laser contact opening. The laser parameters were tuned to completely ablate the SiN_x ARC, creating a uniform line opening with a width of less than 16µm. The FBP produced thin metal lines exhibiting excellent conductivity. Good contact resistance was obtained for a peak doping concentration below 2E+19cm^{-3}. Even though the surface morphology and the emitter profile were modified by the 532nm nanosecond laser during contact opening, the efficiency of the Cu-plated cells demonstrated a 0.2%$_{abs.}$ gain over conventional printed or sintered cells. The best efficiency achieved for 6" plated cells was 21.3%.

Many aspects of this metallization scheme can be improved. Moving to a UV laser source will significantly reduce the thermal effect of the laser and minimize damage to the silicon surface. Optimization of the silicidation process will enhance adhesion and the electrical contact between Si and metal. The vast range of emitter profiles that are possible by using a nickel silicide contact should yield a high-efficiency cell design that optimally combines the emitter, the electrode pattern, and the very fine metal lines provided by Cu plating.

References

[1] Romijn, I. et al. 2012, "Industrial n-type solar cells: Towards 20% efficiency", *Photovoltaics International*, 15th edn, p. 81.

[2] Song, D. et al. 2012, "Progress in n-type Si solar cell and module technology for high efficiency and low cost", *Proc. 38th IEEE PVSC*, Austin, Texas, USA.

[3] Schmidt, J. & Hezel, R. 2002, "Light-induced degradation in Cz silicon solar cells: Fundamental understanding and strategies for its avoidance", *Proc. 12th Worksh. Cryst. Si. Sol. Cell Mater. & Process.*, Breckenridge, Colorado, USA.

[4] Tous, L. et al. 2015, "Evaluation of advanced p-PERL and n-PERT large area silicon solar cells with 20.5% energy conversion efficiencies", *Prog. Photovoltaics Res. Appl.*, Vol. 23, pp. 660–670.

[5] Yu, S. et al. 2014, "20.63% nPERT cells and 20% PR gain bifacial module", *Proc. 40th IEEE PVSC*, Denver, Colorado, USA.

[6] Tous, L. et al. 2013, "A simple copper based plating process resulting in efficiencies above 20.5% using pilot processing equipment", *Proc. 28th EU PVSEC*, Paris, France.

[7] Aleman, M. et al. 2013, "Large-area high-efficiency n-type Si rear junction cells featuring laser ablation and Cu-plated front contacts", *Proc. 28th EU PVSEC*, Paris, France.

[8] Kamp, M. 2016, *Electrochemical Processes for Metallization of Novel Silicon Solar Cells*. Stuttgart, Germany: Fraunhofer Verlag, pp. 61–64 ("Forward bias plating for p-contacts").

[9] Thibert, S. et al. 2013, "Emitter requirements for nickel contacts on silicon solar cells – A simulation study", *Energy*

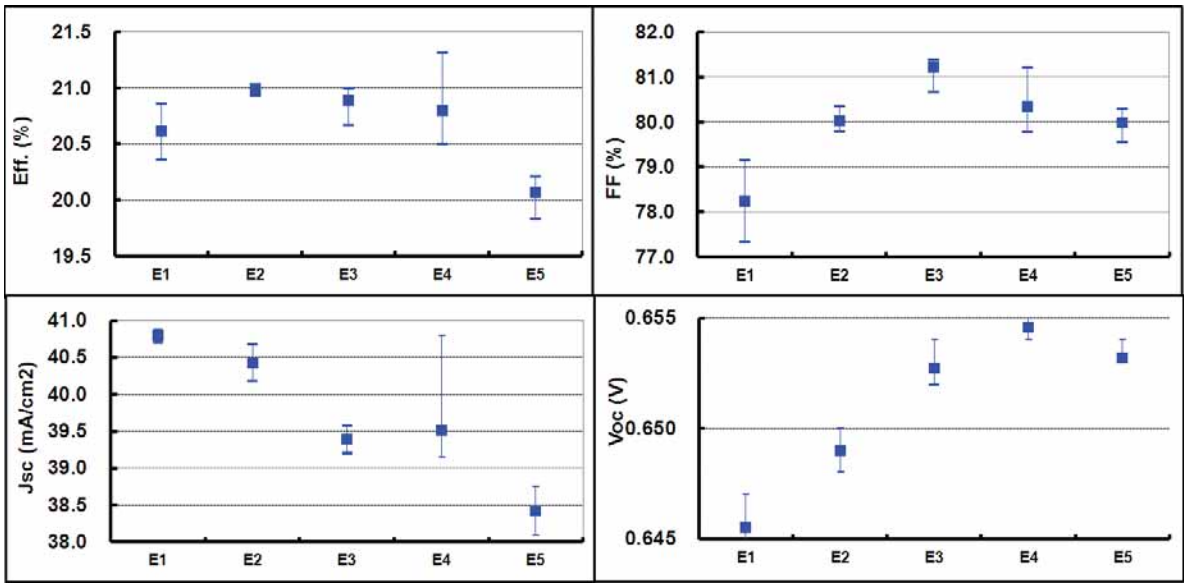

Figure 6. Cell performance for different emitter profiles.

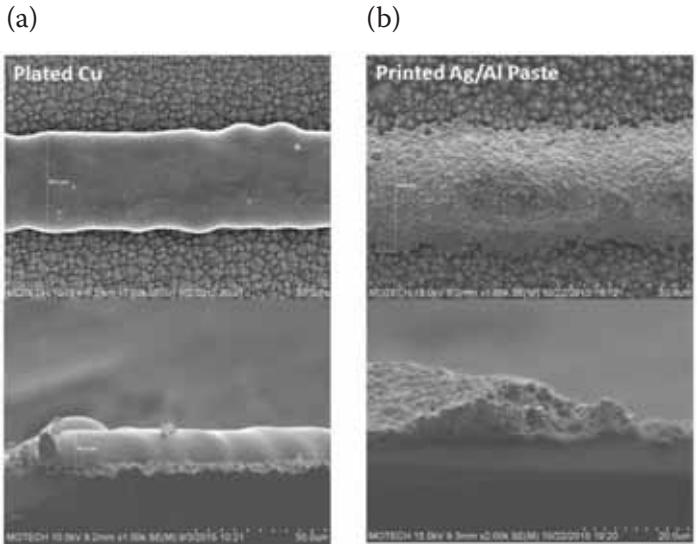

Figure 7. SEM images of (a) a plated Cu finger, and (b) a printed Ag/Al finger.

Procedia, Vol. 38, pp. 321–328.

[10] Hernández, J. et al. 2010, "Application of CMOS metal barriers to copper plated silicon solar cells", *Proc. 25th EU PVSEC*, Valencia, Spain.

About the Authors

Dr. Kuang-Chieh Lai received his Ph.D. in electrical engineering in 2011 from National Cheng Kung University. In 2007 he worked at NexPower Technology Corporation on developing the technology of a-Si thin-film solar cells. He joined Motech in 2011, where is involved in R&D of n-type c-Si solar cell technology.

Dr. Yueh-Lin Lee received his degree in photonics technologies and his Ph.D. from National Tsing Hua University in 2014. He then worked as a principal R&D engineer at Motech, focusing on advanced technologies of electroless plating and electroplating, and high-efficiency silicon solar cells.

Dr. Ming-Shiou Lin received his degree in materials science and engineering in 2005, followed by his Ph.D. from National Chung Hsing University in 2011, with a thesis on ZnO nanorods applied to light-emitting diodes. Since 2014 he has been working in the advanced technology section of Motech, where he is in charge of R&D of high-efficiency silicon solar cells.

Dr. Chia-Chih Chuang received his degree in materials science and his Ph.D. from National Tsing Hua University in 2002 and 2005 respectively. He then worked at the Industrial Technology Research Institute in Taiwan as a solar cell researcher, and later joined Long Energy Group in 2010. Since 2014 he has been at Motech, working as a project leader on developing n-type Si solar cell technology.

Dr. Chi-Chun Li received his Ph.D. in electrical engineering from Princeton University in 1999. From 2000 to 2008 he worked on telecommunication management systems at Alcatel-Lucent, before joining Motech in 2009 to lead the development of new solar cell designs

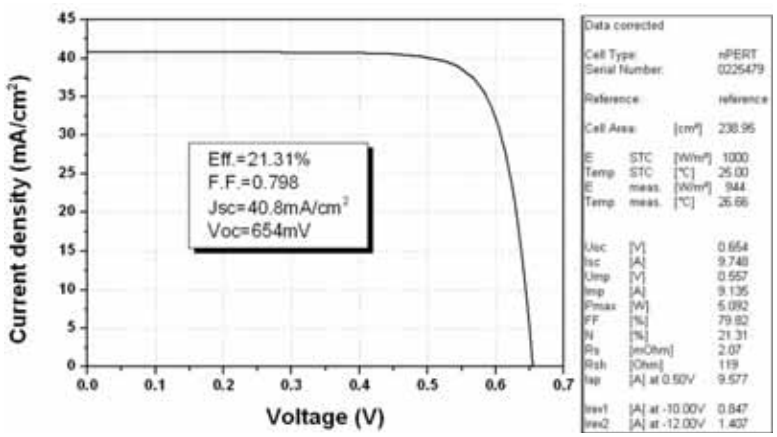

Figure 8. *I–V* curve of a Cu-plated n-PERT solar cell.

Metallization	Eff. [%]	V_{oc} [mV]	J_{sc} [mA/cm^2]	FF [%]
Ag/Al paste	20.8	654	39.8	79.8
Ni/Cu/Sn	21.0	650	40.4	80.0

Table 2. Solar cell performance for printed and plated electrodes.

and processes. He is currently a senior manager of the Advanced Technology Development Department.

Kirin Wang is the RD senior director at Motech, and graduated from the Institute of Material Science and Engineering of National Tsing Hua University in 1991. He joined Motech in 2010 and works on advanced solar cell development (P-PERC, N-PERT, HJT, back contact cell and Cu plating), and on production process development, including double printing, screen design, advanced ingot growth and diamond wire slicing. Before joining Motech he gained 19 years' experience in technology development and mass production in the semiconductor industry.

Enquiries
Chi-Chun Li
Motech Industries, Inc.
No. 96, Dashun 7th Road,
Xinshi District,
Tainan, Taiwan

Tel: +886 6505 0789
Email: chichun_li@motech.com.tw

Analysis and outlook of near-industrial PERC solar cells

Pierre Saint-Cast, Sven Wasmer, Johannes Greulich, Sabrina Werner, Ulrich Jäger*, Elmar Lohmüller, Hannes Höffler & Ralf Preu, Fraunhofer Institute for Solar Energy Systems ISE, Freiburg, Germany

*Now with RENA Technologies GmbH, Gütenbach, Germany

ABSTRACT

This paper presents an in-depth analysis of state-of-the-art p-type monocrystalline Czochralski-grown silicon passivated emitter and rear cells (PERCs) fabricated in a near-industrial manner. PERC solar cells feature a homogeneous emitter on the front side, and an Al_2O_3 passivation layer and local contacts on the rear side. The peak energy conversion efficiencies obtained are 21.1% for a standard anti-reflection coating (ARC), and 21.4% for a double-layer ARC. The loss analysis is based on an extended characterization of the solar cells and of special test samples; this allows the separation of the contributions of each region of the solar cell, including metallization. The impact of the contributions on the open-circuit voltage, the short-circuit current density and the fill factor is determined experimentally. On the basis of the measurements, the devices are numerically simulated, and the free-energy losses are analysed using the simulation model. This simulation allows the calculation of the contribution of the different parts of the solar cell to the efficiency losses. The extensive knowledge of current technology is also the starting point for exploring future technologies for PERC solar cells. An innovative simulation approach allows the future of PERC technology to be mapped out.

Introduction

Passivated emitter and rear cell (PERC) technology [1] using p-type silicon is quickly becoming widespread in crystalline silicon PV, and is expected to establish itself as the industry standard over the next decade. In 2010/2011, major manufacturers began to produce PERC solar cells, with the average energy conversion efficiency in pilot line production using large-area c-Si wafers starting at around 20% [2–3]. In a short period of time, these results could be transferred into mass production [4]. After several years of optimization, the average efficiency has been increased to around 21% in the laboratory and in mass production [5–8]. A few PERC solar cells with an efficiency of 22%, and some with slightly more, have recently been announced by two solar cell manufacturers [9,10]; these, however, are not yet available in mass production.

This paper reports the work carried out in a study of PERC solar cells entirely fabricated at the PV-TEC pilot line [11] at Fraunhofer ISE in a near-industrial manner. The results from several characterization methods applied to solar cells and test samples are combined in order to obtain a detailed analysis of the power losses in the cell. The chosen approach combines experimental evidence and simulation. Previous work has focused only on experimental analysis [12] or simulation [13] in isolation. The approach taken by Fraunhofer ISE, however, combines the realism of experiments with the depth of simulations. These analyses allow a discussion of the strengths and weaknesses of these PERC solar cells, as well as the proposal of further measures to be taken to increase their efficiencies. Going even further, an innovative simulation approach is used to create roadmaps for future PERC technology.

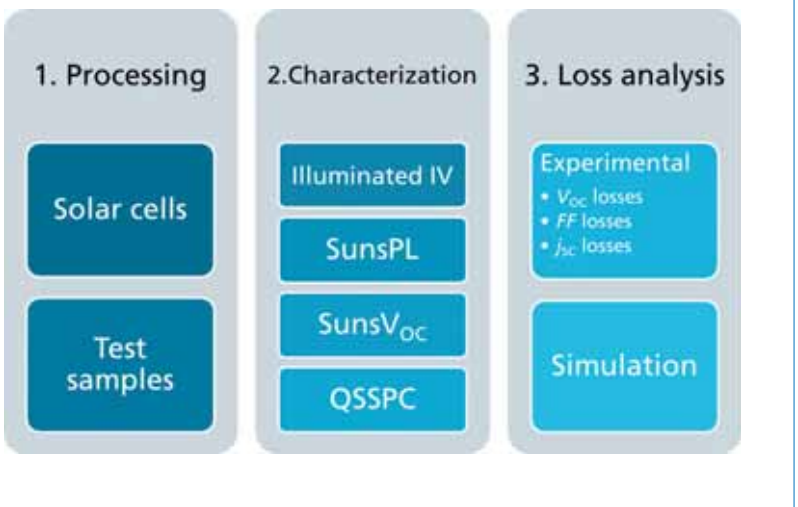

Figure 1. Schematic of the approach used to analyse the losses of Fraunhofer ISE's PERC solar cells.

> "The approach taken by Fraunhofer ISE combines the realism of experiments with the depth of simulations."

Loss analysis approach

The focus of the loss analysis is PERC solar cells; PERC cells and fabricated test samples were therefore produced in parallel to independently characterize different regions of the solar cell. The fabrication of the solar cells and the test samples will be presented in the next section.

The solar cells and test samples are

characterized using several techniques, many of which are injection-dependent techniques that allow the analysis of the solar cell close to its actual operating point. Finally, the results generated by the characterization are analysed. What makes this work special is that two different approaches are used simultaneously to analyse the same set of data:

- The experimental loss analysis is a minor modification of the one presented in Wong et al. [12]. The losses are separated into three different types: 1) recombination losses in open-circuit conditions (V_{oc} losses); 2) fill factor (*FF*) losses; and 3) current losses in short-circuit conditions (j_{sc} losses). This loss analysis is closely derived from the experiments.

- To complement the experimental loss analysis, a simulation is carried out. The experimental data from the experimental loss analysis are used to ensure that the simulation is as realistic as possible. Finally, a simulation-based loss analysis is obtained.

A schematic of the loss analysis approach is given in Fig. 1.

Experimental

Solar cell fabrication

The solar cells used in this study were fabricated entirely in the PV-TEC pilot line at Fraunhofer ISE [11]; the process flow is shown in Fig. 2(a). Commercially available industrial tools were used for each of the fabrication processes. Standard-size pseudo-square wafers with an edge length of 156mm were used. The base material was magnetically cast p-type Czochralski-grown silicon (MCz-Si) with a base resistivity ρ_B = 1.4Ωcm. After an alkaline saw-damage removal, the wafers were alkaline textured, and the rear side was chemically polished. The homogeneous emitter was formed in an industrial tube furnace with a diffusion process using $POCl_3$ [14].

Prior to surface passivation, the rear emitter was wet-chemically removed, followed by a cleaning step (SC1/SC2 [15]). The passivation of the rear surface was obtained by an aluminium oxide (Al_2O_3) layer deposited by fast atomic layer deposition (ALD). The ALD process was followed by an outgassing step performed in a tube furnace. A silicon oxide (SiO_x) and silicon nitride (SiN_y) layer stack (Group 1) or a single SiN_y layer (Group 2) served as capping layers. The capping layers were deposited using plasma-enhanced chemical vapour deposition (PECVD). As regards the front-surface passivation, a double-layer anti-reflection coating (ARC) was applied in the case of Group 1, whereas a standard PECVD SiN_z layer was used for Group 2. All the processes employed up to this stage for what is referred to later as the *front end*.

The processes from this stage on, until the finalization of the solar cells, constitute the *back end*; these processes are associated with the formation of the metal contacts. The rear layer stack was locally ablated using a laser process in order to obtain a line-shaped local contact opening (LCO). The front- and rear-side metallizations were applied using screen printing. The front grid featured five busbars, and the rear electrode consisted of full-area screen-printed aluminium (Al). Finally, the contact firing was performed in an industrial conveyor belt furnace. The front and rear cell design is illustrated in Fig. 2(b).

Test sample creation

In order to separate the recombination currents under open-circuit conditions from different parts of the solar cell, test samples were created in parallel with the fabrication of the solar cells. The wafers and the processes used for these samples were the same as for the solar cells, the only difference being the process sequences.

First, the focus was directed on the samples used for the characterization of the front end. After passivation, the samples were fired without metal present on the wafer surfaces. These samples allow the extraction of the implied open-circuit voltage (iV_{oc}), and are referred to as iV_{oc} *samples*. In order to further characterize the front end, three types of symmetric sample were needed. One type (j_{0e} samples) featured the front surface of an iV_{oc} sample on both sides and allowed the extraction of the recombination

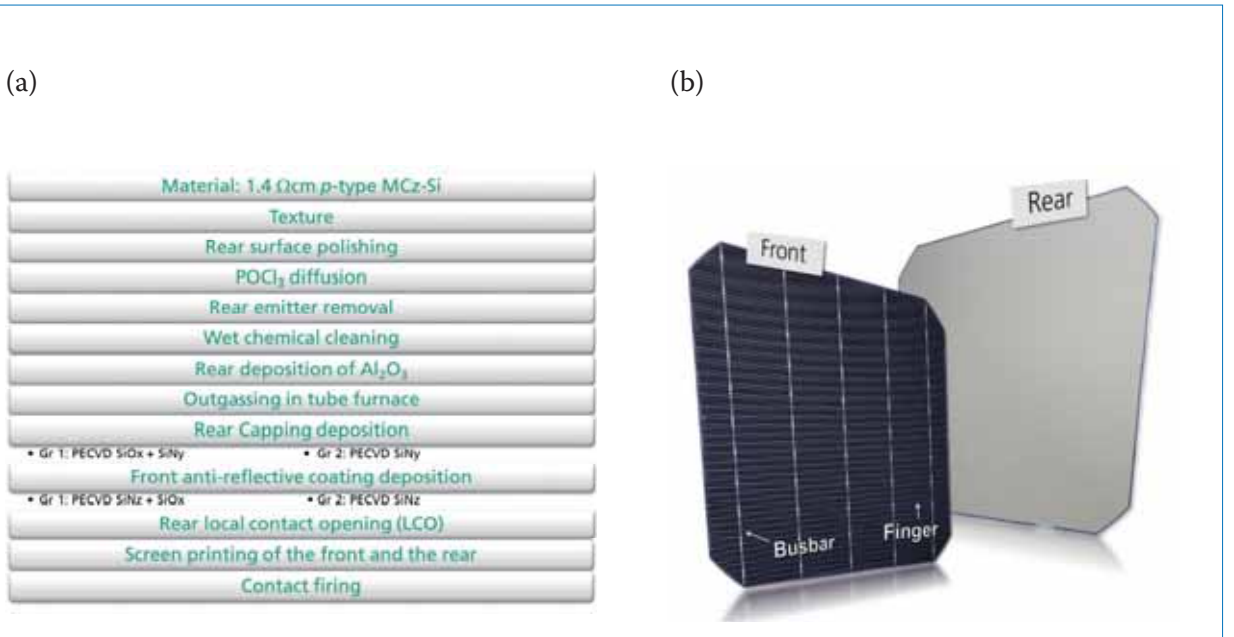

Figure 2. (a) Process flow used for the fabrication of the PERC solar cells at Fraunhofer ISE. (b) The fabricated PERC solar cells, showing the front and rear screen-printed designs.

of the emitter. The second type (S_{pass} samples) featured the rear surface of an iV_{oc} sample on both sides, and allowed the extraction of the recombination due to the rear-side passivation. For the third type, the lifetime of the bulk (τ_{bulk}) was obtained by etching back the passivation layers of the S_{pass} samples using concentrated hydrofluoric acid (HF) and potassium hydroxide (KOH), and then re-passivating both sides with high-quality PECVD AlO_x and subsequent annealing at 425°C.

To study the back end, modified iV_{oc} samples were fabricated:

- iV_{oc} samples with front-side (FS) metallization but no rear-side (RS) metallization. These allowed the loss caused by the front-side metallization to be determined (iV_{oc} + FS Ag).
- iV_{oc} samples with LCO and rear Al. These allowed a determination of the loss caused by the rear contact where a local aluminium back-surface field (Al-BSF) is formed (iV_{oc} + RS LCO).

A schematic of the test sample and the associated recombination in different parts of the solar cell is presented in Fig. 3.

Characterization

Illuminated current–voltage characterization

The current–voltage (I–V) characteristics of the PERC cells were measured using an industrial cell tester. The I–V characteristics of selected samples were independently measured by the Fraunhofer ISE CalLab PV Cells.

The resulting I–V measurements under illumination are summarized in Table 1. Peak energy conversion efficiencies of η = 21.4% and η = 21.1% were obtained for Groups 1 and 2 respectively. The main difference between the groups is the current (j_{sc}), which is higher for Group 1 because of the double-layer ARC and the double capping layers on the rear. The industrial cell tester also includes SunsV_{oc} measurements, I–V measurements in the dark, and busbar-to-busbar resistivity measurements; these will be used later for the analysis of the fill factor. In the following discussion of the work, the characterization and loss analysis focuses on Group 2 (with a single-layer ARC), as it is more representative of current industrial PERC solar cells.

QSSPC, SunsPL and SunsV_{oc} characterization

In order to study the recombination current under open-circuit conditions at 1 sun illumination, and represent it as a function of the injection density for each part of the solar cell, each test sample presented in Fig. 3 needed to be measured by a system with which injection-dependent measurements are possible. The non-metallized samples were measured using quasi-steady-state photoconductance (QSSPC) measurements [16]. The recombination current density j_{rec} as a function of the implied voltage was calculated directly from the measured effective lifetime as a function of the minority-carrier density.

The metallized samples were measured by means of calibrated suns-photoluminescence (SunsPL) [17]. Here, the laser light intensity was varied and measured by a calibrated reference cell. The PL signal was calibrated to implied voltage using two different measurements:

1. The QSSPC measurement of the iV_{oc} samples.
2. The illuminated I–V measurement of the solar cell.

Both of these calibrations yielded very consistent results.

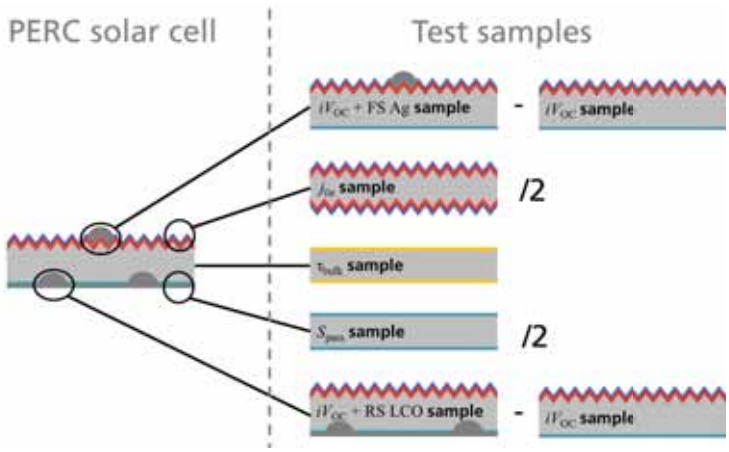

Figure 3. Schematics of the PERC solar cells and of the test samples used for the characterization of the different regions of the cell. To obtain the recombination due to the contacts (front or rear contact), the recombination of the sample without contacts is subtracted from the recombination of a sample with contacts. In order to study the recombination on the front or rear surface, symmetric samples are fabricated whose recombination currents are divided by two, to account for only one surface.

Group		V_{oc} [mV]	j_{sc} [mA/cm^2]	FF [%]	η [%]
1 (double-layer ARC)	Best cell	668	40.0	80.2	21.4*
	Average of 13 cells	664±3	40.1±0.05	80.2±0.4	21.3±0.2
2 (single-layer ARC)	Best cell	665	39.4	80.3	21.1*
	Average of 13 cells	662±5	39.6±0.03	80.1±0.7	21.0±0.3

Table 1. Open-circuit voltage V_{oc}, short-circuit current density j_{sc}, fill factor FF and energy conversion efficiency η for both PERC solar cell groups. The most efficient cell of each group was independently measured at Fraunhofer ISE CalLab PV Cells, and indicated by *.

Finally, the injection-dependent behaviour of the solar cell was obtained using SunsV_{oc} measurements, where the recombination current as a function of the junction voltage was directly measured; therefore, for each test sample, the recombination current was obtained as a function of the implied voltage (Fig. 4). For the experimental loss analysis, only the recombination current at V_{oc} of the finished solar cells (665mV) was used; however, for the simulation-based loss analysis, the entire injection-dependent measurements were taken into account.

Fill-factor-related characterization

The fill factor was first studied by comparing the actual fill factor ($FF \approx 80.1\%$), the pseudo fill factor ($pFF \approx 82.7\%$), and the theoretical maximal fill factor ($FF_0 \approx 83.7\%$) [18]. The FF was determined to have decreased by $2.6\%_{abs.}$ because of resistive losses, and by $1\%_{abs.}$ because of shunt and non-linear recombination as well as possibly inhomogeneous spatial recombination, such as edge recombination (mainly second-diode saturation current density j_{02}). The resistive losses can be further divided using an analytical model of the front-side resistance [19]. The following measured parameters were used as input parameters: the emitter sheet resistance $R_{sh} = 85\Omega/sq.$; the specific contact resistance of the front metal contacts $\rho_c = 3m\Omega cm^2$; and the specific resistance of a metal grid finger $R_{Grid} = 47\Omega/m$. The spreading resistance in the base was obtained by means of an analytical model [20]. The contact resistance at the local rear contacts was neglected, because it is assumed to cause only a gradually vanishing efficiency loss [21].

Short-circuit-current-related characterization

The j_{sc} was studied by measuring the reflectance and spectral response [22]. The shading of the front contacts, the reflectance of the active cell area and the escape light were obtained from the reflection measurements, as described in Thaidigsmann et al. [22]. The emitter recombination was calculated by integrating the internal quantum efficiency in the short-wavelength range ($250nm \leq \lambda \leq 600nm$). The losses corresponding to the bulk and rear recombinations and to the parasitic absorption in the rear metal are determined by performing the same integration in the long-wavelength range ($600nm \leq \lambda \leq 1{,}200nm$). These losses for $600nm \leq \lambda \leq 1{,}200nm$ cannot be separated from one another directly from the measurements alone. The separation of these losses was treated in the simulation part of the loss analysis (see Fig. 5). All losses were weighted with the AM1.5g standard spectrum [23] to obtain a current density.

Loss analysis

Experiment-based loss analysis

For each loss category (recombination at V_{oc}, FF and j_{sc} losses), the losses of the different parts of the solar cell were compared in order to obtain a relative loss in per cent. However, as the losses of different categories cannot be compared with one another, each category needs to be analysed separately. This is the main limitation of this experimental loss analysis, as it

is not possible to obtain the total losses for one specific part of the solar cell. For example, this method allows the calculation of how many per cent of the recombination losses, the *FF* losses and the current losses are accounted for by the front metal grid. However, since the way in which the losses of different categories are related to the total losses is unknown, this method does not allow the calculation of the total influence of the front metal grid on cell efficiency. The relative losses for each category and for each part of the solar cell are shown in Fig. 5.

Simulation-based loss analysis

Numerical simulations of the optics, the special samples and the finished solar cells were conducted using a Sentaurus TCAD; the measurement results of cell Group 2 were used as input to the simulation, and each part of the simulation was compared with the experiment equivalent in order to achieve a realistic model. State-of-the-art physical models [24] were employed. In order to set up the most realistic parameter for the modelling of the PERC solar cell, all the test samples were also simulated for the entire measured range of injection density. The PERC solar cell was then simulated using the acquired calibrated input.

On the basis of these simulations, a free-energy loss analysis was conducted for the finished solar cell. In contrast to the analytical loss analysis, the free-energy loss analysis, including the optical part [25], gives an evaluation of the losses at maximum power point condition and allows the direct comparison of the losses with each other (see Fig. 5).

> "The results from the simulation agreed fairly well with the results obtained experimentally."

The consistency between the experimental and the simulation loss analyses was verified by comparing the distribution of losses between the categories. For the optical losses, the rear parasitic absorption is reflected in the experimental analysis combined with base and rear recombination, and therefore cannot be compared specifically; as for the other optical losses, the measured and simulated distributions differed by less than 3%. For the recombination losses,

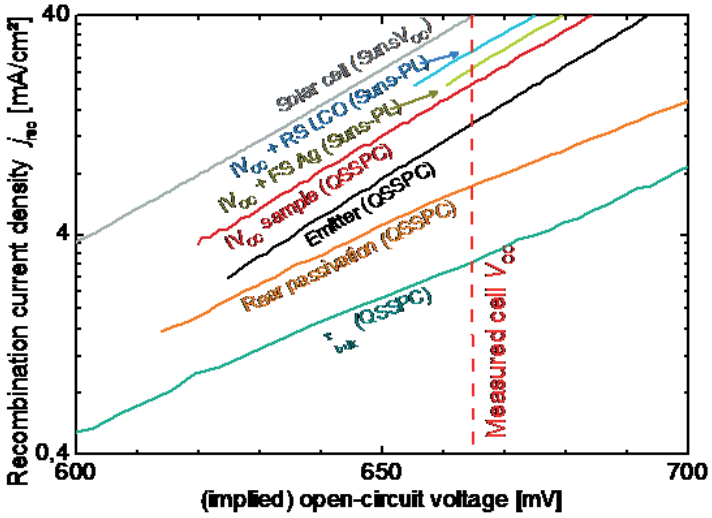

Figure 4. Recombination current density as a function of implied or real open-circuit voltage, for each test sample.

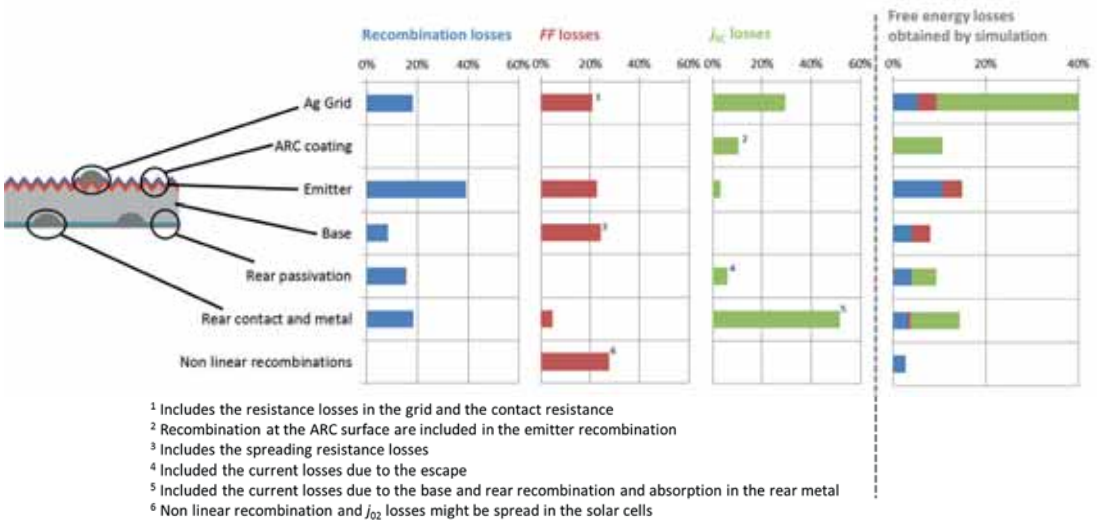

Figure 5. Results of the experiment- and simulation-based loss analyses. For the experiment-based analysis, the recombination, fill factor and current losses are presented separately. For the simulation-based analysis, all the loss categories can be grouped together. This loss analysis focuses on the cell from Group 2 only.

an additional simulation in open-circuit condition was carried out. The measured and simulated distributions of the losses differed by less than 5%, whereas the distributions of the transport losses differed by less than 3%. The highest difference (5%) in loss distribution was thus observed for the recombination losses, which are also the most difficult to characterize. However, it was concluded that the results from the simulation agreed fairly well with the results obtained experimentally (Fig. 5).

Discussion

The main optical losses of the solar cells are due to the front metal reflection and rear absorption, which could be slightly reduced using advanced metallization technologies. The reflectance between the fingers can be decreased using a double-layer ARC (the best cell in this work). However, this approach might not improve the module output power. The recombination on the front side (emitter + front metal grid) is the dominant recombination loss mechanism; this could be reduced by the implementation of a selective emitter. The losses associated with the transport are fairly equally distributed (electron, hole and metal) and represent a small share of the total losses.

In the next section, the focus will be on using simulations to predict the impact of technological developments on the efficiency of PERC cells. With regard to this, a complete loss analysis has been published in more detail in Saint-Cast et al. [26].

Next technological steps

In order to plan the next technology, it is firstly very important to thoroughly understand current technology and its limitations. The work carried out so far has provided a very good and precise knowledge of the status quo, and the model constructed for the calculations relating to the loss analysis is a very good starting point for further simulations. To simulate possible technological improvements, one can start with current technology and proceed to change the parameters corresponding to each improvement in the simulation. Hence, the approach taken here is scenario-based, whereby the improvement that leads to the highest gain in efficiency is iteratively chosen. It is necessary to postulate and simulate different scenarios in order to explore these routes and determine whether or not they can lead to the optimal cell structure in an efficient manner. The downside of this method is that simulation results are only obtained for just a few postulated scenarios, and interesting combinations might therefore remain unexplored.

The obvious solution is then to explore all possibilities. While this might sound very appealing, it would clearly be impossible to achieve, considering the number of simulations required for exploring the entire input space. For example, if 13 variables on five levels are varied in a full-factorial design, this would demand 5^{13} simulations, or more than 1.2 billion simulations in order to cover the input space. Fraunhofer ISE's approach is to simulate monocrystalline p-type PERC cells using a state-of-the-art design of experiment (DoE) and metamodelling approach, formerly also applied to multicrystalline PERC cells [27–29]. It was found that 1,000 simulations are sufficient to preserve the accuracy of the numerical device simulations in the metamodel, which reduces the number of required simulations by a factor of a million. As an example, this kind of arrangement for a three-dimensional space is shown in Fig. 6.

With the application of the metamodel being fairly rapid, it is now possible to iteratively detect the technological improvements that would lead to the highest gain in efficiency. Since the entire input space is readily available, physical and technological constraints on the input parameters (such as series resistance contribution and shading ratio of the front-side metallization, which cannot be varied independently) can be implemented. Furthermore, the distance of the local contacts on the rear side is optimized for every technology in order to obtain a fair comparison in the simulation. The described process leads to a roadmap that anticipates the possibility of producing monocrystalline p-type silicon PERC cells with efficiencies above 23%. Starting with the current technology, the milestones on this roadmap (see Fig. 7) are: the introduction of a selective emitter followed by an improved front metallization, an improved local back-surface field, an improved rear passivation, and finally the use of a double-layer ARC. More details about this approach will be reported in a future publication [30].

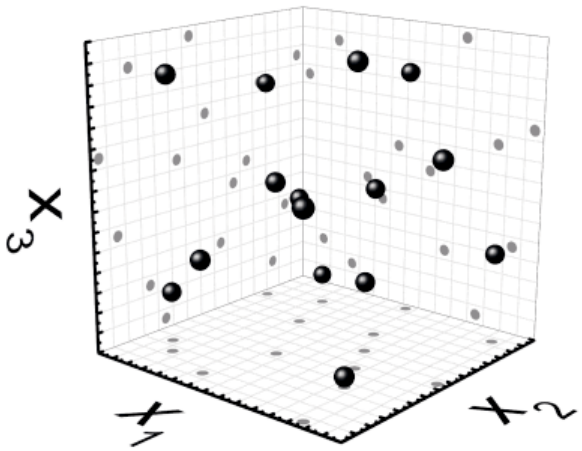

Figure 6. Example of a space-filling DoE for a three-dimensional variable space. The grey points are the projections onto the planes spanned by the axes.

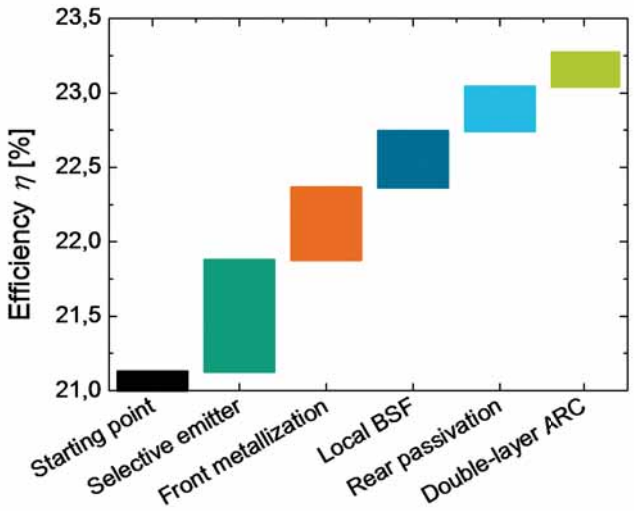

Figure 7. Cell efficiency as a function of the technological improvement for present and future PERC solar cell technology.

"The described process leads to a roadmap that anticipates the possibility of producing monocrystalline p-type silicon PERC cells with efficiencies above 23%."

Summary

The work reported in this paper has provided an extensive loss analysis of PERC solar cells fabricated in the PV-TEC pilot line, with up to 21.4% conversion efficiency. A reliable loss analysis of the current PERC cell technology with homogeneous emitter has been made available thanks to this study. The main losses of the solar cell studied, due first to the front grid and second to the recombination in the emitter, are located on the front surface. This opportunity to build a realistic simulation model of the PERC solar cell was used to advantage; the model allowed a numerically based power loss analysis at the maximum power point. The results were in fairly good agreement with the experimental loss analysis.

With a solid understanding of current technology, a method was developed to explore the effect of technological improvements through simulations. This method allows potential technological improvements of future PERC solar cells to be mapped out on a roadmap. The next stage for improvement is the implementation of a selective emitter, leading to an efficiency close to 22%. Conversion efficiencies of 23.3% could be realized after further improvements to the front metallization, the local rear contact, the rear passivation and the ARC.

Acknowledgements

This work was conducted within the frameworks of the projects CUT-A (0325823) and CUT-B (0325910A), supported by the German Federal Ministry of Economics and Energy (BMWi).

References

[1] Blakers, A.W. et al. 1989, *Appl. Phys. Lett.*, Vol. 55, pp. 1363–1365.
[2] Münzer, K.A. et al. 2010, *Proc. 25th EU PVSEC*, Valencia, Spain, p. 2314.
[3] Engelhart, P. et al. 2011, *Proc. 26th EU PVSEC*, Hamburg, Germany, p. 821.
[4] Tjahjono, B. et al. 2013, *Proc. 28th EU PVSEC*, Paris, France, p. 775.
[5] Neuhaus, H. 2016, PVCellTech Conf., Kuala Lumpur, Malaysia.
[6] Metz, A. et al. 2014, *Sol. Energy Mater. Sol. Cells*, Vol. 120, p. 417.
[7] Dullweber, T. et al. 2014, *Proc. 30th EU PVSEC*, Kyoto, Japan, p. 621.
[8] Gintech 2016, Press Release (Jan. 5), *pv magazine*.
[9] Trina solar 2015, Press Release (Dec. 16), *pv magazine*.
[10] Solar World AG 2016, Press Release (Jan. 14), *pv magazine*.
[11] Biro, D. et al. 2006, *Proc. 21st EU PVSEC*, Dresden, Germany, pp. 621–624.
[12] Wong, J. et al. 2015, *IEEE J. Photovolt.*, Vol. 5, No. 2.
[13] Brendel, R. et al. 2015, *Prog. Photovoltaics Res. Appl.*, DOI: 10.1002/pip.2696.
[14] Werner, S. et al. 2014, *Proc. 29th EU PVSEC*, Amsterdam, The Netherlands, p. 1342.

[15] Kern, W. et al. 1970, *RCA Review*, Vol. 31, pp. 187–205.
[16] Sinton, R.A. & Cuevas, A. 1996, *Appl. Phys. Lett.*, Vol. 69, No. 17, pp. 2510–2512.
[17] Trupke, T. et al. 2015, *Appl. Phys. Lett.*, Vol. 87, No. 9, p. 93503.
[18] Greulich, J. et al. 2010, *Prog. Photovoltaics Res. Appl.*, Vol. 18, No. 7, pp. 511–515.
[19] Fellmeth, T. et al. 2014, *IEEE J. Photovolt.*, Vol. 4, No. 1, pp. 504–513.
[20] Saint-Cast, P. 2012, Ph.D. dissertation, Constance University, Germany, p. 61.
[21] Müller, M. et al. 2014, *J. Appl. Phys.*, Vol. 115, p. 084505, DOI 10.1063/1.4867188.
[22] Thaidigsmann, B. et al. 2009, *Proc. 24th EU PVSEC*, Hamburg, Germany, pp. 2056–2059.
[23] IEC 60904-3:2008, "Photovoltaic devices: Part 3. Measurement principles for terrestrial photovoltaic (PV) solar devices with reference spectral irradiance data".
[24] Altermatt, P.P. 2011, *J. Computat. Electron.*, Vol. 10, pp. 314–330.
[25] Greulich, J. et al. 2013, *J. Appl. Phys.*, Vol. 114, No. 20, p. 204504.
[26] Saint-Cast, P. et al. 2016, "Analysis of the losses of industrial-type PERC solar cells", *physica status solidi (a)*, DOI 10.1002/pssa.201600708.
[27] Wasmer, S. et al. 2016, "Understanding process-related efficiency variations in mc-Si PERC cells", *Photovoltaics International*, 31st edn, pp. 43–52.
[28] Wasmer, S. et al. 2016, "Impact of material and process variations on the distribution of multicrystalline silicon PERC cell efficiencies", *IEEE J. Photovolt.* (10.1109/JPHOTOV.2016.2626145).
[29] Müller, M. et al. 2014, "Sensitivity analysis of industrial multicrystalline PERC silicon solar cells by means of 3-D device simulation and metamodeling", *IEEE J. Photovolt.*, Vol. 4, No. 1, pp. 107–113.
[30] Wasmer, S. et al. 2017 [forthcoming], 7th Int. Conf. Crystall. Si. Photovolt., Freiburg, Germany.

About the Authors

Pierre Saint-Cast received his M.Sc. in micro- and nanoelectronics from Joseph Fourier University, Grenoble, France, and his engineering degree from the Polytechnic Institute of Grenoble, both in 2007. In 2012 he was awarded a Ph.D. by the University of Konstanz, Germany. Since 2008 he has been with Fraunhofer ISE, where his research interests include the development of passivation layers for solar cell applications, and the processing, analysis and analytical modelling of PERC solar cells.

Sven Wasmer studied physics at the University of Freiburg, Germany, and received his diploma in 2013, in collaboration with Fraunhofer ISE. He is currently working towards his Ph.D. at Fraunhofer ISE, with a topic of the characterization and simulation of process variations in solar cell production.

Johannes Greulich studied physics in Heidelberg and in Freiburg, Germany, where he received a diploma degree in 2010. In 2014 he obtained his Ph.D. in physics from the University of Freiburg for his work on the simulation and characterization of novel large-area silicon solar cells. Since 2015 he has been head of a research team at Fraunhofer ISE, working on inline solar cell characterization, device simulation and image processing.

Sabrina Werner studied physics at the University of Freiburg, Germany, and received her diploma degree in 2011. Since 2009 she has been with Fraunhofer ISE, working in the PV production technology and quality assurance division. Her research interests include the investigation and improvement of high-temperature processes and passivated solar cells.

Ulrich Jaeger received his diploma degree in physics in 2008 from the Technical University of Darmstadt, Germany. From 2008 to 2013 he worked at Fraunhofer ISE, both as a Ph.D. student and a postdoctoral researcher in the PV production technology and quality assurance division, on the topic of laser doping for the industrial fabrication of crystalline silicon solar cells and as a project manager for the development of passivated silicon solar cells. Since 2016 he has been with RENA Technologies GmbH, where he is involved in sales and business development for production equipment for PV devices.

Elmar Lohmüller studied physics at the University of Tübingen, and at Nelson Mandela Metropolitan University, Port Elizabeth, South Africa. He received his diploma degree in 2010 for his work at Fraunhofer ISE on the development of p-type MWT-PERC solar cells. He then worked on the development of n-type MWT solar cells, for which he received a Ph.D. from the University of Freiburg in 2015. He is currently a researcher at Fraunhofer ISE, where he focuses on the development of p-type PERC solar cells.

Hannes Höffler studied physics at the University of Freiburg, Germany, and received his diploma in 2010. In 2015 he was awarded a Ph.D. in physics by the University of Freiburg for his work on luminescence imaging and its applications in the processing of silicon solar cells in an industrial environment. He is currently responsible for the offline characterization laboratory in the PV production technology and quality assurance division at Fraunhofer ISE.

Ralf Preu is the director of the PV production technology and quality assurance division at Fraunhofer ISE in Freiburg, Germany, and also teaches photovoltaics at the University of Freiburg. He studied physics at the universities of Freiburg and Toronto, as well as economics at the University of Hagen, Germany, and has a Ph.D. degree in electrical engineering. He joined Fraunhofer ISE in 1993 and has worked in different fields in PV, including system monitoring, and silicon solar cell and module technology, characterization and simulation. His main focus is on the R&D of advanced silicon solar cell technology and its transfer to industrial production.

Enquiries

Pierre Saint-Cast
Fraunhofer Institute for Solar Energy Systems ISE
Heidenhofstraße 2
79110 Freiburg, Germany

Tel: +49 (0)761 4588 5480
Email: pierre.saint-cast@ise.fraunhofer.de

High-performance screen-printable pastes for HJT cells

Stefan Körner & **Markus Eberstein**, Fraunhofer IKTS, Dresden, Germany

ABSTRACT

A highly promising concept for future solar cells is the heterojunction (HJT) architecture; according to the ITRPV roadmap 2016, the market share for HJT solar cells will increase to 10% by 2026. Over this timescale, stabilized cell efficiency will increase to 24%, which is the second-highest predicted efficiency after back-contact cells with n-type mono-Si. Moreover, metallization of HJT cells offers the advantage of using low-temperature steps, which reduces energy consumption and hence production costs. However, attaining the predicted goals requires a further improvement in the performance of metallization pastes in terms of process ability, conductivity, and contact resistance to the indium tin oxide (ITO) layer. Today's paste systems pose difficulties in handling during processing, especially with regard to the storage conditions. In the study reported in this paper, new metallization pastes for HJT solar cells are examined. These new pastes demonstrate excellent electrical performance using an infrared radiation-based curing profile, with efficiencies reaching 21.7%. Along with an additional gain in electrical characteristics, the standard deviation is decreased compared with conventional convection curing. The electrical performance of the new paste is similar to (or even better than) that of currently available reference metallization pastes, while a significantly easier handling and processing behaviour is observed. Using the contemporary generations of new pastes with bimodal silver mixture, the sheet resistance is decreased to 2.7mΩ/sq.

Introduction

The 2016 international technology roadmap for photovoltaics forecasts that the market share for silicon heterojunction (HJT) solar cells will see an increase of up to 10% by the year 2026; over this timescale, HJT cell efficiency is expected to increase to 24% [1]. This is the second-highest predicted efficiency after back-contact cells with n-type mono-Si.

> "The development of high-conductance systems that can be cured at temperatures lower than the required 200°C is a new challenge for paste manufacturers."

The HJT cell architecture includes two temperature-sensitive layers: 1) an intrinsic amorphous silicon for passivation of the base; and 2) a boron-doped amorphous layer as the emitter, obtained by plasma-enhanced chemical vapour deposition (PECVD). These two layers limit the maximum process temperature to 200°C in all subsequent process steps. As the top layer, an indium tin oxide layer (ITO) is deposited as transparent conductive oxide (TCO); this acts additionally as an anti-reflection coating and provides conductivity in the top layer, which decreases the contact resistance between the front-side metallization and the solar cell. As regards the metallization grid on top, the development of high-conductance systems that can be cured at temperatures lower than the required 200°C is a new challenge for paste manufacturers.

In the study reported here, the development of front-side metallization pastes for low-temperature applications was investigated. For low-temperature curable binders, different polymers were evaluated with regard to solubility in various solvents, rheological properties and curing conditions. Silver was added to the organic vehicle as a functional phase in the preparation of the pastes; the amount of silver was systematically varied, and the influence on the electrical properties was investigated. Solar cells were fabricated with these pastes and characterized. Additionally, nanoparticles and low melting point alloys (LMPAs) were examined as paste additions. The curing was carried out on a production scale in a new belt furnace, which provided heat transfer either by convection or by infrared in an air or a nitrogen atmosphere.

Polymer	Type	Glass transition [°C]	Melting point [°C]
A	Epoxy	110	>200
B	Epoxy	130	>200
C	Vinyl	68	135–210

Table 1. Types of polymer used in the study and selected thermal properties.

Solvent	Polarity	Boiling point [°C]
I	++	<100
II	0	>150
III	++	<100
IV	–	>200
V	+	>200
VI	0	>200
VII	– –	<100

Table 2. Polarities and boiling points of the different solvents used in the study.

Experiments

Organic vehicle preparation

For the preparation of the organic vehicle (or *binder*), different polymers were selected because of their thermal properties, such as glass transition and melting point (Table 1). The polymers were then dissolved in various solvents. The polarity of the solvents was varied (Table 2) in order to influence the solubility of the polymers and the binder properties, such as viscosity and curing conditions.

All polymer–solvent combinations were treated in the same way. A mixture of polymer and solvent was prepared and stirred with a magnetic stirrer; the solubility was evaluated after 1, 12 and 24 hours of stirring. Binders with fully dissolved polymer were thermally treated for 10 minutes at 150, 180, 200 and 240°C in order to determine the optimal curing conditions.

Paste production

After the preparation of the organic vehicle, the pastes were created. For this, two binders were chosen and mixed with a flaky silver powder with a particle size of less than 10µm. The powder was added gradually, and after each powder addition the paste was mixed in a centrifugal mixer (Speedmixer DAC150 FVZ). Homogenization using a three-roll mill was then performed. The solids content was varied systematically, and an attempt was made to maximize the content in order to lower the resistance in the final layer. During the curing process, the mass loss was determined so that the evaporation rate of the solvent could be controlled.

In the case of the paste preparation using the LMPA to reduce the amount of silver, a powder with a melting point of 138°C was chosen. The LMPA powder was treated with different organic reduction agents before paste preparation; this inhibited the oxidation of the non-noble powder during the curing of the final paste.

Besides the LMPA, silver nanoparticles were added to the paste; these nanoparticles were suspended in solvent V. The polymer was then added, in an appropriate fraction, to the suspension. Following the preparation of the nanoparticle pre-paste, the flaky silver powder was added.

All pastes were subsequently printed on alumina ceramic as the test substrate, and cured using different time–temperature regimes; electrical characterization was then performed. Additionally, field emission scanning electron microscopy (FESEM) images of cross sections of the chosen pastes were taken, and the relationship of conductivity with structural properties was determined.

Solar cell production

To test paste 7 on the solar cells, ten wafers (Meyer Burger Germany) were printed and cured. For comparison purposes, a state-of-the-art commercial paste was printed on ten wafers as well. The commercial pastes must be stored in a freezer at –20°C, whereas the IKTS paste can be stored in a conventional fridge at 7°C. Next, the wafers were split into two groups: five wafers of each paste were cured for 15 minutes at 200°C with convection heat transfer, and the other five wafers of each paste were cured using the same conditions but with IR heat transfer. All wafers were then electrically characterized using a GridTouch system.

Results and discussion

Organic vehicle

In contrast to conventional high-temperature metallization paste, the polymer remains in the film after thermal processing. In consequence, the polymer in an organic vehicle for low-temperature curable paste fulfils two tasks: 1) it adjusts the viscosity of the binder, which acts as a screen-printing medium; and 2) it facilitates the adhesion between the metal particles of the paste, as well as the adhesion to the surface of the wafer. With these functions in mind, it is important to create a binder system that can provide a high solids content, with a functional phase on the one hand, and excellent screen printability on the other.

Three polymers – A, B and C – were dissolved in the various solvents with different polarity and boiling point properties (Table 2). The first property influences the solubility of the polymer, while the second determines the screen printability. If the boiling point is too low, the paste will dry on the screen, whereas if the boiling point is too high, it will take too long for complete evaporation of the solvent during thermal processing. Table 4 gives an overview of suitable polymer–solvent combinations based

Paste	Organic vehicle [polymer/solvent]	Solids content in paste [%]		
		Silver	LMPA	Nano silver
1	A/V	64.1		
2	A/V	73.6		
3	A/V	77.6		
4	B/V	78.8		
5	B/V	80.2		
6	C/V	84.6		
7	C/V	86		
8	C/V	57.3	28.7	
9	C/V			66
10	C/V	37.2		37.2

Table 3. Paste compositions.

Solvent	Polymer		
	A	B	C
I	++	++	++
II	+	++	+
III	++	++	++
IV	–	0	–
V	+	0	+
VI	–	– –	++
VII	– –	– –	– –

Table 4. Solubility ratings of the polymers used in different solvents for this study.

on an evaluation of the solubility of the polymer in the solvent.

The solubility ratings of the investigated polymers illustrate that with increasing polarity of the solvent, the polymer can be dissolved completely. When less solvent or a non-polarized solvent is used, the solubility decreases and the polymer is not dissolved completely or is simply swollen. With the use of solvent VII (which is the most unipolar solvent), the polymer remained unchanged; after this pre-test, solvent VII was not pursued any further in this study.

After testing the solubility of the solvent, the curing conditions were determined. For this, a small amount of organic vehicle was provided on aluminium plates and cured in a box oven at different temperatures for 10 minutes. Fig. 1 shows the appearance of the cured organic vehicle prepared in the case of polymer B and solvents I to VI. For all curing conditions, a solid transparent film can be obtained; however, its colour ranges from colourless to amber. The latter indicates the first signs of degradation of the polymer, which can be caused either by exceeding a certain thermal budget or by reactions between solvent and polymer. Curing the polymer alone without any solvent will result in a colourless layer. In general, discolouring increases with increasing temperature: all solvent–polymer combinations, apart from solvents II and V, begin to discolour at 180°C. For solvents II and V, discolouring starts at the lowest temperature and increases with the thermal budget; in these cases it is concluded that there is a negative interaction between the solvents and the polymer.

When the highest curing temperature of 240°C is used, the thermal degradation for all solvents can be evidenced by the dark appearance of the samples. This temperature was chosen despite the maximum process temperature allowed by the HJT wafer, in order to determine if any effects of polymer degradation could be seen using this simple set-up.

The images for polymer A are not shown here; degradation effects cannot be seen because of the initial reddish colour of the polymer. The use of polymer C results in colourless layers, which did not show any negative influences from temperature or from solvent–polymer interactions. With this in mind, and taking into account the boiling points of the solvents, further experiments were performed just using solvent V. When solvents with boiling points below 100°C are used, this will probably result in fast-drying pastes which would be difficult to screen print. With the solvents II, IV and VI, which have the highest boiling points, it is possible that evaporation of the solvent will take too long and thus the pastes would not be a practical solution. Solvent V, however, should be a good compromise between solubility and curing conditions.

Paste characterization

The electrical conductivity of a polymer–silver composite depends on the solids content of silver in the cured layer. If the silver content is high enough, the conductivity in the dried layer is provided by percolation between the metal particles. Assuming a density of the organic vehicle of roughly 1g/cm^3, the critical silver content for percolation to occur between the particles is in the range 20–30vol% (72–82wt%) [2]. With this in mind, the paste was dried in order to increase the solids content, but still maintain its screen-printability. (See Table 3 for the composition of the pastes tested.)

Fig. 2 depicts the sheet resistances of the cured layers for pastes 1–7 as a function of curing temperature (black bar = 150°C, red bar = 200°C). Pastes 1–3 with polymer A demonstrate that a paste-curing temperature of 200°C reduces the resistivity of the final layer. For paste 1 the difference in resistance for the two temperatures is 18Ω/sq.; in contrast, for pastes 2 and 3 the difference is less than 60mΩ/sq. When

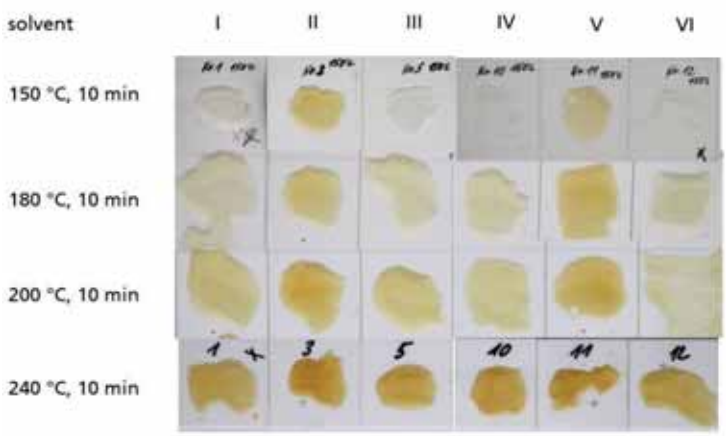

Figure 1. Images of polymer B dissolved in solvents I–VI and cured for 10 minutes at 150, 180, 200 and 240°C.

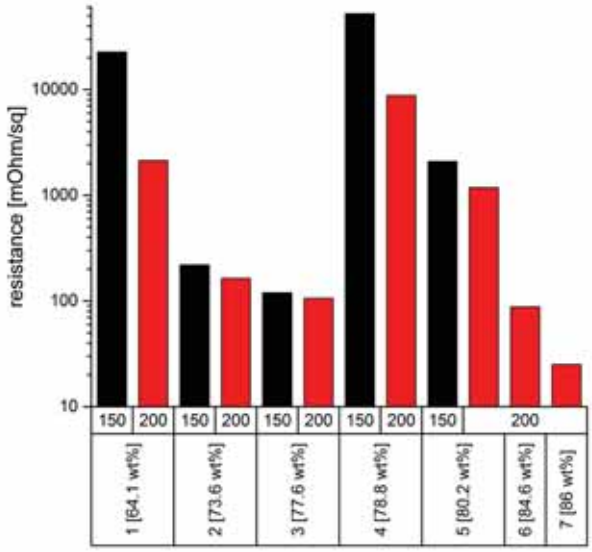

Figure 2. Sheet resistance of the cured layer as a function of paste composition and curing temperature (black bar = 150°C; red bar = 200°C). (The curing time was 10 minutes in all cases.)

the solids content is increased from 64.1wt% (paste 1) to 77.6wt% (paste 3), the resistance falls by approximately 2,000mΩ/sq. at 200°C. The corresponding difference for pastes 2 and 3 is of the order of 60mΩ/sq.

Increasing the amount of silver in the paste system increases the probability of creating percolation paths, and therefore of decreasing the resistance. However, a further increase in solids content was not possible with polymer A, and so the polymer matrix was changed to polymer B. Because of the change in polymer, it now became possible to increase the wt% of silver to 80.2.

The influence of temperature is similar to that for polymer A: with increasing temperature, the resistance decreases. At the same time, a higher temperature results in complete evaporation of the solvent used during organic vehicle preparation. With this in mind, it is reasonable to expect that somewhat better layer formation, especially the creation of percolation paths, could occur. Because of the higher temperature, the vapour pressure of the solvent is higher, and hence the rate of evaporation is increased. Earlier release of the solvent means that the particle arrangement in the polymer (which has not yet fully cross-linked) can happen more easily: more percolation paths are created and the resistance drops. The antagonist to this mechanism is the kinetics of the cross-linking of the polymer chains. If the cross-linking velocity is high, then the polymer hardens and consequently the solvent cannot evaporate completely. Residual solvent can increase the resistance in the final layer; moreover, the arrangement of the silver particles is hindered by the rapid cross-linking polymer matrix, which becomes very stiff and does not soften during the curing. The cross-linking for polymer B occurs somewhat faster than for polymer A, resulting in the higher resistances for paste 5 with 80.2wt% silver than for paste 3 with 77.6wt% silver.

> "Residual solvent can increase the resistance in the final layer."

In contrast, polymer C in the pastes 6 and 7 used in this study did not cross-link during curing; therefore, the solvent can evaporate completely and the silver particle arrangement can occur. By providing an optimal viscosity for paste preparation it is also possible to increase the solids content further in comparison to the pastes with other polymer matrices; when the silver content is maximized, it is possible to decrease the resistance to 25.1mΩ/sq. As regards the results for the other pastes, only the high temperature was chosen for curing in order to obtain the lowest possible resistance.

Fig. 3 shows FESEM images of cross sections of paste 3 (left) and paste 7 (right). For paste 3, the brightest regions are the silver particles, the black areas are the polymer, and the medium grey indicates inorganic inclusions from the polymer matrix (both types of particle are indicated by arrows in the figure). Between the silver particles there are black areas roughly 5µm in diameter; these are accumulations of polymer, and represent areas that are not fully homogenized with the other paste components. The image for paste 3 also shows particles that are medium grey in colour and have a diameter of around 4µm; energy dispersive X-ray (EDX) measurements were performed on these particles, and they were determined to be inorganic inclusions from the polymer.

To verify that these particles do not originate from paste preparation, the original polymer was investigated; the particles were also present in the original polymer. The commercial polymer is red, and so the conclusion is that these inorganic particles are the pigment for colouring the polymer. The cross-sectional image for paste 3 provides explanations for both the low silver content and the relatively high resistance of 106mΩ/sq. As a result of the inhomogeneous mixing of silver and polymer, the solids content is limited; additionally, these areas and

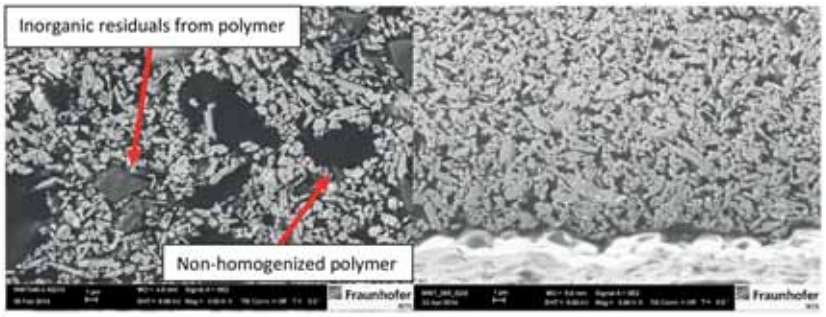

Figure 3. FESEM images of cross sections of paste 3 (polymer A; left hand side) and paste 7 (polymer C; right). Both pastes were printed on alumina for characterization and cured for 10 minutes at 200°C. (Images taken at 3,000× magnification.)

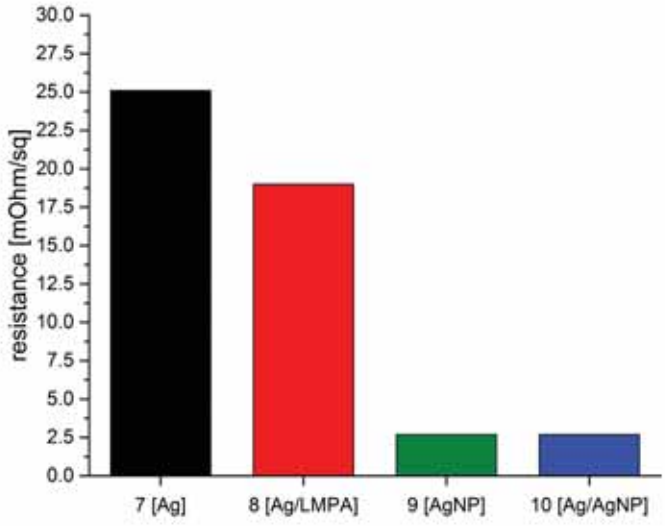

Figure 4. Sheet resistances of pastes 7–10 vs. their functional phases. All pastes were cured for 10 minutes at 200°C.

the inorganic particles are insulators and therefore increase the resistance of the cured layer.

The cross section for paste 7 (Fig. 3, right) shows a homogeneous distribution of the silver particles. The bright layer at the bottom of the image is the alumina substrate. In the paste layer itself, there are no areas of non-dispersed polymer or inorganic particles. The silver particles are close together, and there do not appear to be any insulating areas, despite the thin polymer layers between the silver particles. The probability of creating percolation paths, and hence decreasing the resistance, is high.

Another approach for decreasing the resistance by increasing the probability of conductive paths is the addition of an LMPA, which is a metal alloy with a melting point below 200°C. In most compounds of this type, the main metal is a non-noble one, and oxidation during heating is an issue. To prevent oxidation, the particles are coated with a reducing agent and then added to the metallization paste. With the controlled melting of the LMPA, conductivity is generated not just through the percolation paths between the silver, but also through the connection of the silver particles in the paste. A second effect is the decrease in cost because of the reduced amount of silver in the paste.

Yet another possibility for decreasing the resistance is to use bimodal silver powder mixtures. With these, there is an increase in packing density and thus in the number of connection points between the silver particles. If the particles are small enough, a second effect can occur: sintering can be induced because of the reduction in sintering temperature as a result of the phenomenon of melting point reduction.

Fig. 4 shows the sheet resistances of pastes 7–10 vs. their functional phases. Paste 7 (black) contains only micron-scale silver powder, providing conductivity simply by percolation paths. Paste 8 (red) includes as an additive an LMPA, which melts during curing. Because of this melting process, the silver particles are connected with each other. The conductivity in this case is provided both by percolation paths and by the silver particles connected during the melting phase. With the use of an LMPA, the resistance can be reduced from 25.1mΩ/sq. (paste 7) to 19.0mΩ/sq. (paste 8). Additionally the silver content can be lowered by one-third, which also decreases the cost of the paste.

Pastes 9 and 10, both of which contain silver nanoparticles, yield even lower resistances. Paste 9 (green) contains only nanoparticles in the metallization phase, whereas paste 10 (blue) contains a mixture of micron-scale and nano silver powder. Paste 9 delivers a sheet resistance of 2.7mΩ/sq., which is around one-tenth of that for micron-scale silver powder (paste 7). A mixture of small and large particles, as used in paste 10, can produce a similar resistance of 2.7mΩ/sq. In comparison to paste 9, however, only half of the functional phase for paste 10 consists of the cost-intensive nanoparticles. For both pastes, the silver content can be reduced by 11.6wt% compared with paste 7.

FESEM images of cross sections of pastes 7–10 are shown in Fig. 5. (Paste 7 is shown again for comparison purposes.) Paste 8 (Fig. 5, top right) contains two kinds of material: small particles of silver, and large particles of LMPA. The black areas indicate the polymer matrix. The areas without LMPA are comparable to those for paste 7 without additives (Fig. 5, top left). The LMPA particles are larger than the silver particles by a factor of ten. After curing, the surface is rough and the insides of the LMPA particles are bloated; this indicates partial melting of the particles, which results in a local melding of silver and LMPA. Controlled melting is necessary in order to prevent damage to the polymer matrix. If the LMPA is completely melted in an uncontrolled fashion, the polymer dissolves and disintegrates in the liquid metal phase, resulting in low adhesion to the substrate, as well as low adhesion of the particles to each other.

In paste 9 (Fig. 5, bottom left), the silver particles are dispersed homogeneously in the polymer matrix (black areas). For better visualization of the connections between the particles, this image has been taken at a higher magnification. The particle size is well below 500nm; with this, an initial sintering process can be provided, which results in sinter necks between the particles. This clearly results in a reduction in resistance to 2.7mΩ/sq.

Similar results can be obtained using a mixture of micron-scale and nano silver powder, as in paste 10 (bottom right). The nanoparticles are sintered together, resulting in the creation of sinter necks. Additionally, the nanoparticles are sintered with the micron-scale particles and connect them with each other. In this way, the quantity of expensive nanoparticles can be reduced without a loss in performance.

Solar cell production

Paste 7 was used to print the front-side metallization of some MeyerBurger HJT solar cells. For comparison purposes, a state-of-the-art commercially available paste for solar cell metallization was also used. To demonstrate the influence of oven atmosphere, both pastes were cured using the same profile (10 minutes at 200°C), but with different systems of

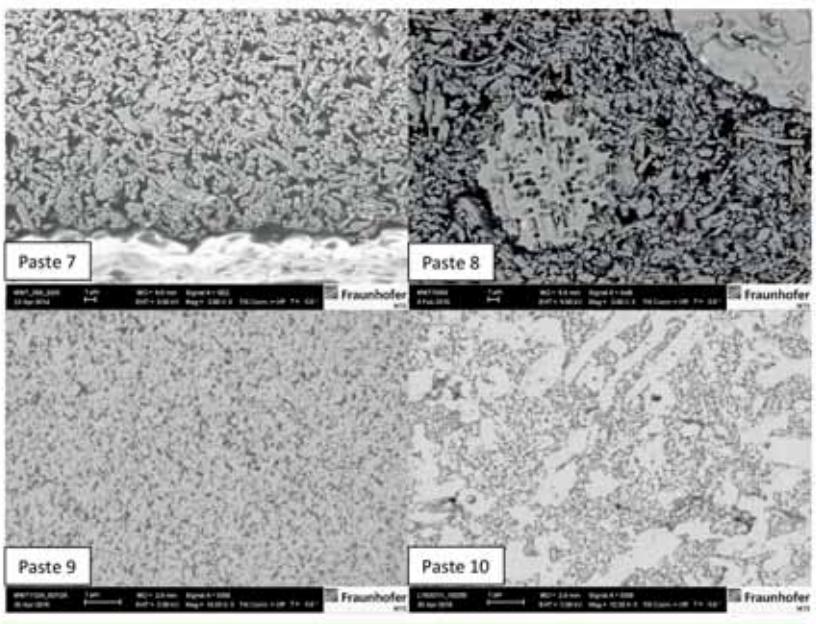

Figure 5. FESEM images of cross sections of pastes 7–10. Each paste was printed on alumina for characterization and cured for 10 minutes at 200°C. (Images for pastes 7 and 8 taken at 3,000× magnification, and for pastes 9 and 10 at 10,000× magnification.)

heat transfer in the oven: one system involves supplying heat via infrared radiation, the other via conventional convection. Fig. 6 shows the electrical data for the solar cells prepared in this study, where the red and blue columns indicate curing by infrared radiation and by convection respectively.

The short-circuit current J_{sc} (Fig. 6(a)) for the commercial paste is of the order of 37mA/cm^2. With the infrared radiation profile, J_{sc} is around 0.1mA/cm^2 higher than with convection heating. In the case of the IKTS paste, a J_{sc} of 36.7mA/cm^2 is obtained, and the IR profile again also results in slightly higher values than with convection

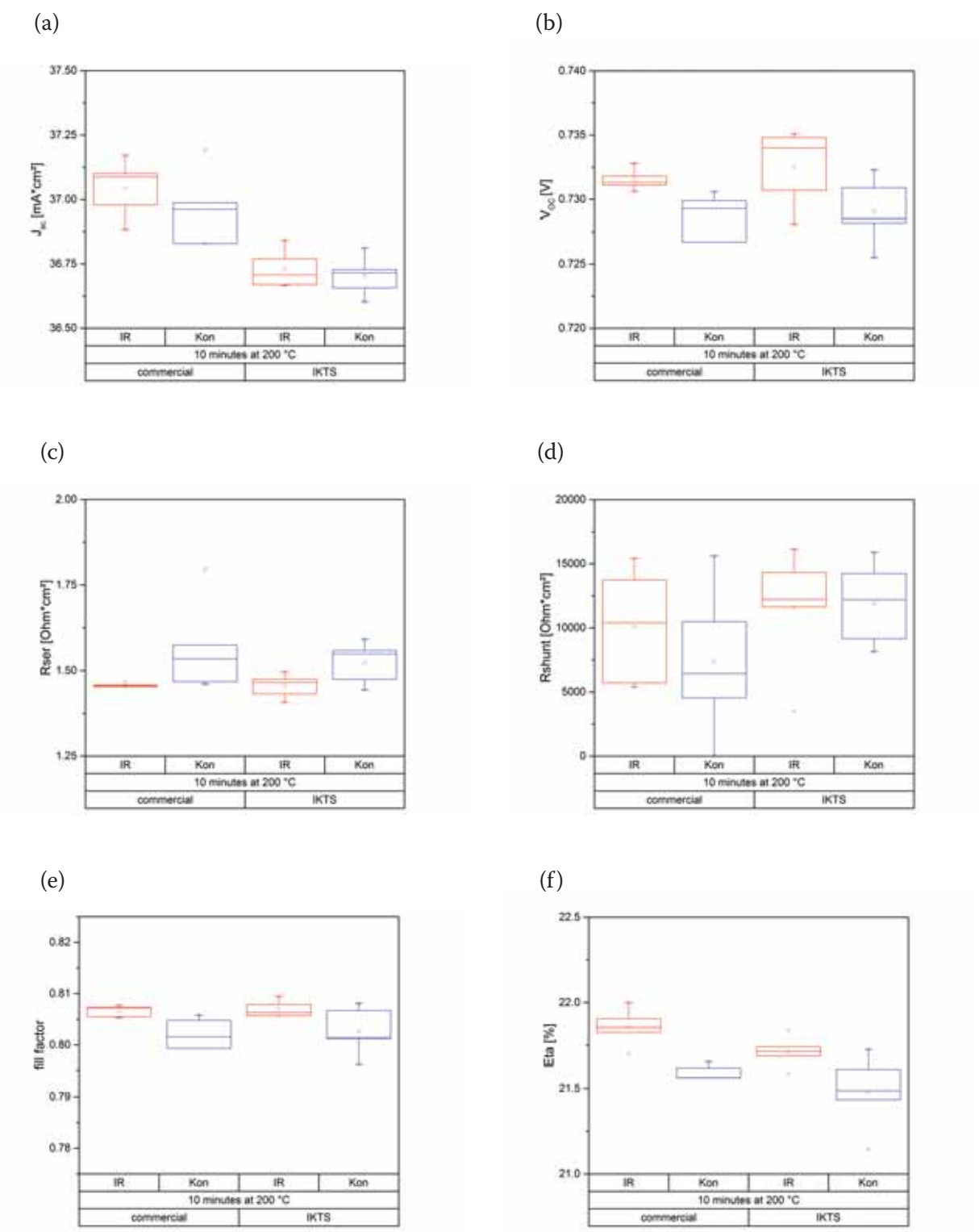

Figure 6. Electrical data for the solar cells prepared in this study as a function of the heat transfer and the paste used for printing: (a) short-circuit current J_{sc}; (b) open-circuit voltage V_{oc}; (c) series resistance R_{ser}; (d) shunt resistance R_{shunt}; (e) fill factor FF; (f) efficiency. Red columns = IR radiation; blue columns = convection. Each graph depicts the results for two pastes: commercial paste (left two columns), and IKTS paste (right two columns).

heating. A comparison of both pastes reveals that the commercial paste generates an approximately 0.25mA/cm^2 higher J_{sc} than the IKTS paste, an increase due to less spreading of the commercial paste and thus a smaller area shaded by the metallization grid.

The V_{oc} (Fig. 6(b)) for the commercial paste is ~0.73V with both curing conditions, which is comparable to that for the IKTS paste. For both pastes, the IR radiation results in a slightly higher voltage, and for the commercial paste the standard deviation is lower.

Similar results can be observed for the series resistance (Fig. 6(c)). As regards IR radiation, both pastes produce a value of R_{ser} below 1.5Ω·cm^2, with a low standard deviation; the resistance is roughly 0.1Ω·cm^2 higher using convection heating. The shunt resistance is comparable for both pastes and both curing systems.

On the basis of the data, the fill factor is greater than 80%: with the use of IR curing, a FF of 80.5% for both pastes is measured, whereas with convection heat transfer, the FF is 80.1%. The result is an efficiency level of more than 21.0%. The commercial paste yields efficiencies of 21.9% using IR curing, with a maximum cell efficiency of 22% recorded. With convection heat transfer, efficiencies of 21.6% (maximum 21.7%) are obtained. For the IKTS paste, however, the efficiency levels are somewhat lower: 21.7% efficiencies (maximum 21.8%) are achieved with IR curing, and 21.5% efficiencies (maximum 21.7%) with convection profiles. However, the use of IKTS paste offers a significant advantage with regard to handling: unlike the commercial paste, it can be stored in the fridge rather than in the freezer, which means that processing is easier because no thawing and freezing times need to be considered. Moreover, future optimization of the rheology of the paste should minimize spreading, which will result in less shading-induced J_{sc} loss.

IR curing has the advantage of moderate improvements in electrical performance. The use of radiation-based profiles results in a deeper heat transfer because of IR absorption in the wafer as well as in the silver; this means that the heat spreading in the printed layer is more homogeneous than in the case of convectional heating. With conventional heat transfer, the heat must be conducted from the surface by the metal particles to the deeper layers of the paste. This is time consuming and so the thermal budget is somewhat lower than with IR radiation; for this reason, IR is favoured for HJT cell curing.

> "The IKTS paste can be stored in a fridge instead of a freezer, which makes it a lot easier for handling by the operator."

Conclusion

In this paper an investigation of material concepts for new low-temperature contact pastes for HJT solar cell preparation has been reported. Screen-printable pastes, which are curable at 150–200°C, can be prepared using suitable polymer–solvent combinations. However, the evaporation rate and polymer cross-linking kinetics must be carefully matched. If the cross-linking occurs too fast, solvent evaporation is hindered; moreover, if fast cross-linking polymers are used, particle arrangement is inadequate, and the percolation path creation is impeded. Both of these effects lead to an increase in the resistance (R = 106.1mΩ/sq. for paste 3, compared with R > 1,000mΩ/sq. for paste 5).

If the reaction kinetics is controlled by using a suitable polymer, the resistance can be further reduced to 25.1mΩ/sq. as a result of optimized particle arrangement (paste 7). Another improvement in resistance can be obtained by means of additives, such as LMPA, or by using silver nanoparticles. The LMPA melts during curing and promotes interconnections between the silver particles; this results in decreased resistance, and lower paste costs because of the reduction in the amount of silver used.

With the use of nano silver (paste 9), an additional sintering at low temperatures can be triggered, and the resistance can be decreased to 2.7mΩ/sq. as a result of conduction through sinter necks. This is also possible by using a combination of micron-scale and nano silver powder (paste 10). Both of the nanoparticle pastes offer the second advantage of lowering the solids content, which in turn decreases the cost.

Solar cells were prepared using paste 7; with this IKTS paste, it was possible to achieve efficiencies similar to those of a state-of–the-art commercial paste. A major advantage of the IKTS paste, however, is that it can be stored in a fridge instead of a freezer, which makes it a lot easier for handling by the operator.

Finally, it was found that curing the pastes with an IR radiation profile improves electrical performance, while at the same time decreasing the standard deviation.

References

[1] SEMI PV Group Europe 2016, "International technology roadmap for photovoltaic (ITRPV): 2015 results", 7th edn (Mar.), Version 2, pp. 30–32 [http://www.itrpv.net/Reports/Downloads/].

[2] Lovinger, A.J. 1979, "Development of electrical conduction in silver-filled epoxy adhesives", *J. Adhesion,* Vol. 10, No. 1, pp. 1–15.

About the Authors

Stefan Körner is a Ph.D. student at the TU Dresden, Germany. He received his diploma in chemistry from the Chemnitz University of Technology in 2012 for research on the topic of gold nanoparticles for biochemical applications, in cooperation with the Leibniz IOM (Leipzig). He then joined the division of thick-film pastes and photovoltaics at Fraunhofer IKTS, where he works on paste development for low-temperature applications, such as HJT solar cells, and on high-temperature pastes for crystalline solar cells.

Markus Eberstein studied materials science at TU Berlin, with a particular focus on glass, and received his Ph.D. in 2001 in the field of microelectronics materials from the BAM Federal Institute for Materials Research and Testing, Berlin. He is currently the manager of the thick-film technology and photovoltaics group at Fraunhofer IKTS. The main topics of his research are structure–properties relationships of glass and ceramic thick-film materials, sintering kinetics, paste rheology and microstructure engineering.

Enquiries

Stefan Körner
Fraunhofer IKTS
Winterbergstraße 28
01277 Dresden
Germany

Tel: +49 351 2553-7817
Email: stefan.koerner@ikts.fraunhofer.de

Thin Film

News

First Solar cancels Series 5 module migration in favour of Series 6

Leading thin-film producer First Solar has decided to skip the previously planned migration to its Series 5 module platform, while bringing plans forward to migrate to its large-area Series 6 module technology to 2018.

The company made the radical decision due to cost competitiveness issues as global module prices have declined around 25% in the third quarter of 2016 alone. The Series 6 module technology will be ramped to around 3GW of capacity in 2019. This would mean that its current Series 4 product would be completely phased out in this timeframe.

The major move will also result in a workforce reduction at First Solar's manufacturing facilities both in the US and in Malaysia, while additional reductions in administrative and other staff are also planned. The workforce reduction equates to around 1,600 jobs, or 27% of First Solar's global workforce. The plant in Ohio US will be the first plant to be closed and migrated to Series 6.

Credit: First Solar

First Solar is reducing its workforce in the US and in Malaysia.

The facility is First Solar's leading production efficiency and pilot line operations. A production facility in Vietnam for Series 3 expansion several years ago but never utilized by the company will also be used for Series 6 migration.

Results

Ascent Solar's sales showed signs of life in Q3

Struggling flexible CIGS thin-film consumer product producer Ascent Solar Technologies' third quarter 2016 sales almost doubled but losses continue to mount.

Third quarter sales were US$452,674, up from US$255,323 in the previous quarter due to a catalogue of woes. Specific customer issues from the last quarter remained unresolved as the company noted that gross shipments for the period would have equated to around US$1.1 million, but due to a deferment in revenue recognition as a result of a customer contract modification as well as allowances for RMA (return merchandize authorization), sales were reported much lower.

Total revenue for the first nine months of 2016 was only US$1.42 million, compared to US$4.14 million in the prior-year period. Although the company cut costs in the quarter, operating losses for the first nine months of 2016 reached US$20.18 million.

Financing

Heliatek adding OPV thin-film capacity with €80 million funding

Organic photovoltaic (OPV) thin-film producer Heliatek has raised €80 million (US$88 million) in a new funding round to expand its 'HeliaFilm' manufacturing capacity by one million m² per annum.

It plans to establish a new manufacturing roll-to-roll facility at its existing site in Dresden over the next 18 months. Demand globally for its HeliaFilm products for the building material and the automotive industry were behind the expansion. The manufacturing expansion should create more than 50 new high-tech jobs in Saxony, Germany, the company said.

The Series D financing round comes via a €42 million equity issue, €20 million in debt and about €18 million in grants and subsidies. Innogy SE led the round of funding, while new investors included ENGIE, BNP Paribas and CEE Group.

Suntech and Trina Solar funding UNSW perovskite R&D

Research at the Australian Centre for Advanced Photovoltaics (ACAP), based at The University of New South Wales (UNSW) has reported a 12.1% efficiency rating for a 16 cm² perovskite solar cell, partially funded by Suntech and Trina Solar and AUD$3.6 million in funding through the Australian Renewable Energy Agency (ARENA).

Although much higher conversion efficiencies have been reported for perovskite solar cells, the results are the highest achieved on a larger glass substrate and were independently confirmed by Newport Corp.

Successful commercialization will require similar durability and low degradation rates to conventional c-Si solar cells. However, sacrificing of high efficiency for durability to work as a tandem layer with conventional cells could be the fastest route to commercialization.

Swedish OPV firm receives €5.2 million funding from Fortum

Finland-based energy firm Fortum has invested €5.2 million in Exeger Sweden AB, dye sensitive OPV thin-film start-up, to help support the launch of commercial products in 2017.

The funding gives Fortum a 5% ownership in Exeger, which prints OPV thin-film materials to produce a range of consumer related products and potentially bigger markets such as building-integrated photovoltaics.

Giovanni Fili, CEO of Exeger Sweden AB said: "Fortum's strategic investment is the last piece in our puzzle to prepare for our first global product launch. It will allow us to ramp up our production capacity even further in order to start accepting commercial orders in 2017. In the coming years, we will invest €100-200 million in the most promising start-ups and funds."

Hanergy Thin Film to appoint financial advisers on efforts to restart stock trading

PV thin-film equipment and module producer Hanergy Thin Film Power Group (Hanergy TF) will be appointing financial advisers and conducting an audit on its consolidated financial statements through its auditors as it attempts to meet Hong Kong Stock Exchange's Securities and Futures Commission (SFC) demands.

Credit: Singulus

Singulus has seen a delay in completing two orders despite a strong order backlog of CIGS thin-film equipment.

Hanergy TF was forced to update investors on the protracted dealings with the SFC, after news reports that the SFC has made several specific demands ahead of a trading resumption, including the appointment of a financial adviser to submit a resumption proposal and a 'clean' audit report on its accounts. The company gave no timelines to meet compliance with the SFC.

University of Delaware in US$1.25 million funding for IBC solar cell cost reductions with SolarCity

The University of Delaware's Institute of Energy Conversion (IEC) has been awarded US$2.1 million from the US government's SunShot Initiative for two research projects aiming to improve the performance of interdigitated back contact (IBC) solar cells while reducing their production costs and new techniques for CIGS deposition.

Although IBC cells have provided the highest efficiencies in volume production via SunPower, production costs have remained higher due to difficulties in patterning and isolating the positive and negative electrodes on the back of the solar cell.

Senior scientist Steven Hegedus will lead a three-year, US$1.25 million project on cutting IBC solar cell production costs. Hegedus and his team are to explore the use of advanced laser patterning techniques to overcome these challenges.

Orders

Manz updates on major 'CIGSfab' purchase orders

PV and electronics equipment manufacturing and automation specialist Manz AG had delays in expected 'CIGSfab' purchase orders that would be the largest in the history of the company and these are not expected to be signed in 2016.

Manz noted in third quarter 2016 financial results that the contracts from turnkey CIGS thin-film module production lines would be in the 'hundreds of millions' (euro) range, the first time the company has provided such details since announcing a deal in early November.

Dieter Manz, founder and CEO of Manz AG, said: "Our future collaboration partners will immediately assume the expense of operating our CIGS research site, relieving us of costs in the low tens of millions per year.

Singulus warns of two solar orders commissioning delays

Specialist PV manufacturing equipment supplier Singulus Technologies has noted a delay in assembling and commissioning two previously shipped orders to customers that were expected to have been operational in 2016.

Revenue recognition for the shipped orders could impact guided full-year revenue, which was recently guided to be in the range of €68 million to €78 million. Singulus said that it would update on the customer delays should revenue recognition be postponed into 2017. Singulus has a very strong order backlog, primarily attributable to Chinese orders for CIGS thin-film equipment that accounted for around €110.0 million of its €134.0 million order backlog at the end of the third quarter.

Midsummer gets follow-on CIGS thin-film equipment order

Swedish CIGS thin-film equipment supplier Midsummer has secured a follow-on order from an undisclosed customer for its flexible CIGS thin-film process tool. The repeat order was for Midsummer's 'DUO' a volume production flexible CIGS (copper, indium, gallium and selenium) thin-film solar cell sputtering tool.

In 2015, the company received a 'multi-million' (US$) order for the DUO from an unidentified 'multinational corporation'.

The new equipment order was received in connection with Midsummer's first system at the customer going into production with a solar cell efficiency of over 15%, which was 2 percentage points higher than the promised specification. The company did not provide delivery schedules to the customer in Asia, nor provide any financial details.

Use of a perovskite layer to boost the efficiency of CIGS modules

Tom Aernouts, imec, Leuven, Belgium

ABSTRACT

Perovskite microcrystals have properties that make them uniquely suitable as a basis of thin, light, semi-transparent solar modules. However, there are some remaining challenges, including lifelong stability, that need to be tackled before this technology can become commercially available. Once these have been resolved, perovskites can also be deployed for boosting established solar technology, such as silicon or copper indium gallium selenide (CIGS) modules. As an example, a record efficiency of 17.8% has recently been reported for a stacked perovskite/CIGS module, surpassing the highest efficiencies achieved so far for both stand-alone perovskite modules and CIGS modules.

Introduction

Perovskite microcrystals are a promising material for manufacturing high-yielding thin-film solar cells. Although these microcrystals have excellent properties, they also present a number of challenges, especially with regard to stability. Perovskites can be processed into thin, light, semi-transparent modules that could eventually be integrated in building materials, such as windows or curved construction elements. In addition, they can be used to enhance established solar technology, such as silicon or copper indium gallium selenide (CIGS) modules. A record efficiency of 17.8% was recently reported [1] for a stacked perovskite/CIGS module (Fig. 1), surpassing the highest efficiencies achieved so far for both stand-alone perovskite modules and CIGS modules.

> "A record efficiency of 17.8% was recently reported for a stacked perovskite/CIGS module."

Imec started its R&D in perovskite solar cells in 2014, with an emphasis on developing a scalable, stable and lead-free technology [2,3]. This research is embedded within Solliance [4,5], a transnational partnership between expert companies and research institutes collaborating on thin-film solar technology. Imec's PV research is part of EnergyVille, the Flemish expertise centre for energy technology.

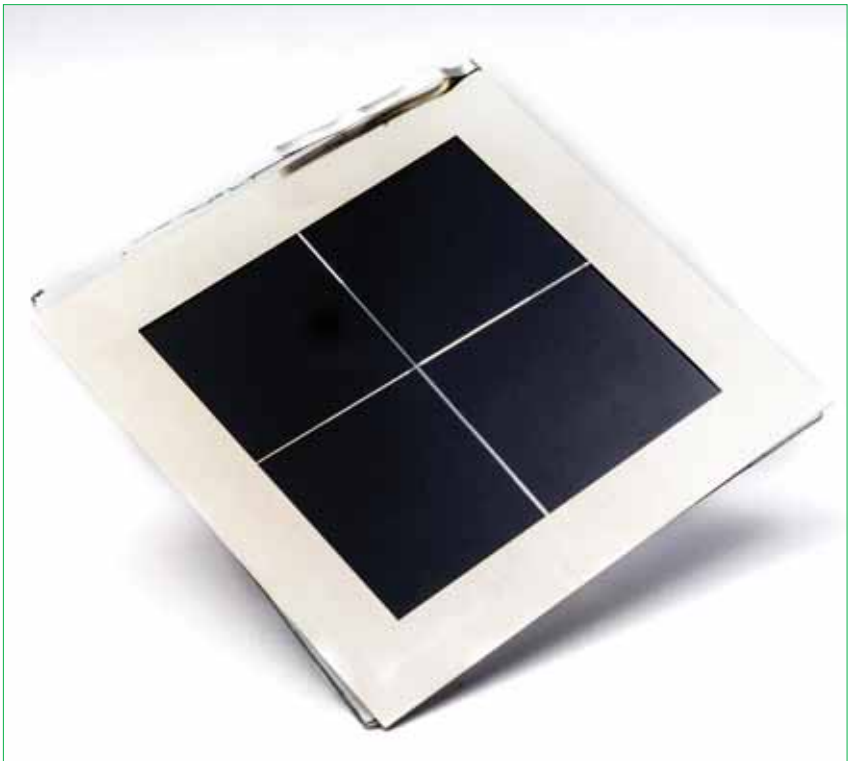

Figure 1. Module of stacked perovskite on CIGS technology.

Searching the perovskite grab bag for gold

Perovskite solar cells are made up of a carefully engineered stack of functional layers, with a central photoactive layer made from microcrystals of perovskites. Perovskites comprise a well-known family of materials that form microcrystals with the structure ABX_3. Solar cells typically use an organometal halide perovskite, in which material A is an organic cation, material B is a metal ion (such as lead), and X is a halide anion (such as iodide, bromide or chloride).

With these three elements, a great many variations of perovskites may be engineered, each having specific characteristics; some of these perovskites will be very useful in harvesting solar energy, others less so. However, there is no direct way of knowing in advance which will be best suited to solar cells. An element of the R&D work therefore entails painstakingly screening compounds and their behaviour, literally searching the perovskite grab bag for gold.

The first use of perovskites in solar cells dates back to only 2009, when they were integrated using a dye-sensitized solar cell architecture, generating a very modest 3.8% conversion efficiency. Moreover, these cells were only stable for a few minutes before they degraded. Since then, labs around the world have steadily improved the efficiency, now achieving values of around 20% in lab cells, with the expectation of even higher values in the future.

Excellent properties, but stability needs improving

Apart from their efficiency, perovskite solar cells have many desirable properties. For example, they are potentially cheap to produce, because they can be constructed using simple fabrication techniques, such as coating and printing with ink-like materials on flexible or glass substrates. In addition, perovskite layers have a high absorption efficiency for sunlight; consequently, not much of the material is needed, a layer of at most a few hundred nanometres being sufficient.

As previously mentioned, the microcrystalline material can be carefully engineered to achieve various optical and electronic properties. This allows, for example, the colour and transparency of the cells to be adjusted, depending on how and when they will be used. However, it also allows a spectrum to be chosen that is complementary to the absorption spectrum of another type of PV technology, such as cells based on silicon or CIGS materials. With semi-transparency and complementarity absorption, it therefore becomes possible to design tandem cells – stacks of solar cells based on different technologies.

The benefit of perovskite solar cells is that the bandgap can be tuned by adjusting, for example, the amount of bromine (Fig. 2). In this way, a solar cell with a bandgap of around 1.8eV can be created; according to calculations, this produces the best combination with a silicon solar cell (to achieve an efficiency higher than that of the silicon solar cell alone).

Whereas the efficiency of perovskite-based PV has dramatically improved, the cell stability has not followed suit: perovskite cells still degrade too quickly, lasting only weeks or months instead of years or decades.

> "One of the challenges is to make the perovskite layer stable under higher temperatures."

One of the challenges is to make the perovskite layer stable under higher temperatures; currently, the material remains stable only for operating temperatures of up to 80°C. Together with a university group that specializes in engineering materials (IMOMEC at Hasselt University, Belgium), the researchers at imec have been developing new perovskite compounds which should remain stable up to 150°C. In parallel, imec is also refining the processing techniques in order to optimize the microcrystalline structure of the active layer.

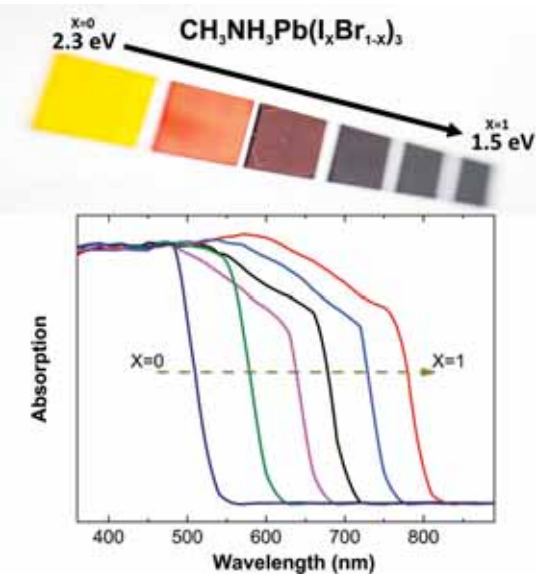

Figure 2. Tuning the bandgap by adjusting the amount of bromine in a perovskite solar cell.

A second issue concerns the hole-conducting layer; this is the layer that guides the holes to the contacts after they have separated from the electrons in the perovskite active layer. In the case of perovskite solar cells, typically a so-called *spiro layer* is used, a layer that was developed for dye-sensitized solar cells. However, being organic, this material degrades rather fast; alternatives are therefore needed here as well.

In addition, the best perovskite materials available today are still very sensitive to moisture, greatly limiting their outdoor use. One way to overcome this is to finish the PV stack with an excellent moisture barrier, for example by sandwiching it between two glass plates.

Unrelated to stability, but also very important, is the concern of toxicity of the material, particularly since the perovskites in use today contain lead. Although the concentration in final PV systems will be very low, it is vital to find a lead-free material with good stability in order to produce a sustainable PV technology and consumer products that adhere to the WEEE (waste electrical and electronic equipment) and RoHS (restriction of hazardous substances) regulations.

On all these issues, imec is slowly making progress, carefully tuning the recipes and processing steps. It is expected that, as in the case of efficiency, advances in the stability of the technology will also be made, with the achieved lifetimes measured in years rather than weeks.

From stand-alone to tandem modules

Cells are one thing, but if it is ever hoped to get this technology out of the lab and into production, it is essential to develop processes that can be scaled to an industrial level. This means processing large-area cells with good efficiencies, and integrating cells into modules without much efficiency loss, as well as eventually integrating them in fully fledged PV systems.

Recently, in May 2016, the team at imec presented the first-ever semi-transparent perovskite PV modules. These were fabricated with scalable coating techniques, and demonstrated efficiencies of 12% on sizes as big as 4cm^2 and 10% on sizes as big as 16cm^2, which was a world best for such large areas. Comparable modules may be realized on flexible (plastic film or metal foil) carriers as well as on rigid (glass, metal) carriers. In addition, by carefully mixing in the right materials, the optical and electrical properties of the cells may be tuned, which also results in colour and transparency variations at the module level.

Aside from making perovskite layers that are transparent, it is also possible to engineer them to absorb specific spectral ranges. If this is done, the layers will be found to have a sharp absorption cut-off, meaning that there is very little parasitic absorption from nearby spectral ranges. This naturally leads to the idea that perovskite cells could be stacked on top of other solar cells, such as silicon cells or other thin-film cells.

Using silicon PV, imec has managed to stack a transparent perovskite

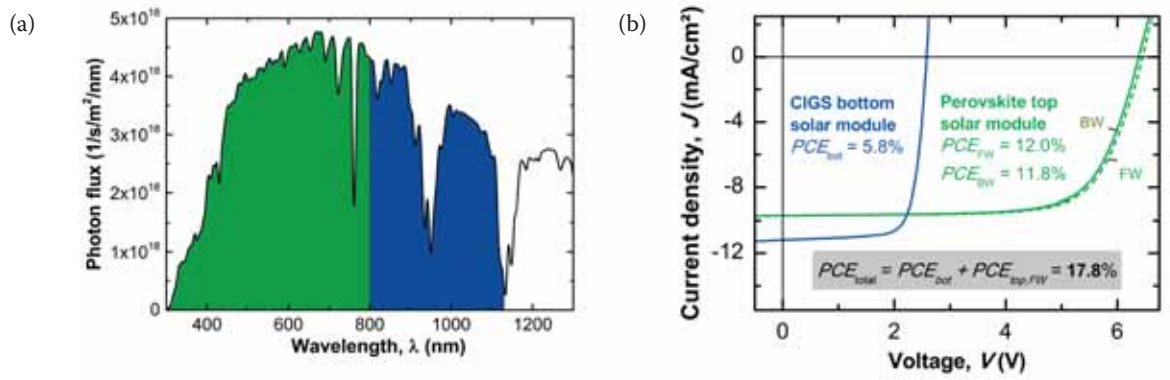

Figure 3. (a) AM1.5 photon flux, with coloured wavelength regions representing the spectral range that is harvested by the perovskite top solar module (green) and the CIGS bottom solar module (blue). (b) *I–V* characteristics of the stacked perovskite top solar module and the CIGS bottom solar module.

module on top of interdigitated back contact (IBC) silicon solar cells of the same size. In this set-up, the perovskite top module passed 70% of the incoming light to the silicon cells. In this way, a conversion efficiency of 20.2% was measured for a 4cm^2 stack and 17.2% for a 16cm^2 stack, a record result for this size.

One of the challenges of combining technologies is that it is preferable to work with state-of-the-art expertise and technology, and these are rarely found at a single lab. For the next combination that will be discussed, perovskite on CIGS, imec therefore worked together with an international team, resulting in the announcement of another record-performing module.

Perovskite on CIGS modules

CIGS is an established thin-film PV technology: the current world record for stand-alone CIGS cells stands at 22.6%, and was established at Germany's ZSW (Zentrum für Sonnenenergie- und Wasserstoff-Forschung Baden-Württemberg). The scientists at imec therefore teamed up with those at ZSW and at another German lab at the Karlsruhe Institute of Technology (KIT). KIT focuses on the optics in multijunction perovskite solar modules and develops specialized nanophotonic materials for these devices.

The result of the work carried out for this project was a thin-film stack with a conversion efficiency of 17.8%; this was realized mainly by efficiently exploiting the solar spectrum (Fig. 3). The higher-energy part of the spectrum is harvested by the semi-transparent perovskite module on top, while the lower-energy light passes through and is harvested by the bottom CIGS module. The stack, with an efficiency of 17.8%, outperforms imec's world-record upscaled perovskite module (efficiency of 15.3%), as well as the highly efficient stand-alone upscaled CIGS module from ZSW (efficiencies near 15.7%).

The new module (3.76cm^2) makes use of the so-called *4-terminal architecture*, where a perovskite solar module in superstrate configuration is stacked on a CIGS solar module in a substrate configuration. Both submodules are constructed using a fully scalable interconnection scheme, offering a route towards solar modules on the scale of a few square metres.

To see what the maximum potential of this technology might be, imec has quantified the various losses still present in the presented prototype, and also identified the key challenges and possibilities of eventually reaching power conversion efficiencies above 25%.

> "Perovskite solar technology is definitely a solid contender for inclusion in the PV technology mix that will power our future world."

Outlook: a perovskite-powered environment

Perovskite solar technology is definitely a solid contender for inclusion in the PV technology mix that will power our future world. Perovskite has demonstrated its potential both as a booster material for various other technologies, and as an inexpensive technology for powering up large surfaces in, for example, buildings or cars. The next few years will tell if the right mix of efficiency, stability and scale can be formulated which will lead to large-scale application of this fascinating and very versatile material.

References

[1] Paetzold, U. et al. 2016, "Towards scalable perovskite/Si multijunction solar modules", Poster Session, Int. Conf. Perovskite Sol. Cells Optoelectron. (PSCO), Genoa, Italy.

[2] Imec 2015, "Perovskites: The new gold?", *imec magazine* (Sep.) [http://magazine.imec.be/data/69/reader/reader.html?t=1471856446229#!preferred/1/package/69/pub/75/page/0].

[3] Imec 2015, 'The perfect marriage: Silicon and perovskite solar cells', *imec magazine* (Apr.) [http://magazine.imec.be/data/59/reader/reader.html#preferred/1/package/59/pub/65/page/4].

[4] Solliance website [http://www.solliance.eu/].

[5] Solliance 2015, "Dyesol joins Solliance as an industrial partner", Press Release (Jun.) [http://www.solliance.eu/news/item/?tx_ttnews%5Btt_news%5D=308&cHash=8fda8d06616e33d1f40d3c5790a8b91c].

About the Author

Tom Aernouts heads the thin-film PV research at imec. After obtaining his Ph.D. in physics from KU Leuven (Belgium), he began his research career at imec, working on organic oligomer-based diode structures and organic PV. He has overseen the group's successful growth in manpower, expertise and covered thin-film technologies, while authoring or co-authoring more than 80 journal publications, book chapters and conference contributions.

Enquiries

Tom Aernouts
imec
Kapeldreef 75
B3001 Leuven, Belgium
Tel: +32 16 28 12 11
Email: tom.aernouts@imec.be
Website: www.imec.be

PV Modules

74

86

News

Mixed fortunes for module makers in Q3 results

There were mixed results for module manufacturers in Q3 of this year with some raising guidance but most lowering it.

JinkoSolar has raised its full-year PV module shipments to be in the range of 6.6GW to 6.7GW, compared to previous guidance of 6.0GW to 6.5GW, contrasting with weaker than expected third quarter shipments. Hanwha Q CELLS said that previously upwardly revised shipment guidance would be retained for the full year after reporting a 10.9% increase in revenue for the third quarter of 2016.

Trina Solar significantly missed its third quarter 2016 PV module shipment guidance range that makes meeting previous full-year shipment projections almost unattainable. It also said it would not be releasing 2017 guidance because of its pending privatisation.

Yingli also lowered its full-year guidance for 2016 off the back of its Q3 results from 2.2GW to 2.1GW.

Yingli Solar

Yingli was one module producer to lower its full-year guidance for 2016.

Certification and warranties

HT-SAAE 'HIGHWAY' PV modules pass 'Triple IEC Standard' test

China-based n-type monocrystalline module manufacturer Shanghai Aerospace Automobile Electromechanical Co., (HT-SAAE) has confirmed its 'HIGHWAY' PV modules (265-270W, 60-cell) have gained TUV Rheinland's 'Ultimate Reliability Certification.'

HT-SAAE said that according to TUV Rheinland, there were only a few PV module producers around the world that have completed the 'Triple IEC Standard' test. Every piece of module sampled must remain reliable and safe in the long-term (25 to 30 years) and have output degradation less than 5%.

Shi Lei, general manager of the PV business department at HT-SAAE said: "The HIGHWAY PV modules have topped their peers in the market. They've already hit overseas markets such as Japan, Brazil and India. It gives our clients confidence and assurance for them to make informed investment decision."

Munich Re supporting Suntech's 25-year solar module warranty scheme

Wuxi Suntech, the PV module manufacturing arm of renewable energy group Shunfeng International Clean Energy (SFCE) has secured insurance from Munich Re to support its 25-year module warranty scheme.

The new third-party insurance was said to provide back-up coverage of all Suntech PV modules produced in 2016 and 2017 based on an upfront unspecified lump sum premium payment for modules shipped outside of China.

"Munich Re values our new partnership with Suntech as during our risk management evaluation we were very convinced of their key component suppliers, the high quality materials for its modules and its intensive quality assurance process," said Michael Schrempp, Munich Re's head of green tech solutions.

SFCE PV product shipments (wafer, cell, modules) outside China in the first half of 2016 generated around US$182 million in revenue, 31.1% of total revenue.

The company also owns US-based PV module manufacturer Suniva, which is expected to have completed a doubling of capacity to around 430MW.

Assembly

Trina dumps Japanese module assembly partner

Trina Solar has pulled out of a deal to have its PV modules assembled in Japan by module assembly equipment supplier and assembly sub-contractor, NPC Group.

Trina Solar Japan Ltd had signed a long-term, large-scale module assembly contract with NPC Group in April, 2016 which would last through December 2018 for the production of 130MW of module per annum.

However, NPC Group said in recent financial filings that Trina Solar had breached the contract and had not provided any production materials to begin module assembly as well as not providing purchase orders against the contract.

NPC Group noted that there were no further prospects for the production of modules under the contract, despite the company having undertaken production preparation that included remodelling its module assembly line and expanding its factory facilities and workforce to accommodate the contract assembly agreement.

As a result, NPC group said that the cancelled contract impacted sales by around US$4.8 million in FY Q2 and profit by around US$3.8 million and its module assembly order backlog stood at zero.

Trina Solar previously reported Q2 2016 shipments to Japan had accounted for 3.1% of total external shipments, or around 50MW. However, since the end of the second quarter of 2016 there has been a major change in industry dynamics, due to a collapse in demand in China after feed-in tariff changes that have led to overcapacity and plummeting ASPs across the supply chain.

Trina Solar

Trina Solar has pulled out of a deal to produce its modules in Japan by NPC Group.

Astronergy to produce mono PERC solar modules at German assembly plant

PV manufacturer Astronergy Solarmodule GmbH, a subsidiary of China-based producer, Astronergy and part of Chint Group, has said it will start production of modules using the latest generation of PERC cells with monocrystalline wafers to produce high-efficiency 'all black' modules in the 295 to 310Wp power classes.

Astronergy noted that the new modules, which will enter production in October 2016 had undergone extended stress tests from TÜV Rheinland, resulting in successful tensile loads of 5,400 pascals and minimal performance degradation of under 1%.

"We tested the black cells of several established tier-one cell manufacturers, but only two were able to meet our high expectations concerning the colour depth and uniformity of the cells," noted Thomas Volz, CEO at Astronergy Solarmodule.

The manufacturer offers a product warranty of 12 years and a linear performance warranty of 25 years. Major distributor BayWa r.e. renewable energy is one of the first to be highlighted as a distributor of the new modules.

"Black mono modules are in high demand for family homes," noted Günter Haug, managing director of BayWa r.e. renewable energy. "We were especially impressed with the extremely uniform appearance of the Full Black Module. For this reason, we are delighted that Astronergy, as one Germany's leading module manufacturers, has expanded its product range."

1500V

Canadian Solar takes major 1500V module order as new architecture takes hold

Canadian Solar has said that its recently launched 72-cell 1500V multicrystalline modules will be deployed at two planned PV power plants in Australia with a cumulative capacity of 47MWp.

Canadian Solar noted that the two solar power projects that are to be located in Longreach (17MWp) and Oakey 30MWp, Queensland and have a 20-year government-backed Contract for Difference deal in place.

The construction of both projects is expected to start in the first quarter of 2017 and achieve completion in January, 2018 or earlier, according to the company.

Jeffrey Barnett, president of GCL System Integration Americas said the need to keep improving project economics would be a huge factor in adoption of 1500V in 2017, even if that adoption is not yet being represented in installs.

"It's a significant part of strategy but it is not a significant part of project deployment today. In the second half of 2017 we will see more. It's when the large-scale projects are demanding it that they will drive this technology. With PPA prices around US$0.04 kWh in Mexico, they are going to need to squeeze every last bit out of the installation cost without sacrificing quality," said Barnett.

USA

SEIA launches new module recycling programme

The Solar Energy Industries Association (SEIA) has launched a first-of-its-kind national PV recycling programme — designed to ensure the sustainability of the US solar market.

Collaborating with major solar companies and developers such as First Solar, SunPower, Flex, JinkoSolar, Panasonic, SolarCity and Trina Solar, SEIA has orchestrated a state-of-the-art network of recyclers that can handle PV waste and the disposal of solar panels.

Tom Kimbis, SEIA's interim president, said: "Our goal is make the entire solar industry landfill-free. By establishing a national network of collection points, recycling facilities and an easy-to-use consumer web portal, this proactive programme will help drive down the cost of recycling for all parties involved. This means the environment wins and so do our solar consumers and companies."

While PV panels can last for decades, they are mainly made up of easily recyclable materials such as glass and aluminium — which can be recovered and reused once a panel has run its course.

Marty Neese, SunPower chief operating officer, said: "As solar energy becomes mainstream, it's critical that industry leaders focus on recycling and diverting waste from landfills."

Alex Heard, senior vice president, global technical services at First Solar, added: "With more than 227GW of solar modules installed worldwide, recycling is important for all PV technologies and the sustainability of the industry as a whole. By making affordable PV recycling solutions more accessible to consumers, SEIA's recycling programme will help to ensure that today's clean energy solutions do not pose a future waste burden."

PID –1,500V readiness of PV modules: Some solutions and how to assess them in the lab

Benoit Braisaz[1], Benjamin Commault[2,3], Nam Le Quang[4], Samuel Williatte[4], Marc Pirot[2,3], Eric Gerritsen[2,3], Maryline Joanny[2,3], Didier Binesti[1], Thierry Galvez[4], Gilles Goaer[4] & Khalid Radouane[5]

[1]EDF R&D, ENERBAT, F-77250 Moret sur Loing; [2]Univ. Grenoble Alpes, INES, Le Bourget du Lac; [3]CEA, LITEN, Le Bourget du Lac; [4]EDF ENR PWT, Bourgoin-Jallieu; [5]EDF EN, La Défense, France

ABSTRACT

Even though it is now more than five years since potential-induced degradation (PID) began to proliferate, and despite the fact that solutions are under development, it is currently still the most discussed mode of degradation associated with cracking in PV modules. This is probably because of the serious consequences that can rapidly be triggered when PV systems are affected. Although test specifications have been established (IEC 62804), there is no pass or fail criterion for identifying a PID-free module. This paper presents several ways of addressing the problem of PID at the module and cell levels, by considering glass, encapsulants, thin-film barriers and ion-implanted cells. The proposed solutions are tested in accordance with a specific test protocol, and an applied voltage of 1,500V is used in order to prepare for the future increase in DC plant voltage. An initial PID test was conducted on mini-modules at room temperature (25°C and Al foil), before proceeding to a more severe test at 70°C (Al foil); this made it possible to clearly differentiate the influences of the different tested materials on PID degradation of the modules. These tests were carried out on 60-cell modules under the following conditions: test duration of 192h, temperature of 75°C, relative humidity of 85% and applied voltage of –1,500V. In contrast to ethylene-vinyl acetate (EVA) and standard glass modules, no evident degradation was observed with thermoplastic polyolefin (TPO), ionomer (ION), and thin chemically tempered glass modules; similarly, no degradation was evident with Al_2O_3-layer (deposited under the SiN layer at the cell level) modules or ion-implanted cell modules. The use of one of these components can therefore be a potential solution to the problem of PID.

Introduction

The development and operation of solar power plants requires a good knowledge of the types of module degradation and their sensitivities to different stresses – temperature (T), relative humidity (RH), bias-voltage frame cells (V), UV, etc.

Potential-induced degradation (PID) is caused by a high negative voltage between module–cell polarities and the ground (the module frame). This type of degradation is highly dependent not only on humidity and temperature, but also on:

- Cell components: junction technology, thin-film materials, etc.
- Module components: EVA, anti-reflection (AR) layer, frame, glass, etc.
- Module ageing and soiling
- System: type and topology of inverters, system voltage, DC and AC grounding system, etc.
- Mounting system: frame grounding, metallic or wood support, fixing plates, dielectric characteristics of rubber, frame-support contact, tightening torque, etc.
- Environment: weather, irradiance, etc.

The topic of PID, which has been very active in terms of international publications since 2010 (see Fig. 1) thanks to the papers of Solon [1,2] and NREL [3], came to light several years ago when PV system voltages increased. The degradation was initially identified in 1978 by Jet Propulsion Labs [4]. At present, no testing standard exists for differentiating 'PID-prone' modules from 'PID-free' modules. Research into finding PID-free solutions is currently ongoing, and PID-free modules are appearing on the market. The IEC 62804 test specification was published in 2015, but without any pass or fail criterion for identifying a PID-free module.

The physics that explains the PID phenomenon in c-Si modules, which assumes that sodium ions are responsible for the degradation, was reported in the paper by Naumann [5].

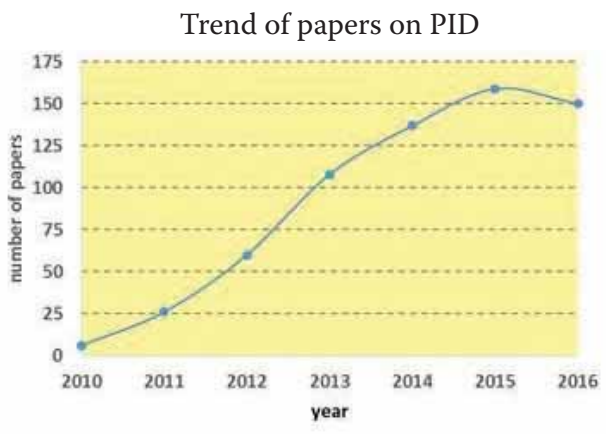

Figure 1. Trend of papers since 2010 that have included a discussion of PID.

ZERO MEANS A LOT
WHEN IT COMES TO PID

Potential induced degradation (PID) can cause significantly reduced efficiency – or even premature failure and replacement – of photovoltaic modules. So, it's good to know that **modules made with encapsulant films featuring ENGAGE™ PV Polyolefin Elastomers (POEs) exhibit virtually no PID.**[1]

Compared to solar module systems using ethylene vinyl acetate (EVA) encapsulants, the "PID Zero" performance of ENGAGE™ PV POEs offers excellent opportunities for:

- Improved electrical efficiency
- Increased power generation/retention
- Greater reliability
- Longer lifespan
- Lower total costs

Learn more about why PID Zero ENGAGE™ PV POEs are the material of choice for leading PV module manufacturers around the world by visiting www.dowpv.com or contacting your nearest Dow representative.

ENGAGE™ PV
polyolefin elastomers

[1] Tests conducted by the Fraunhofer Center for Silicon Photovoltaics CSP. Additional information available upon request.

According to this paper, the electrical field (between frame and cells) triggers the diffusion of sodium ions from the glass into the encapsulation material and cells; these ions are then released and accumulate at the surface of the silicon nitride (the AR layer). Sodium ions propagate through Si stacking faults in the p-n junction (Fig. 2). In the case of p-type cells, these charges generate local shunts in the p-n junction, which dramatically affects shunt resistance and V_{oc}.

There are many parameters associated with the module that can mitigate or suppress the consequences of PID – for example, EVA resistivity and glass resistivity [6], intermediate diffusion layer, thickness of the glass and EVA, AR coatings [7], cell and silicon features.

"The increase in power plant voltage to 1,500V will accentuate PID stresses."

Several approaches to solving the PID issue are currently being studied. However, these solutions have not always been authenticated: for example, a module announced by a manufacturer to be insensitive to PID may in actual fact be sensitive in a lab test. The degradation mechanism due to the potential is not entirely understood at the material and microscopic levels. In addition, the increase in power plant voltage to 1,500V will accentuate PID stresses.

The earlier work reported in the previously cited publications has identified possible electrical causes (Fig. 3) of degradation processes at the microscopic level for c-Si and CdTe modules. Moreover, the impacts on PV plants, the testing methods used by laboratories, and a range of solutions at three levels – cell, module and system – have been discussed [8,9].

Since the degradation occurs initially to the shunt resistance, measurements taken under standard test conditions (STC) are not adequate for measuring the consequences of PID [10]; the low-light behaviour should be a mandatory criterion for pass/fail results in a PID test. Indeed, the module tested in Braisaz [10], for example, exhibited no degradation at 1,000W/m^2, but demonstrated severe degradation at 200W/m^2, after 96 hours at 60°C/85%RH/–1,000V (IEC TS 62804 [11]). It would have passed the requirements of the standard if the only criterion had been 1,000W/m^2 (because the power loss was below 2%).

In Braisaz [12], a representative, selective and reproducible test protocol with a pass or fail

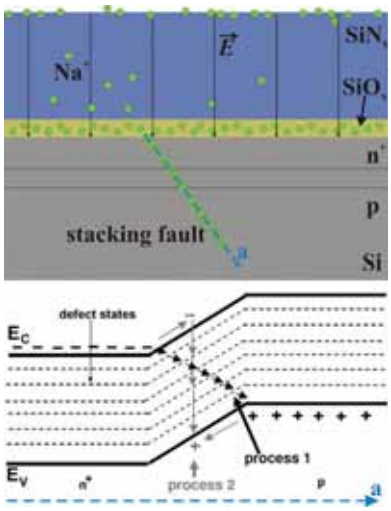

Figure 2. Schematic view of a solar cell cross section: the electrical field causes a drift of Na^+ ions through the p-n junction [5].

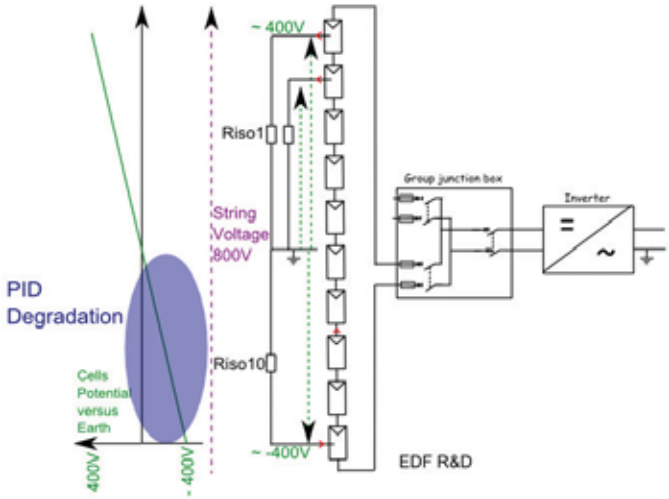

Figure 3. PID in operation in a PV system.

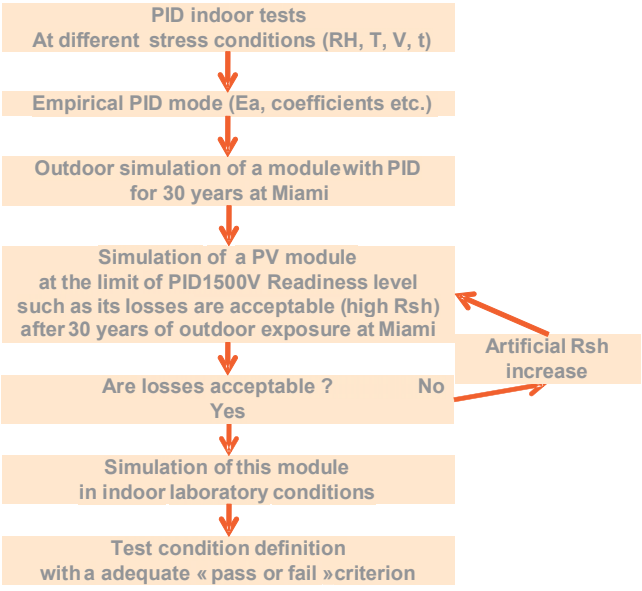

Figure 4. Method for developing a PID test [12].

criterion has been proposed: 192h/75°C/85%RH/–1,500V, with a maximum power loss of 5% at 200W/m^2. Outdoor degradation has been estimated on the basis of indoor accelerated test results and an empirical PID model. After several iterative simulations, an indoor test protocol with a specific 'pass or fail' criterion has been determined: there are limited losses after 30 years' outdoor exposure in Miami for a module at the end of a 1,500V string. According to this test protocol, all the PID solutions tested and reported by Braisaz [13] appear to be suitable.

Establishing a test protocol for PV modules

Many tests under various conditions were conducted on several 60-cell c-Si modules from the same manufacturer in order to determine the role that the factors T, RH, V and time play in PID. The approach to creating a test protocol is summarized in Fig. 4.

From these indoor test results, basic laws were deduced by fitting two-diode model parameters to the measurement data (I–V curves and flashes), and a PID behaviour model was formulated. The degradation is considered to satisfy:

- a linear law with respect to time;
- a linear law with respect to voltage;
- a sigmoid law with respect to moisture;
- an Arrhenius law with respect to temperature.

On these assumptions, the degradation rate Rd can be expressed as:

$$Rd = \mathrm{A}*V*\frac{\mathrm{B}}{1+e^{-C.RH+\mathrm{D}}}*e^{-\frac{E_a}{k_B T}} \quad (1)$$

where A, B, C and D are coefficients that are calibrated using the least-squares method on the measurements; V is the voltage; T is the temperature; RH is the relative humidity; k_B is the Bolztmann constant (1.38×10^{-23}J·K^{-1}); and E_a is the activation energy of the PID phenomenon. An empirical law can then be established from the evolution of R_{sh} during the accelerated PID tests:

$$R_{sh} = \frac{R_{sh0}}{1+b*Rd*t} \quad (2)$$

where R_{sh0} is the initial shunt resistance, b is a coefficient and t is the time (hours). This model is based on a set of empirical parameters.

Up until this point, $R_{sh}(t)$ has provided an indication of the level of degradation under steady-state conditions (constant temperature, humidity and voltage); however, outdoor stresses are continually changing. An incremental algorithm based on previous work [14] calculates iteratively the PID degradation with variable temperature and humidity; the degradation is updated at each time step of 1 hour. The steps for computing the evolution of the outdoor shunt resistance during the module's lifetime are presented in Fig. 5.

If the temperature at time t, $T(t)$, and the state of the reaction at a time step t–dt, $X(t–dt)$, are known, then it is possible to determine the time t_{eq} that would represent the achievement of the same degree of reaction for indoor conditions at a constant temperature $T(t)$. This quantity t_{eq} is the reciprocal function of the shunt resistance function.

If the derivative of the function R_{sh} at (RH , T, V , X), along with $T(t)$, $RH(t)$ and $V(t)$, is used, the slope of the shunt resistance can be calculated at any point in time, for any module conditions, and for any state of reaction:

$$\dot{R_{sh}}(t_{eq}, RH, T, V) = \left(\frac{dR_{sh}}{dt}\right)_{t_{eq},RH,T,V} = \frac{-b*Rd*R_{sh0}}{(1+b*Rd*t)^2} \quad (3)$$

The shunt resistance at time t can then be calculated by numerical integration over the time period from 0 to t:

$$R_{sh_{outdoor}}(t) = \int_0^t \dot{R_{sh}}(t_{eq}(u), RH(u), T(u), V(u))\,du \quad (4)$$

With an hourly weather data set consisting of irradiance, temperature and relative humidity, the outdoor-related degradation after 30 years was calculated for a module at the end of a 1,500V string (negative side). In this study, the weather data set is for one full year in Miami, taken from the Meteonorm database. Degradation is measured at 1,000W/m^2 and at 200W/m^2; these will be the PID degradation references. The hypothesis is that the PV plant operator desires a maximum degradation of less than 1% at STC (1,000W/m^2) and 6% at 200W/m^2 after 30 years' outdoor exposure for a module at the end of a 1,500V string (negative side). The characteristics of such a module were therefore determined by calculating an adequate 'artificially increased' shunt resistance R_{sh}.

The module in question, which is just at the limit of the PID-1,500V readiness level, was simulated in order to check that after 30 years the degradation is less than 1% at 1,000W/m^2 and 6% at 200W/m^2. This module with a new R_{sh} was then simulated in laboratory conditions (constant T, RH, and V stresses). On the basis of what is experimentally possible with test chambers, and in order to accelerate the tests, a protocol was established with an adequate 'pass or fail' criterion, specifically 192h/75°C/85%RH/–1,500V, with a maximum power loss of 5% at 200W/m^2.

Materials and methods

Mini-modules

Two single-cell mini-modules incorporating standard solar cells (p-type monocrystalline silicon with $POCl_3$-diffused emitter, SiN_x AR coating, Al-BSF) were created with:

- Four encapsulants:
  - a classic EVA with a 33% vinyl acetate content
  - a 28% vinyl acetate EVA
  - a thermoplastic polyolefin (TPO)
  - an ionomer (ION)

Two other modules with four cells in series were constructed:

- Two glass backsheet assemblies:
  - standard glass and a Tedlar–polyester–Tedlar (TPT) backsheet
  - special thin chemically tempered glass and a TPT backsheet

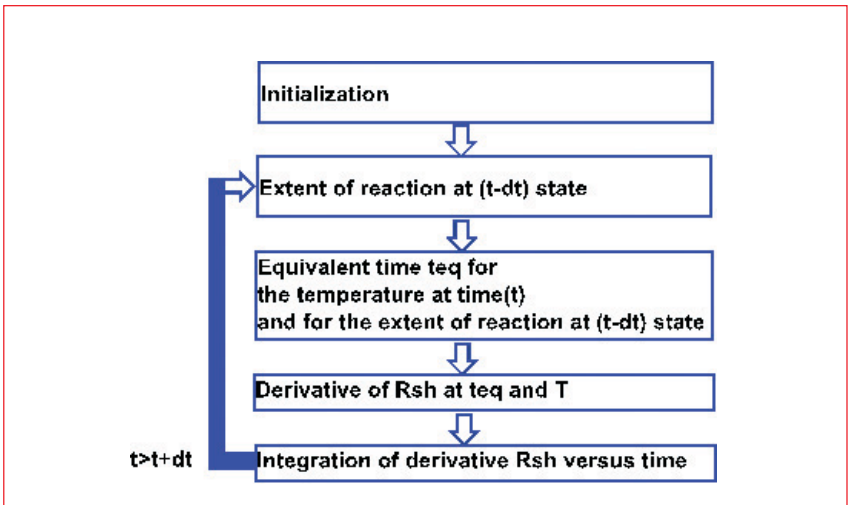

Figure 5. R_{sh} degradation method.

The sensitivity of the modules to PID was evaluated using the following set-up. The modules were stacked together (glass to glass) with an aluminium foil between them. The aluminium foils were connected together to the positive terminal of the voltage generator, while the cell strings were connected together to the negative terminal. The voltage of 1,500V delivered by the generator was thus set between the aluminium foil and the cells. An initial test at 25°C and a relative humidity below 60% was conducted on all modules for 192 hours, i.e. test conditions 192h/25°C/<60%RH/–1,500V. Subsequently, a more severe test was carried out at a temperature of 70°C for 128 hours, i.e. 128h/70°C/<60%RH/–1,500V.

60-cell modules

In the study reported in this paper, the test protocol '192h/75°C/85%RH/–1,500V, with 5% of maximum power loss at 200W/m^2, was used on 60-cell module prototypes to evaluate various PID solutions that had previously been tested on the mini-modules:

- Three encapsulants (Fig. 6):
  - a classic EVA
  - a TPO
  - an ION
- Three glass backsheet assemblies (Fig. 7):
  - standard glass and a TPT backsheet
  - special thin chemically tempered glass and a TPT backsheet
  - special doubly thin chemically tempered glass module and a TPT backsheet
- One module with an ALD-deposited Al_2O_3 barrier under the SiN_x layer of the solar cells (Fig. 8)
- One module with implanted cells (Fig. 9)

The test chamber and the system used are presented in Fig. 10.

Mini-module test results

Encapsulant tests

Fig. 11 presents the maximum power variation of the modules during the tests at 25°C. The maximum power is stable, except in the case of the modules encapsulated with 33% vinyl acetate EVA.

"The modules with a TPO or ionomer encapsulant showed no degradation."

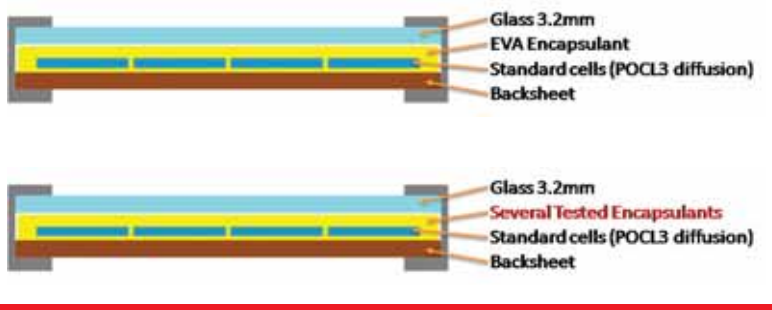

Figure 6. Sectional view of the reference module (top), and the module with the tested encapsulants (bottom).

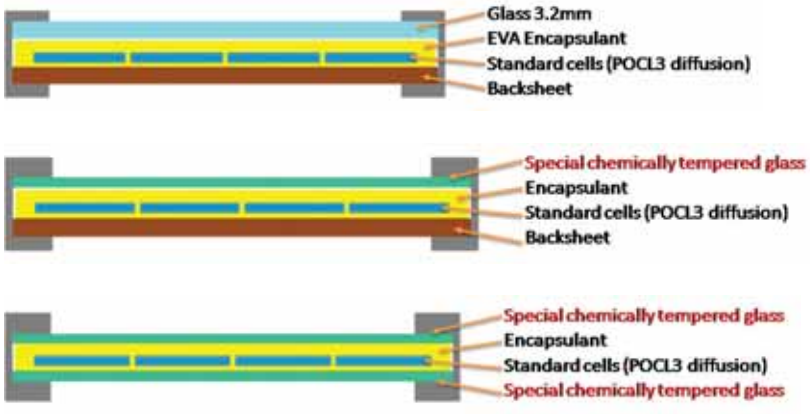

Figure 7. Sectional view of the reference module (top), the tested new glass module (middle), and the tested double-glass module (bottom).

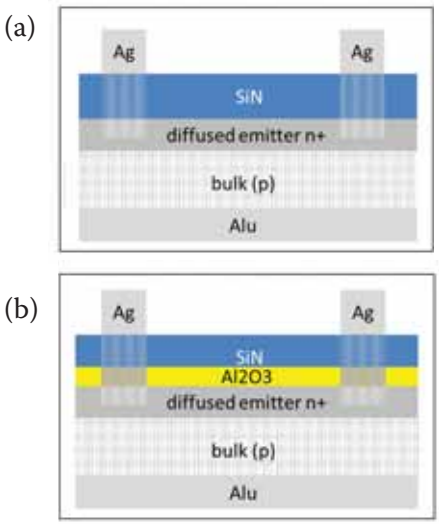

Figure 8. Stack of (a) a standard cell, and (b) a cell with an Al_2O_3 barrier under the SiN_x layer of the solar cells.

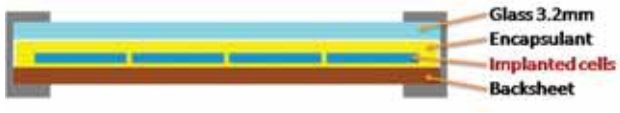

Figure 9. Sectional view of the tested module with implanted cells.

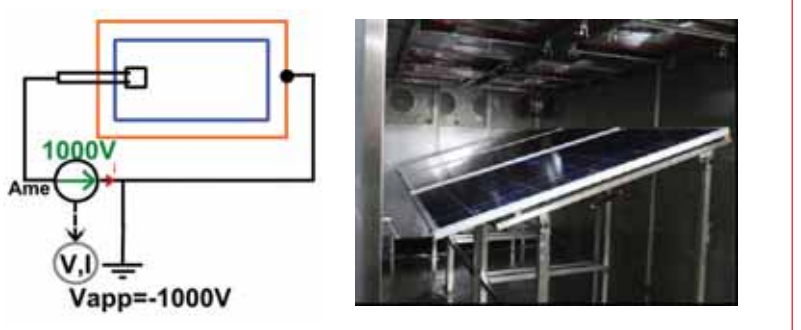

Figure 10. PID mounting system and picture of the test chamber with the bias voltage applied to the frame.

To compare the different impacts of the three encapsulants TPO, ION and 28% vinyl acetate EVA on PID, a PID test at 70°C was carried out. The electroluminescence (EL) images of the mini-modules during the test are shown in Fig. 12. A very good cell response before the test was obtained for the modules, all of which remained stable during the test, apart from that with the 33% vinyl acetate EVA, as seen in Fig. 11. Even if the EVA encapsulant is made with 28% vinyl acetate, the material is clearly not suitable for curbing the PID during testing at 70°C (see the *I–V* Curves and the EL images in Fig. 12). On the other hand, the modules with a TPO or ionomer encapsulant yielded a very good and stable cell response, as indicated in Fig. 12. Degradation was observed for the module with EVA at 28%, while the modules with a TPO or ionomer encapsulant showed no degradation.

Glass tests

The two 4-cell mini-modules with a chemically tempered thin glass (0.85mm thick) were subjected to the PID tests at –1,500V, as was a 4-cell mini-module with a standard solar glass. The results, in terms of the variation in maximum power at 1,000W/m^2 during the tests, are presented in Fig. 13. The degradation rate is limited by the use of the chemically strengthened thin glass, compared with the module with a standard solar glass. Nevertheless, the resistance to PID afforded by the chemically strengthened thin glass is not sufficient to keep the degradation of the initial module power below 5% at higher temperatures.

Standard-size module results

Encapsulant tests

Fig. 14 shows the module efficiency as a function of the irradiance at three stages of a PID test: initially, after 96h and after 192h. No losses at all were observed for polyolefin and ionomer modules, even at low irradiances of 200W/m^2. These modules showed slight increases in power, as opposed to the EVA module, which lost 66% in STC conditions, and 88% at 200W/m^2 (not visible on the graph in Fig. 14).

EL images of the EVA module are given in Fig. 15; the affected cells are those on the edges, where the electrical field (between the frame and the cells) is stronger. As PID degrades the shunt resistance, the affected cells are visible at low currents.

Glass tests

In Fig. 16 no PID is observed on thin chemically tempered glass using a chemically strengthened cover glass. However, the EVA module (created using a different EVA from the one in Fig. 14) lost 15% in STC conditions, and 31% at 200W/m^2; nevertheless, this EVA performs better than the previous one in terms of PID resistance.

Temperature coefficients

The temperature coefficients were also measured after PID testing (–1,500V/75°C/85%RH/192h) of an EVA module. The power was observed to be very low (a decrease of more than 66%), but now virtually independent of temperature (Fig. 17). Further investigations are necessary in order to assess and explain this phenomenon (reported by Desharnais [15]). It seems that the shunt resistance is too degraded to be sensitively dependent on temperature in order to have a consequential effect on power.

Al_2O_3 thin layer under the SiN

In this 60-cell module, each cell contains an Al_2O_3 layer deposited under the SiN layer; no degradation was observed after the PID test (Fig. 18).

Ion-implanted cells

A 60-cell module with ion-implanted cells (p-type monocrystalline silicon with SiO_2/SiN_x stack on the front side, ion-implanted emitter, Al-BSF) was subjected to PID testing and compared with a 60-cell module with standard diffused cells (Fig. 19). No degradation for the module with EVA and ion-implanted cells was observed; it seems that ion-implanted cells are PID resistant. Further investigation needs to be carried out, however, in order to validate this interesting result, probably due to the formation of an oxide layer during the implantation process (reported by Zhu [16], Basame [17] and Han [18]).

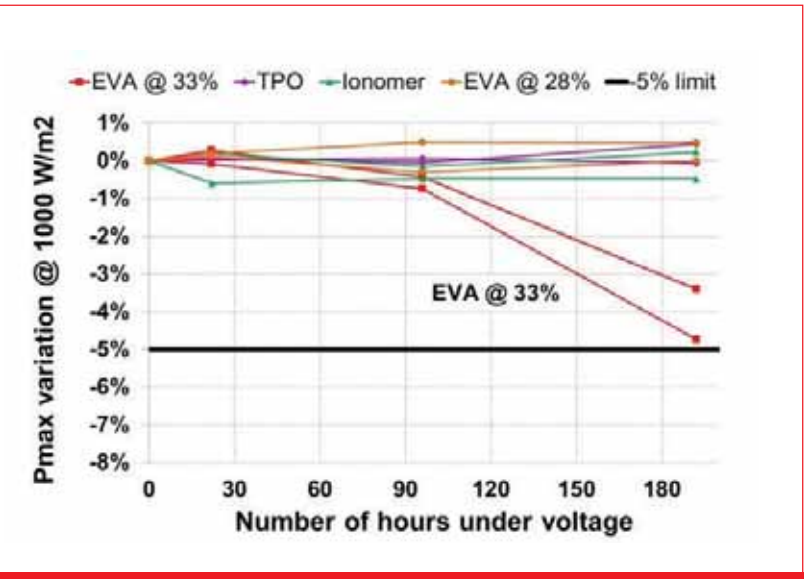

Figure 11. STC relative power evolution for mini-modules with different encapsulants (33%-EVA, 28%-EVA, ionomer and polyolefin) during PID at –1,500V/25°C/with aluminium foil.

> "The most promising solution, in terms of cost, is the use of ion-implanted cells."

Conclusions

With this new empirical approach for establishing test protocols through modelling and testing, it is possible to assess PID resistance. The PID model developed here is an initial empirical approach that entails validation by additional indoor and outdoor tests, but it could be used for other tests (damp heat, thermal cycling, etc.). The model needs to be supplemented by:

- New tests to refine the parameters, laws and hypothesis.
- A regeneration-effect model, as reported in Lechner [19].
- Tests on other modules with different surface–perimeter ratios.
- A sub-module model of the electrical field at the surface (see Pingel [6]), in order to take into account both the decrease in shunt resistance at the cell level and the mismatch.
- Uncertainty calculations and outdoor validation.

It has been demonstrated that possible solutions offering module

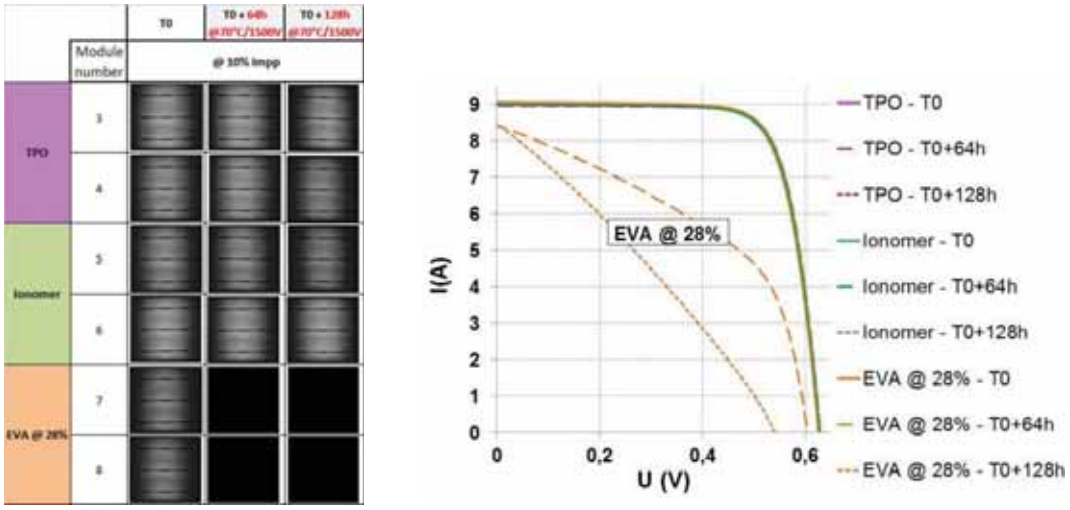

Figure 12. EL images and *I–V* curves after the PID test (–1,500V/70°C/with aluminium foil).

resistance to PID are: TPO, ionomer, thin PID-free glass with lower Na content (chemically strengthened glass), Al_2O_3 layer under the SiN, and ion-implanted cells. The most promising solution, in terms of cost, is the use of ion-implanted cells.

Acknowledgements

The authors wish to thank ADEME (Agence française pour l'environnement et la maitrise de l'énergie) for funding these studies. The work was carried out within the framework of the ADEME PID1500 project, in which the goals are to define an adequate PID test protocol for 1,500V systems and to develop ways of addressing PID issues at the cell and module levels. The project partners are EDF R&D, EDF ENR PWT, CEA Tech and Certisolis.

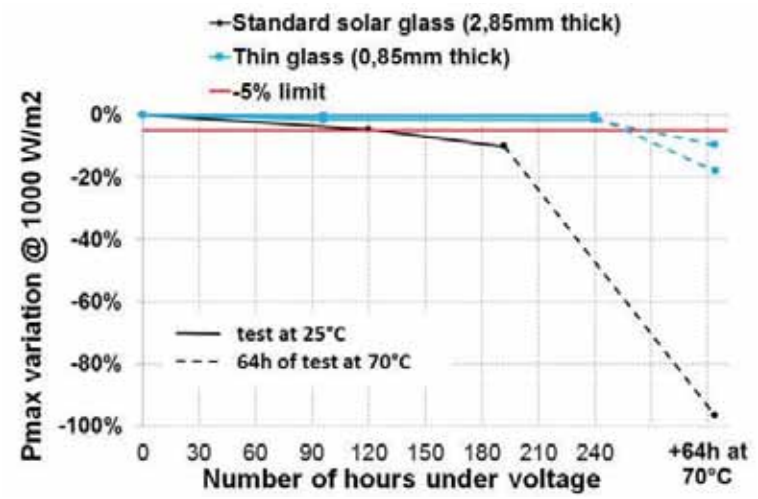

Figure 13. STC relative power evolution for mini-modules with different glass during the PID test (–1,500V/25°C/with aluminium foil).

References

[1] Pingel 2010, "Potential induced degradation of solar cells and panels", *Proc 35th IEEE PVSC*, Honolulu, Hawai, USA, pp. 002817–002822.

[2] Pingel 2010, "Potential induced degradation of solar cells and panels", *Proc. 25th EU PVSEC*, Valencia, Spain, pp 3753–3759.

[3] Hacke 2010, "Test-to-failure of crystalline silicon modules", *IEEE*, CP-5200-47755.

[4] Hoffman 1978, "Environmental qualification testing of terrestrial solar cell modules", *IEEE*, pp. 835–842.

[5] Naumann 2013, "Explanation of potential-induced degradation of the shunting type by Na decoration of stacking faults in Si solar cells", *Sol. Energy Mater. Sol. Cells*, Vol. 120, pp. 383–389.

[6] Pingel 2014, "The local potential distribution as driver of PID", *Proc. 30th EU PVSEC*, Kyoto, Japan, pp 2335–2341.

[7] Berghold 2012, "PID effects on crystalline silicon cells with various AR coatings", *Photovoltaics International*.

[8] Berghold 2013, "PID and its correlation with experience in the

field", *Photovoltaics International*.
[9] Kastl 2011, "Dealing with high voltage stress", *pv magazine*.
[10] Braisaz 2014, "PID results at low irradiances on c-Si modules", *IEEE*.
[11] IEC TS 62804:2014, "Test methods for detection of potential-induced degradation of crystalline silicon".
[12] Braisaz 2015, "Evaluation of 'PID 1500V ready' modules: A new test protocol", *IEEE*.
[13] Braisaz 2016, "Improved 1500V PID resistance encapsulants cover glass and ion implanted cells", *Proc. 32nd EU PVSEC*, Munich, Germany.
[14] Braisaz 2012, "An ageing model of PV modules and a link between indoor accelerated tests an outdoor degradation", *Proc. 32nd EU PVSEC*, Munich, Germany.
[15] Desharnais 2014, "Characterizing the impact of potential-induced degradation and recovery on the irradiance and temperature dependence of photovoltaic modules", *Proc. 30th EU PVSEC*, Kyoto, Japan.
[16] Zhu 2014, "Cost-effective industrial n-type bifacial and IBC cells with ENERGi™ P and B ion implantation", *Proc. 8th SNEC Int. PV Power Gen. Conf.*, Shanghai, China.
[17] Basame 2013, "Ion implanted high efficiency PID free cells for today's solar market", *Proc. 28th EU PVSEC*, Paris, France.
[18] Han 2013, "Ion implantation – An effective solution to prevent c-Si PV module PID", *Proc. 28th EU PVSEC*, Paris, France.
[19] Lechner 2013, "PID-behaviour of thin-film and c-Si PV-modules", *Proc. 28th EU PVSEC*, Paris, France.

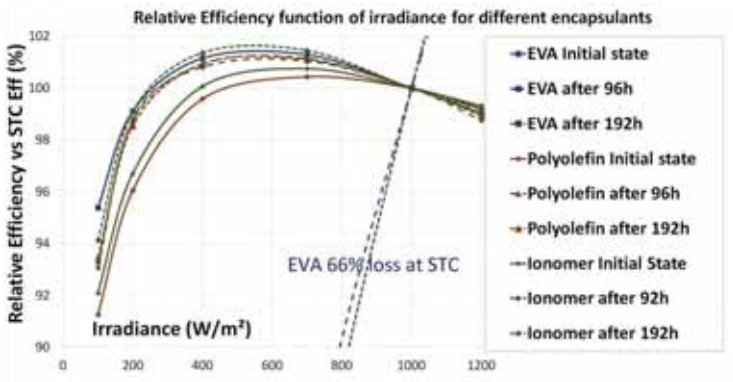

Figure 14. Relative efficiency vs. STC efficiency as function of irradiance for different module encapsulants (PID conditions: –1,500V/75°C/85%RH).

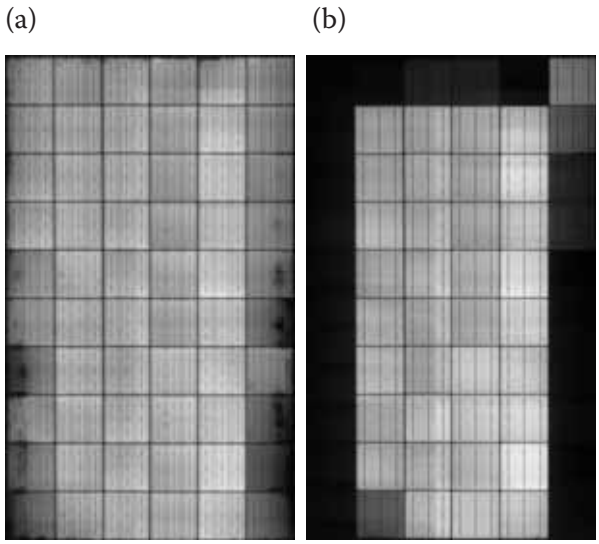

Figure 15. EL images after the PID test (–1,500V/75°C/85%RH/96h): (a) 9A; (b) 0.9A.

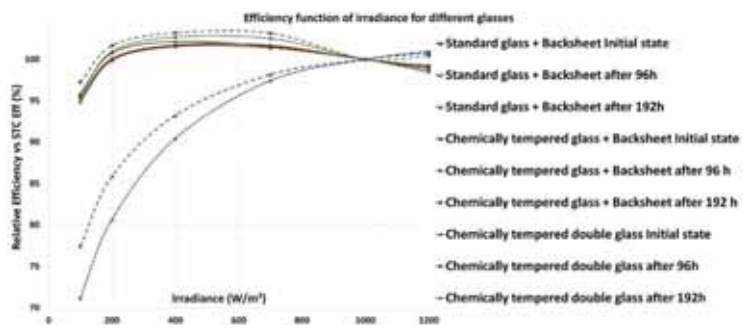

Figure 16. Relative efficiency vs. STC efficiency as a function of irradiance for different module glass (PID conditions: –1,500V/75°C/85%RH).

About the Authors

Benoit Braisaz graduated in 2008 from CentraleSupélec Engineering School in Paris, and specializes in electrical engineering and physics. For seven years he has been working as a research engineer in the PV installations group at EDF R&D, where his main research topics are PV system modelling and electrical characterization (indoor and outdoor measurements). He has been in charge of R&D activities at the Certisolis lab since 2016.

Benjamin Commault graduated as a materials engineer from Polytech Nantes in 2011, and since then has been working as a research engineer in PV at the French Institute for Solar Energy (INES). At CEA-INES he has gained more than two years' experience in the development and production of heterojunction solar cells, and since 2014 he has been working on the R&D of c-Si PV modules.

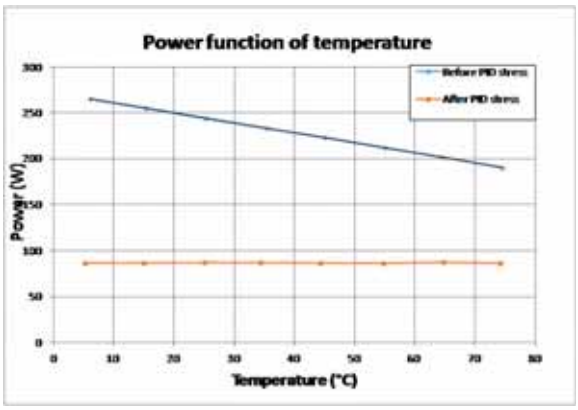

Figure 17. Power as a function of temperature, before and after PID stress testing. After the test there is virtually no temperature dependency.

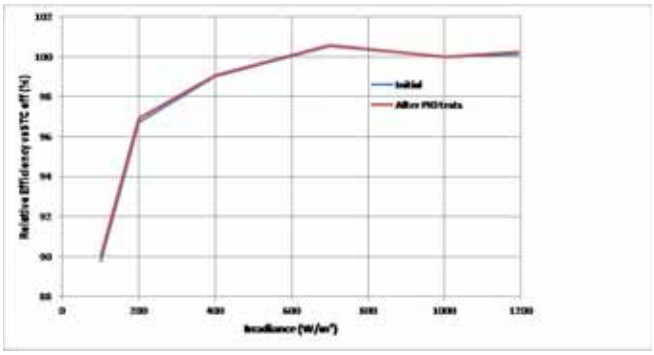

Figure 18. Relative efficiency vs. STC efficiency as a function of irradiance for a module with diffused cells and an Al_2O_3 layer, before and after the PID test (PID conditions: –1,500V/75°C/85%RH/192h).

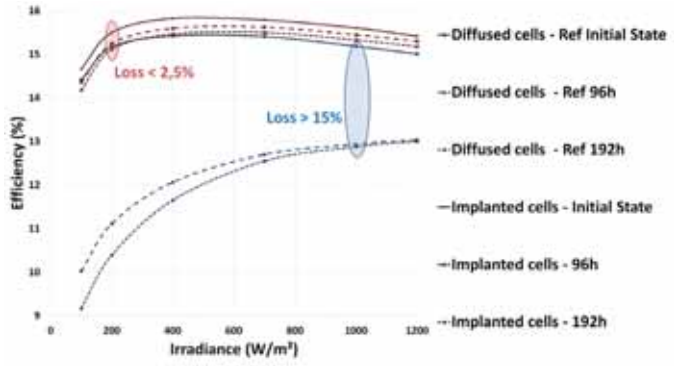

Figure 19. Efficiency as a function of irradiance for a module with implanted cells and for a module with diffused cells (PID conditions: –1,500V/75°C/85%RH).

Nam Le Quang has a Ph.D. in physics and more than 35 years' experience in the field of PV. He began his PV activities in various laboratories, including the Solid State Physics Laboratory (LBSB) at CNRS, ESAT and imec. He has been involved in many locally and EU-funded research projects relating to PV, several of which he has coordinated (PV-16, REDUCOP, Solar Nano Crystal (SNC)). He joined Photowatt (EDF ENR PWT) in 1992 and is now head of R&D programmes.

Marc Pirot began his career at the CEA-LETI, working on manufacturing processes for microelectronics devices. He joined the silicon solar cell team at the National Institute of Solar Energy in 2001, and currently works as a project leader on p-type Al-BSF and PERC solar cells.

Eric Gerritsen received his M.Sc. in 1983 and his Ph.D. in 1990. For more than 20 years he held various scientific and engineering positions at Philips (Research, Lighting and Semiconductors) in the Netherlands, Germany and France, where his work mostly concerned the development and industrial transfer of materials processing technologies. Since 2008 he has been at CEA-INES, the French national institute for solar energy, dealing with all aspects of module design, performance and reliability testing.

Didier Binesti received his Ph.D. in materials science in 1986. After two years at the Centre National de la Recherche Scientifique, he joined Electricité De France, successively working on various materials for electrotechnics, energy and buildings, and PV plants, while leading R&D teams and projects.

Khalid Radouane received his Ph.D. in plasma physics in 1999 from the Laplace Institute in Toulouse, and has more than 20 years' experience in the fields of microelectronics, LCD display, PV and storage. He began his PV activities at the University of Orléans, and has held various positions with different companies, including Total and Soitec. He joined EDF EN in 2009 and is now head of the solar PV and storage department.

Enquiries
Benoît Braisaz
Certisolis
39 Allée du Lac de Come
F-73375 Le Bourget du Lac
France

Tel: 0033 632460245
Email: benoit.braisaz@certisolis.com

Improving the efficiency of PV modules using glass with reflective strips

Salvador Ponce-Alcántara & **Guillermo Sánchez**, Valencia Nanophotonics Technology Center – UPV, Spain

ABSTRACT

Conventional ribbons used for interconnecting solar cells in PV modules act like mirrors, causing a large proportion of incident light to be lost. Experimental results indicate that only around 5% of the perpendicular incident light on the connections can be reused; as a result, this area contributes very little, if at all, to the current generation. In order to reduce the mirroring effect, a new glass with reflective strips placed on top of the solar cell busbars has been tested. The use of white reflective strips with high reflectivity and good Lambertian behaviour is responsible for a theoretical increase in efficiency of 0.28%$_{abs.}$ in a standard PV module processed with three-busbar solar cells. Different PV mini-modules were fabricated in order to study the real effect of the glass with reflective strips. The experimental results showed that the average short-circuit current density increases by 1.2%$_{abs.}$ with this new glass, which equates to an increase in PV module efficiency of 0.23%$_{abs.}$, or a gain of 0.033% per cm^2 of connecting ribbon. In consequence, the glass with reflective strips helps to reduce cell-to-module losses. Moreover, and using the same effect, reflective strips can be placed on the glass, in the spaces between the solar cells in a PV module; this helps to improve the current density, mainly in glass–glass and bifacial modules. The study of this new type of PV module is currently under way, with the publication of results forthcoming. The technology is simple and inexpensive; it is compatible with polished and textured glasses, and supports glasses with anti-reflection coatings. In addition, no degradation has been found in PV modules after various tests carried out in a climate chamber. This reflective strip technology is therefore almost ready for use at the industrial level.

Introduction

Reducing the costs associated with PV is an important contribution towards making this type of renewable energy more competitive. On account of the facts that over the last few years PV production capacity has exponentially increased, and that the industry has seen significant development in Asia, the price per watt of a PV module has currently reached a level of around $0.50/Wp [1]. Because of this low average price and the excellent efficiencies achieved, 93% of the actual PV industry was associated with silicon-wafer-based technology in 2015; around 96% of that percentage is attributable to double-side-contacted silicon solar cells. By 2026 this percentage is still expected to be very high (around 80%) [2].

There are two main reasons for this tendency: high efficiency and low price per watt. One way to reduce the latter is to increase the efficiency of the PV device. In this respect, the efficiency of a solar cell has increased more rapidly than that of a PV module; resistive and optical losses are the major reasons for this difference.

In recent years a lot of effort has been put into increasing the efficiency of PV devices; as a result, efficiencies of 19.8% have been achieved for multicrystalline silicon solar cells at the industrial level. For PV modules, however, the average industrial efficiency has been reduced to 17.1% [3]. Given this, the approaches to increasing PV module efficiency have focused on optical and electrical losses at the module level. Optical losses are mostly due to light absorption and/or reflection by the glass, the encapsulant and the metalized area of the solar cell. Electrical losses are mainly caused by series resistance in the string connectors; indeed, because of the interconnection between the cells, and on the basis of the above-mentioned achievable efficiencies, experimental studies have shown that the fill factor decreases by around 3%$_{abs.}$ for a PV module compared with that for a solar cell [4].

Many avenues of investigation are being pursued to reduce the loss in fill factor. One possibility is the use of solar cells with multiple busbars. This arrangement leads to a reduction in series resistance at both cell and module levels; moreover, the impact of grid damage (such as an accidental finger interruption in the metallization grid of the solar cell) is decreased. Another advantage of the use of a greater number of busbars is the reduction of the stresses associated with the ribbon-soldering step [5]. As a result, and according to the International Technology Roadmap for Photovoltaic (ITRPV 2016) [6], the industry will gravitate to the use of four (or even more) busbars in the near future. However, it must be borne in mind that any electrical improvement is partially negated by shading losses.

With standard PV glass, currently around 92% of the incident light is transmitted to the solar cells. The percentage can be improved by using textured glass and/or glass with an anti-reflection coating layer, resulting in around 96% of the incident light reaching the cells. A lot of effort has therefore been put into increasing the transmission of light in the glass; however, in glass design the light reflected by the solar cells is not considered. In particular, it is important to take into account the light reflected by the busbars. In today's industrial solar cells, around 3% of the total area is covered by the three busbars, which is even higher if more busbars are used.

When attempting to increase the efficiency, the optical utilization of the inactive areas of the solar cells and PV modules becomes an important issue. In particular, following encapsulation some of the light reflected by all the inner PV module surfaces can be reused. Taking into account the refractive indices of the encapsulant, the glass and the air, Snell's law shows that the critical angle for achieving total internal reflection of the light reflected by the inner PV module surfaces is 42°. For lower angles, most of the light will escape from the PV module and does not contribute to increasing the current photogenerated by the solar cells.

"It is essential to increase the percentage of incident photons striking the solar cell ribbons and redirect them to the active area."

In order to reduce the shading effects mentioned earlier, it is essential to increase the percentage of incident photons striking the solar cell ribbons and redirect them to the active area. One way to achieve this objective has been proposed by Hamann et al. [7], who proposed the use of white-painted ribbons. They reported an experimental improvement in efficiency of $0.20\%_{abs.}$ if the area covered by ribbons is 3.5%; this implies a $0.023\%_{abs.}$ increase in efficiency for each cm^2 of ribbon. However, because of the possibility of degradation and the reduction in optical properties during the soldering step of a solar cell series, white-painted ribbons have not yet gained (according to the authors' knowledge) the expected acceptance at the industrial level.

In this paper, another method for taking advantage of the ribbon area is presented; this method is based on the use of a new glass with reflective strips placed on top of the tabbing ribbons. The reflective strips are created with a white paint based on titanium oxide nanoparticles (NPs). These NPs are responsible for a high global reflectance, with a diffuse component close to the ideal Lambertian one. Calculations show a theoretical increase in PV module efficiency of $0.28\%_{abs.}$ if the area covered by ribbons is 2.9%. In this case, the improvement in efficiency per unit area of the ribbon is $0.040\%/cm^2$ as a result of the use of a glass with reflective strips.

Different PV mini-modules were fabricated in order to study the real effect of the glass with reflective strips. Three different glasses were used: 1) polished side facing the air, and textured side facing the cell; 2) textured side facing the air, and polished side facing the cell; and 3) both sides polished. In all cases, an improvement of $0.033\%_{abs.}$ per cm^2 of the tabbing ribbon was obtained experimentally, which implies a $0.23\%_{abs.}$ gain in efficiency for a standard PV module containing three-busbar solar cells. In consequence, the glass with reflective strips helps to reduce cell-to-module losses.

An interesting technology that is growing and expected to reach a 20% market share in 2026 is the bifacial solar cell concept [6]; here, the effect of the use of a glass with reflective strips will be even more notable. They can be placed on top of the busbars and in the spaces between solar cells, thus reducing the inactive areas of the PV module.

Reflective strips are compatible with any type of PV glass – polished or textured, and with anti-reflection coating layers. It is essential, however, that these strips remain stable in outdoor conditions. Different accelerated ageing methods have been studied for PV modules processed with glasses with reflective strips: no variation in module efficiency has been found compared with that for PV modules used as references.

There is also the possibility of using reflective strips on top of the interconnections between the solar cells in a series. Furthermore, and depending on the demand for architectonic integration, it is possible to use reflective strips of different colours.

Optical behaviour of the metallization grid in a PV module

When trying to increase efficiency, the optical utilization of the inactive areas of solar cells and PV modules is vitally important; in particular, following encapsulation some of the light reflected by all the inner PV module surfaces can be reused. Taking into account the refractive indices of the encapsulant, the glass and the air, Snell's law shows that the critical angle for achieving a total internal reflection of the light reflected by the inner PV module surfaces is given by:

$$\theta = \arcsin [n_{air} / n_{glass\text{-}EVA}] \quad (1)$$

On the assumption that the glass and the encapsulant have a refractive index of 1.5, the internal reflectance angle θ at the glass–air interface must be greater than 42°. For smaller angles, most of the light will escape from the PV module and does not contribute to increasing the current photogenerated in the solar cells.

By considering the spacing of cells, and given a Lambertian reflector (ideal diffuse surface) embedded in EVA and glass, it can be shown that the maximum percentage of incident light that can be reused is 56% [8]. In this respect, it has been experimentally shown that the percentage varies from 43% to 52%, depending on the PV backsheet selected [9].

In standard industrial specifications, the area of the metallization grid of typical crystalline silicon solar cells occupies between 6 and 8% of the cell surface; this area has a low contribution to current generation because it is shaded by the metal. As shown in Fig. 1, shading losses can be reduced after encapsulation by the total internal reflection (RTI) from the metallization grid of a certain percentage of photons, which are redirected back to the cell.

Fig. 1 shows the case of a ray of light which falls perpendicular to the PV module. From the point of view of the optical properties of the metallization grid, the ribbons soldered to the busbars have a high specular component. As will be discussed later in this paper, it has been experimentally determined that less than 5% of the incident light is reused. This percentage is well below the theoretical limit of 56% mentioned previously, and implies only a 0.12% improvement in the short-circuit current of the solar cell.

A novel means of reducing the shadowing effect of the solar cell metallization grid is presented; the method is compatible with the vast majority of crystalline silicon solar cells, as well as with current industrial PV module fabrication processes. It is not necessary to impose restrictions on the ribbon selection and/or on the soldering step, both of which play an important part in reducing the series resistance of a PV module, and hence in increasing its efficiency. The method presented in this paper is based on the use of a glass with reflective strips placed on top of the solar cell metallization grid.

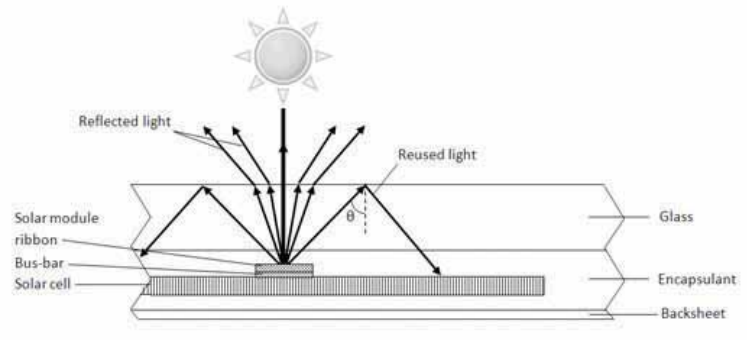

Figure 1. Schema of the reflection of a ray of incident light striking a tabbing ribbon.

"The method is based on the use of a glass with reflective strips placed on top of the solar cell metallization grid."

Glass with reflective strips

To usefully exploit the light reflected from the solar cell ribbons, a glass with reflective strips was experimentally developed and tested in the laboratory at Valencia Nanophotonics Technology Center. As a result of the improvements obtained in performance, the glass with reflective strips has been patented.

The reflective strips are placed on the inner side of the glass, and on top of the solar cell metallization grid; a schema of a PV module with a reflective strip is shown in Fig. 2.

A white paint based on titanium dioxide pigments was used to define the reflective strip; as well as its high global reflectance, it efficiently scatters the light. As a result, a significant percentage of the incident photons can be reused by light trapping (Equation 1); these photons are subsequently absorbed by the solar cell active area.

The combination of high global reflectance and the short distance from the interconnection ribbon also allows an efficient use of a percentage of light transmitted through the reflective strip placed in the glass. In addition, as will be revealed below, the influence of the angle of incidence of the light is minimal.

The reflective strips discussed in this paper can be used to cover all the metallization grid of a solar cell, which includes the fingers and the busbars. Depending on the fabrication technology, two solar cells with the same number of busbars can have a different number of fingers. However, for a given number of busbars, the busbar positions on the solar cell surface are fixed; therefore in order to obtain a more general result, reflective strips placed only on top of the busbars have been studied.

Optical characterization of the reflective strips

Reflectance, transmittance and absorbance

Global reflectance and transmittance measurements of the reflective strips were obtained using a SpecWin Light CAS 140CT spectrophotometer and an Instruments Systems 150mm integrating sphere. Absorption was calculated from the equation:

$$\text{Absorption} = 1 - \text{Reflection} - \text{Transmission} \quad (2)$$

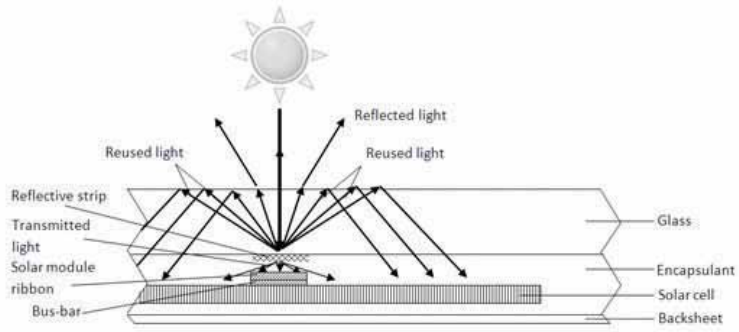

Figure 2. Schema of the behaviour of a ray of incident light hitting a reflective strip.

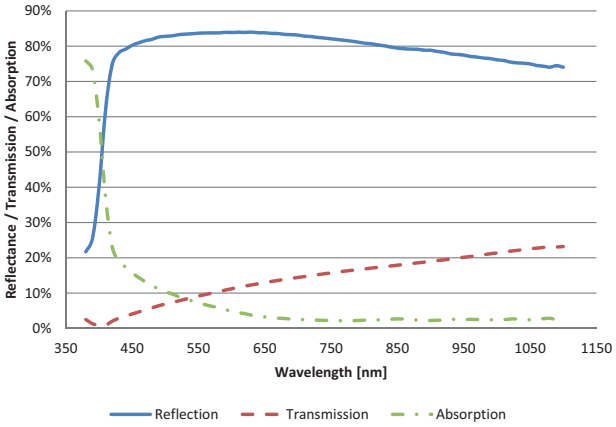

Figure 3. Global reflection, transmission and absorption of the white paint used to define the reflective strips.

Measurements as a function of wavelength are shown in Fig. 3. An average global reflectance of 79.3% and transmittance of 14.6% were determined for the reflective strips.

Angular dependence of the reflected and transmitted light

According to Equation 1, and in order to estimate the percentage of the incident light on the reflective strip that can be sent to the active area of the solar cell, it is important to study the angular dependence of the reflected and transmitted light. To this end, and depending on the relevance of the specular component, a variation of $9\%_{abs.}$ for the reflected light that undergoes total internal reflection can be found in reflective layers with similar global reflectances [9].

An angular measurement set-up (Thorlabs optical components) was performed in order to determine the angular dependence of the light reflected by and transmitted through the reflective strip. Fig. 4 shows a schema of the set-up used.

To measure the angular dependence, both the laser and the sample were kept in fixed positions. The spectrometer was turned using a Thorlab's NanoRotator 360° rotation stage and their APT precision motion controller. The angular measurement cannot be performed at angles between ±5° with respect to the laser position, because the laser beam and the spectrophotometer cannot be superimposed.

A 633nm red laser from JDS Uniphase was selected for this study. The reasons for this choice are its stable characteristics, the high reflectance of the white paint at 633nm, and the fact that the external quantum efficiency of a standard crystalline silicon solar cell reaches its maximum close to the laser emission wavelength.

For a quasi-normal incidence, Fig. 5 reveals the angular dependence of the reflected and transmitted light of the white paint used in the reflective strip. As a reference, the response of a standard metallic ribbon is also indicated (in green) in the figure.

According to Fig. 5, no specular peaks are visible in the case of the reflective strip. In addition, the reflected and transmitted light is markedly diffused. A different phenomenon is observed with a standard PV ribbon, for which the specular component is much greater

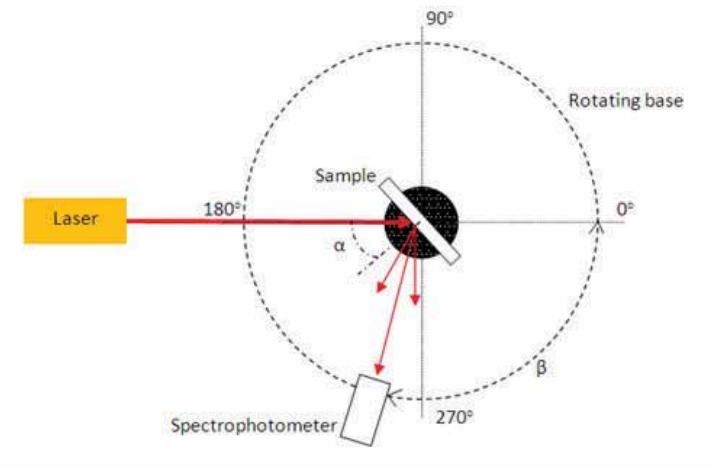

Figure 4. The set-up used to measure the angular dependence of the backsheets. The laser is placed in a fixed position, where α is the angle between the laser beam and the perpendicular to the sample. The sample can be rotated through the range α = 0 to 90°, but is kept fixed while a measurement is being taken. β is an angle related to the position of the spectrophotometer, which can be rotated from 0 to 360°.

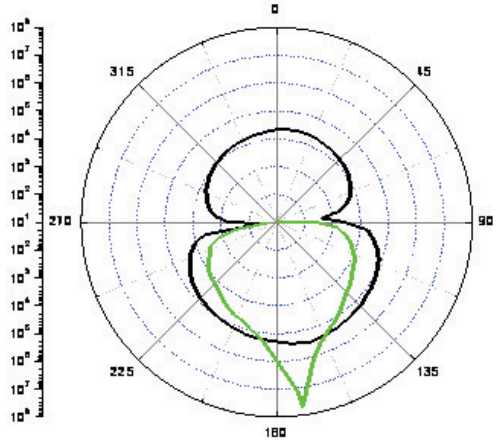

Figure 5. Angular dependence of the light reflected by and transmitted through the reflective strip (black) compared with a standard PV ribbon (green). In this set-up, the light incidence takes place at 180°. In order to measure the specular component of the reflected light, the sample is rotated by an angle α = 5°. The reflectance response is located in the second and third quadrants, and the transmittance in the fourth and first quadrants.

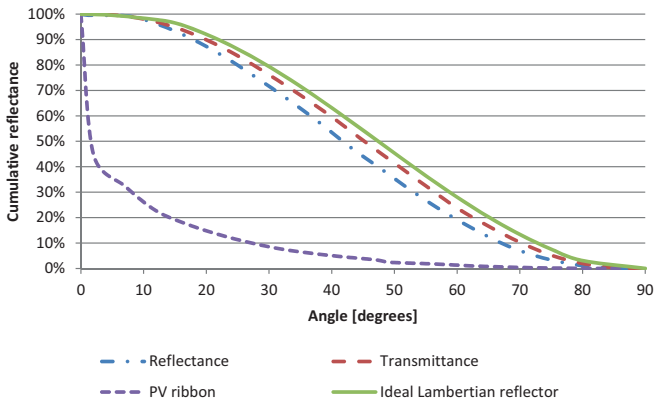

Figure 6. Cumulative reflectance and transmittance of the reflective strip and a PV ribbon, for a quasi-normal light incidence.

"No specular peaks are visible in the case of the reflective strip."

For a quasi-normal incidence of light (α = 5°), the cumulative reflectance was calculated by integrating the measured light over the solid angle of 2π; the results are shown in Fig. 6. A standard PV ribbon acts like a mirror; in this respect, as shown in Fig. 6, its specular component is important. On the other hand, and mainly in the case of transmitted light, the reflective strip has an angular dependence similar to that of an ideal Lambertian surface.

Depending on the position of the reflective strip in a PV module, and on the light reflected, the use of a significant fraction of the light transmitted through the module is possible; a greater percentage of the light directed towards the metallization grid can therefore be utilized. Bearing in mind that total internal reflection at the glass–air interface takes place for angles of incidence greater than 42°, for a standard PV ribbon the percentage of the reflected light that can be reused is close to 5%. In contrast, the percentage values achieved for the reflected and transmitted light that can be reused in the case of a reflective strip are around 50% and 55% respectively. It is therefore expected that improvements to the current of a PV module can be made because of the better utilization of the light directed towards the solar cell metallization grid and module interconnections.

Dependence of the reflectance and transmittance on the angle of incidence of the light

The following characterization step consists of studying the optical response of a standard PV ribbon and a reflective strip as a function of the angle of incidence of the light. Three angles were selected: α = 5°, 30° and 60±2° (low- to high-gloss regions). Figs. 7 and 8 summarize the results; according to Fig. 7, a standard PV ribbon has a significant specular component, which increases slightly with the angle of incidence.

As regards the reflective strip, the percentage of reflected light increases as the angle of incidence increases, which is consistent with the Fresnel equations [10]. This behaviour is mainly due to a reduction in the transmitted light through the reflective strip. No specular peaks are observed, and a significant

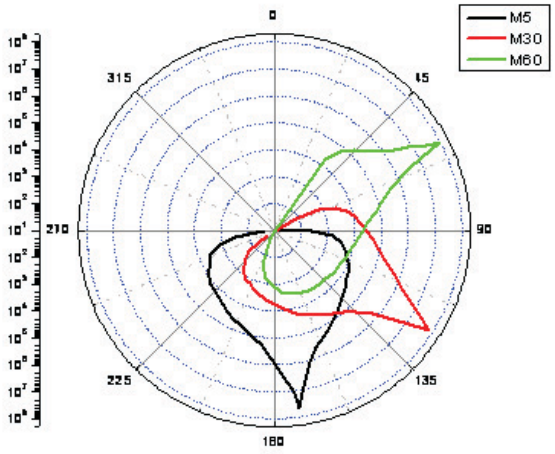

Figure 7. Angular dependence of the light reflected by a standard PV ribbon, for three different angles of incidence.

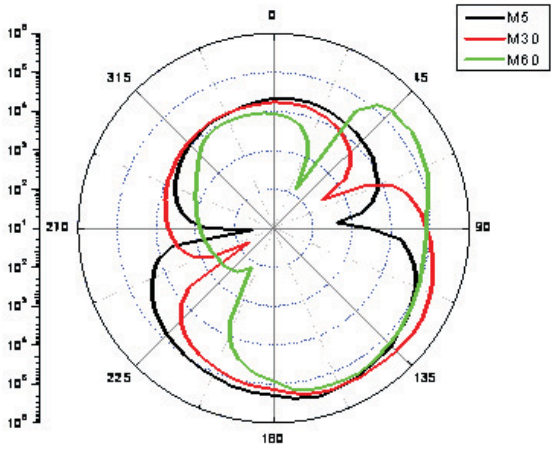

Figure 8. Angular dependence of the light reflected by and transmitted through a reflective strip, for three different angles of incidence.

diffused component is present in all cases. The reflective strip therefore acts like an ideal Lambertian surface.

Effective optical surface area calculation

With the previous characterization measurements in mind, and neglecting multiple internal reflections, the optically active surface area (S_{opt}) of a PV ribbon was defined. This surface area can be deduced from the metallization grid area and can be added to the active area of the solar cells. As shown in Equation 3, S_{opt} depends on the ribbon's global reflectance and transmittance, and on the angular response to the light:

$$S_{opt} = [(G_R \times R_{lr}) + (G_T \times T_{lr})] \times S_{ribbon} \quad (3)$$

where G_R is the global reflectance of the ribbon, R_{lr} is the reflected light due to total internal reflection at the glass–air interface and which can be reused, G_T is the global transmittance of the ribbon, T_{lr} is the transmitted light that can be reused, and S_{ribbon} is the PV ribbon surface area. In an ideal case, where the global reflectance and the reflected light of an inactive area of the PV module that can be reused is 100%, the entire surface would be active.

In the case of a standard PV ribbon, the average global reflectance is close to 85%, the reflected light due to the total internal reflection at the glass–air interface and which can be reused is 5%, and the global transmittance is 0%. Because of this, only 4.3% of a standard PV ribbon surface is optically active.

In comparison, for a reflective strip placed on top of a PV ribbon, the average global reflectance is 79.3%, the reflected light due to the total internal reflection at the glass–air interface and which can be reused is 50%, the global transmittance is 14.6%, and the percentage of the transmitted light that can be reused is 55%. In this case, around 47.7% of the PV ribbon surface is optically active on account of the effect of the reflective strip. The metallic surface area that is optically active thanks to this effect is increased by a factor of more than 10, because of the use of reflective strips; this equates to a short-circuit current gain of 1.35% for a standard PV module fabricated with three-busbar solar cells. This improvement becomes more significant with an increase in the number of busbars and/or their surface area.

> "Around 47.7% of the PV ribbon surface is optically active on account of the effect of the reflective strip."

Experimental results

Electrical parameters

Three-busbar high-efficiency 156×156×0.18mm multicrystalline silicon solar cells with similar electrical parameters were used to study the effect of the reflective strips on the short-circuit current and efficiency of PV mini-modules. Each glass had two different configurations on two independent solar cells: one of them had reflective strips, and the other was used as a reference. The same low-iron PV glass, encapsulant and backsheet were utilized in each case.

Three mini-modules were fabricated with each type of glass (polished side facing the air, and textured side facing the cell; textured side facing the air, and polished side facing the cell; and both sides polished).

The electrical characterization of the mini-modules was carried out under standard test conditions using a class A solar simulator from Abet Technologies. A black mask with a separation of 2±0.3mm between the solar cell and the mask edges was utilized. The incident light was perpendicular to the PV mini-modules, and at least three measurements were taken in each case.

Fig. 9 shows a reference module with a standard PV glass, and a test module with the same glass, but with reflective strips painted on its inner side. According to Fig. 9, there is a pronounced difference between the PV modules in terms of the light reflected by the connecting ribbons. In the standard module, the connecting ribbons have a high specular reflection, as mentioned previously. As a result, the light is reflected away from the camera, and they have a dark appearance. On the other hand, in the case of the module with a glass incorporating reflective

Figure 9. (a) Standard PV module. (b) PV module with a glass incorporating reflective strips.

strips, a large percentage of the light directed towards the connecting ribbons is reflected back to the camera. This effect highlights the different reflection behaviours of the two mini-modules.

The short-circuit current of the PV modules processed with a glass incorporating reflective strips showed an average improvement of 1.2±0.2%$_{abs.}$, which is close to the theoretical value of 1.35%. This short-circuit current improvement implies a reduction in cell-to-module efficiency losses of 0.23%$_{abs.}$ due to optical effects alone. If the surface of the busbars in the solar cells used in this study is taken into account, the improvement in efficiency is 0.03%$_{abs.}$ per each cm^2 of busbar. For three-busbar solar cells, according to the theoretical results a variation in efficiency of 0.28%$_{abs.}$ (0.04%$_{abs.}$/cm^2) is achievable.

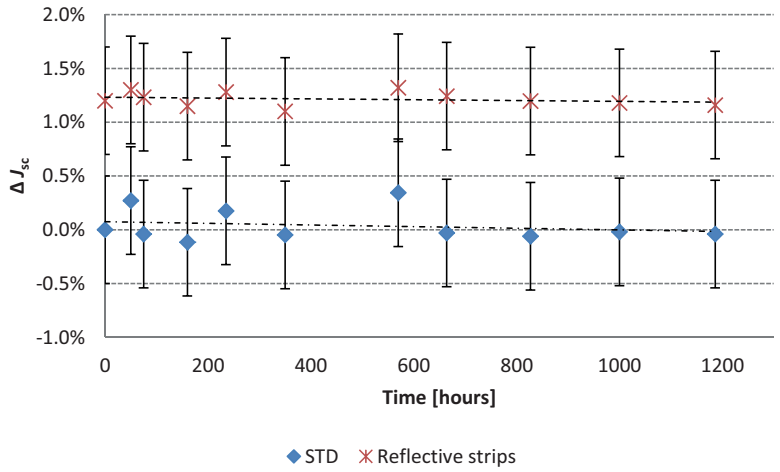

Figure 10. Short-circuit current density variations during the damp-heat test.

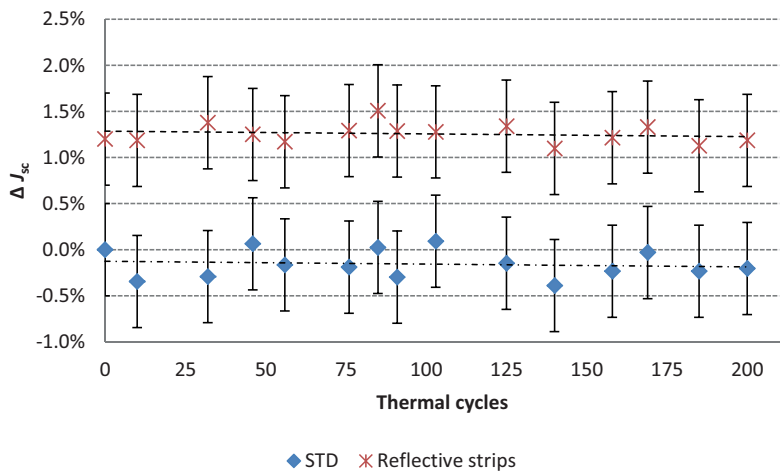

Figure 11. Short-circuit current density variations during the thermal-cycling test.

Degradation

In general, different methods of accelerated ageing have traditionally been used on PV modules, for example the UV exposure, thermal-cycling and damp-heat tests, as well as the highly accelerated stress test (HAST). The application of simultaneous multiple stresses – such as temperature, humidity and UV radiation – is also common. In this study, two degradation tests were investigated: damp heat (IEC 61215) and thermal cycling (TC200) [11]:

- Damp-heat test: a module is subjected to 1,000 hours at 85°C/85% RH in accordance with IEC 61215, which corresponds to 20 years' outdoor exposure. For this study, however, the duration of the test was extended to 1,200 hours.
- Thermal cycling test: performed for 200 cycles (TC 200), this test aims to simulate the thermal stresses on materials as a result of extreme changes in temperature (between –40°C and +85°C).

In this study, one mini-module with a glass having both faces polished was used as a reference, while another mini-module with the same glass but incorporating reflective strips was investigated. An Espec Global N environmental chamber was used to perform the degradation. Special attention was paid to the variation in short-circuit current, with the initial short-circuit current of the standard PV module taken as the reference. Figs. 10 and 11 show the degradation results, as well as the standard deviations.

No adhesion problems between the reflective strips and the glass were observed. Moreover, no important variations were discovered between the initial short-circuit current density and the value after both degradation processes. In this respect, the resulting

trends for the reference module and for the module with reflective strips were similar, leading to the conclusion that neither case demonstrated any appreciable degradation.

Conclusions

A new glass with reflective strips has been presented, which aims to reduce cell-to-module losses and to improve the efficiency of standard PV modules. The technique allows the use of the otherwise inactive area of the solar cells. The reflective strips are placed on the inner side of the glass, as well as on top of the solar cell metallization grid. The benefit of these strips has been demonstrated by studying their effect on the connecting ribbons.

Because of the high specular reflection of a standard PV ribbon, only around 5% of the incident light falling on it is utilized for increasing the current of the solar cells. With the use of a glass incorporating reflective strips, this percentage is increased by a factor of 10, an improvement that is due to the high global reflectance and the Lambertian response of the said strips. In addition, their transmitted light is highly diffused, and so some of that light can be reused.

With a normal light incidence, a theoretical short-circuit current improvement of 1.35% was obtained for a PV module processed from solar cells with three busbars, which equates to an improvement in efficiency of $0.28\%_{abs.}$ Experimentally, average improvements of 1.20% in the short-circuit current, and $0.23\%_{abs.}$ in the efficiency, of different PV mini-modules were obtained. These values imply a theoretical gain of $0.04\%_{abs.}$, and an experimental gain of $0.03\%_{abs.}$, per cm^2 of tabbing ribbon. Owing to the Lambertian behaviour of the strips, this improvement is expected to be almost constant for any angle of incidence of light.

If the reduction in the shading effect is taken into account, a new solar cell metallization grid can be designed to reduce the series resistance losses. In this respect, the glass with reflective strips favours the use of a large number of busbars.

Glass incorporating reflective strips can be integrated in the vast majority of PV modules fabricated with crystalline silicon solar cells – in other words, in modules constituting more than 90% of the current market. Given the presence of metallization grids on both of the main surfaces, bifacial solar cells would benefit even more from the use of reflective strips on the glass. Moreover, reflective strips can be placed in the spaces between solar cells, which helps to reduce the inactive areas of this type of PV module.

> "Because there are no technical obstacles, and no incompatibility issues with existing industrial fabrication procedures, reflective strip technology is almost ready for implementation at the industrial level."

The reflective strip approach is simple and inexpensive; it is compatible with polished and textured glasses, and supports glasses with anti-reflection coatings. In addition, no degradation was found in PV modules after various stress tests carried out in a climate chamber. The method offers the possibility of independently optimizing each PV module fabrication process in general, and the soldering interconnection step in particular. Moreover, the use of this novel glass does not require any additional fabrication processes. Because there are no technical obstacles, and no incompatibility issues with existing industrial fabrication procedures, reflective strip technology is almost ready for implementation at the industrial level.

References

[1] PVinsights 2016, Solar PV Module Weekly Spot Price (June) [http://pvinsights.com].

[2] Fraunhofer ISE 2016, Photovoltaics Report, updated: 6 June.

[3] Hanwha Q CELLS, May 2016, Industrial Data Sheets.

[4] Braun, S. et al. 2013, "Multi-busbar solar cells and modules: High efficiencies and low silver consumption", *Energy Procedia*, Vol. 38, pp. 334–339.

[5] Nakamura, M. 2011, "Improvement of reliability using four bus bar cell", NREL PVMRW, Golden, Colorado, USA.

[6] SEMI PV Group Europe 2016, "International technology roadmap for photovoltaic (ITRPV): 2015 results", 7th edn (Mar.) [http://www.itrpv.net/Reports/Downloads/].

[7] Hamann, L., Prönneke, L. & Werner, J.H. 2012, "Colored ribbons achieve $+0.28\%_{abs.}$ efficiency gain", *IEEE J. Photovolt.*, Vol 2. No. 4, pp. 494–498.

[8] McIntosh, K., Swanson, R.M. & Cotter, J.E. 2006, "A simple ray tracer to compute the optical concentration of photovoltaic modules", *Prog. Photovoltaics Res. Appl.*, Vol. 14, pp. 167–177.

[9] Ponce-Alcántara, S., Vivas, A. & Sánchez, G. 2014, "The importance of the photovoltaic backsheets optical characterization to improve the power of solar modules", *Photovoltaics International*, 26th edn.

[10] Casas, J. 1985, *Óptica*. Zaragoza, Spain: Coop. Artes Gráficas-Librería General.

[11] Arndt, R. & Puto, R. 2010, "Basic understanding of IEC standard testing for photovoltaic panels", Report, TÜV SÜD America Inc.

About the Authors

Salvador Ponce-Alcántara has a master's in electronics engineering, and a Ph.D. from the Solar Cell Institute – UPM, Spain. He has been a member of the R&D departments of several companies (Pevafersa, Isofotón), and joined the Valencia Nanophotonic Technology Center – UPV in 2011 as a leader in the PV module area. Since 2015 he has combined his research activities with a position as a professor in the Faculty of Electronics Engineering at UPV.

Guillermo Sánchez Plaza is co-founder of the Valencia Nanophotonic Technology Center – UPV, where he is currently the director of technology. He began working in the PV research area in 2009, and has extensive experience in nanomanufacturing processes for optoelectronic devices, on both an industrial and a laboratory scale.

Enquiries

Dr. Salvador Ponce-Alcántara
Valencia Nanophotonics Technology Center – UPV
Building 8F
Camino de Vera s/n
46022 Valencia
Spain

Tel: +34 96 387 70 00 (Ext. 88101)
Email: salponce@ntc.upv.es

Photovoltaics International

Advertisers & Web Index

ADVERTISER	WEB ADDRESS	PAGE NO.
Dow Chemical	www.dowpv.com	77
Energy Storage Summit	storage.solarenergyevents.com	22
Guangzhou Bothleader Electrical Materials Co., Ltd	www.gzbld.com	81
Horiba UK Ltd	www.horiba.com	17
Innolas Solutions GmbH	www.innolas-solutions.com	49
Intersolar	www.intersolarglobal.com	9
Intevac	www.intevac.com	47
JA Solar Holdings Co., Ltd.	www.jasolar.com	IFC
KUKA Industries	www.kuka.com	29
LERRI Solar Technology Co Ltd	www.lerri.com	5
Linde Group	www.linde.com/electronics	31
Meco Equipment Engineers B.V	www.besi.com	51
PV-Tech Membership	marketing@solarmedia.co.uk	83
The Quartz Corporation	www.thequartzcorp.com	19
RCT Solutions	www.rct-solutions.com	43
Schmid Group	www.schmid-group.com	21
Sentech Instruments GmbH	www.sentech.com	55
SNEC 2017	www.snec.org.cn	IBC
PV Celltech Conference	celltech.solarenergyevents.com	32
Solar Expo - Abu Dhabi	solarexpo.ae	15
Solar Middle East	www.energisingtheindustry.com	27
Talesun	www.talesun.com	7
Technic, Inc.	www.technic.com/epd	57
Von Ardenne GmbH	www.vonardenne.biz	25
Wuxi Suntech Power Co., Ltd.-	www.suntech-power.com	OBC

To advertise within Photovoltaics International, please contact the sales department: Tel +44 (0) 20 7871 0122

Top five solar module manufacturers in 2016

PV Tech, the sister website of *Photovoltaics International*, can reveal the preliminary top five solar module manufacturers in 2016, based as usual on final shipment guidance from third quarter financial results.

The top five ranked PV module manufacturers in 2016 are all current members of the 'Silicon Module Super League' (SMSL), which remains a six-company ranking, based on module shipments being significantly ahead of any other rivals.

This is typically at least 1GW below the sixth (bottom) ranked SMSL member and more than 2GW to 3GW below the topped-ranked SMSL.

These companies have typically increased both manufacturing capacity and product shipments significantly faster than other companies that could be included in a top 10 or top 20 ranking by shipments, clearly separating themselves from the pack, therefore justifying their own ranking category.

Indeed, such is the gap from the pack that SMSL members are typified by outpacing global end-market demand growth rates and gaining constant market share in the last few years, while others have sunk or trod water with global growth rates.

Despite the introduction of the SMSL rankings, one thing hasn't changed in the last 10 years: namely the challenge the leading PV manufacturer has in keeping the top ranking position for more than a couple of years.

This year was no different for the former SMSL leader for two consecutive years, Trina Solar; in 2016, Trina Solar has been leapfrogged by 2015 third-ranked JinkoSolar to become the leading global PV module manufacturer.

As a result of higher revised guidance provided in its third quarter financial results, JinkoSolar has guided full-year shipments to be in the range of 6.6GW to 6.7GW, surpassing those of Trina Solar of 6.3GW to 6.55GW.

JinkoSolar's final guidance range is notable due to the fact that it is only a 100MW difference from the low to high range. This compares to its initial shipment guidance for 2016 that varied by 500MW (6GW to 6.5GW). The wide range had been typical for JinkoSolar in the past.

Regular readers should not be surprised at JinkoSolar taking the top spot for the first time, as we highlighted in late August that the company had reported the second consecutive quarter of solar module shipments higher than Trina Solar.

Trina Solar also had another strong year and the shipment guidance figures reflect how close the leadership battle had been in the first half of the year. What is clear though is that JinkoSolar had that little bit more momentum than Trina Solar, which has been impacted greatly by the demand drop in China in the third quarter.

Ranked 2015	Ranked 2016	Company	2016 guidance range
3	1	JinkoSolar	6.6-6.7GW
1	2	Trina Solar	6.3-6.55GW
2	3	Canadian Solar	5.073-5.173GW
4	4	JA Solar	4.9-5GW
5	5	Hanwha Q CELLS	4.8-5GW

JinkoSolar has taken the lead slot in PV Tech's league table of 2016's top PV manufacturers. Source: PV Tech

Hanwha Q CELLS

Despite a reshuffling of positions, the top five module producers in 2016 remain unchanged from 2015.

Trina Solar did not provide fourth-quarter guidance or reiterate previous guidance and would need to ship around 1,858MW in the fourth quarter to meet the low end of its former guidance but would still fall short of JinkoSolar.

However, in respect to Canadian Solar it was clear from initial shipment guidance that it would have had to significantly raise guidance to catch Trina Solar or JinkoSolar. Indeed, Canadian Solar's downward revised shipment guidance in reporting third quarter results sealed the drop from being ranked second in 2015 to being ranked third in 2016.

Much closer to call are the rankings of JA Solar and Hanwha Q CELLS. Only 100MW separates them at the low end of their guidance ranges.

Both companies are tracking similar quarterly shipments, although we have to estimate Hanwha Q CELLS since it withheld actual quarterly figures after Q1.

However, based on momentum over three quarters it would seem possible that Hanwha Q CELLS could just edge past JA Solar after retaining upward revised Q2 guidance, while JA Solar lowered guidance in Q3.

There is also a wild card at play for fifth ranked position in the form of SMSL newcomer, GCL System Integrated (GCL SI). Strong first-half-year shipments and revenue, due to its focus on the Chinese market, meant the company tracked Hanwha Q CELLS.

However, the sudden collapse in downstream projects in China in the third quarter could have thwarted all attempts to surpass Hanwha Q CELLS. A strong rebound in fourth-quarter demand for GCL SI would need to happen for it to resume its ranking fight.

Should that not happen then GCL SI is not guaranteed to automatically finish the year in sixth position of the top 10 rankings. The main reason is that CdTe thin-film leader First Solar, with slightly lowered guidance of 2.8GW to 2.9GW, could beat its silicon rival.

This is an edited version of a blog post that first appeared on pv-tech.org

Mark Osborne, Senior News Editor, Photovoltaics International

SNEC 2017
PV POWER EXPO
Dialogue & Conference & Exhibition

www.snec.org.cn

11th (2017) International Photovoltaic Power Generation Conference & Exhibition

April 19-21, 2017

Shanghai New International Expo Center
(2345 Longyang Road, Pudong District, Shanghai, China)

关注SNEC微信

Follow us at WeChat

◎Asian Photovoltaic Industry Association / Shanghai New Energy Industry Association

◎Show Management: Follow Me Int'l Exhibition (Shanghai), Inc.

Add：Room 902, Building No. 1, 2020 West Zhongshan Road, Shanghai 200235, China

Tel：+86-21-33561099 / 33561095 / 33561096 Fax：+86-21-33561089

◎For exhibition: info@snec.org.cn For conference: office@snec.org.cn

10th EDITION
WORLD FUTURE ENERGY SUMMIT
PART OF ABU DHABI SUSTAINABILITY WEEK 2017
16-19 JANUARY 2017
ABU DHABI NATIONAL EXHIBITION CENTRE

We sincerely invite you to visit our booth at Hall 8

#110

SUNTECH